

## ABSTRACT

Title of Dissertation:                   CHARACTERIZING HYDROLOGICAL  
  PROCESSES WITHIN THE DATA-SCARCE  
  ENVIRONMENT OF THE CONGO BASIN

Yolande A. Munzimi,  
Doctor of Philosophy, 2019

Dissertation directed by:           Professor Matthew C. Hansen,  
  Department of Geographical Sciences

The Congo Basin in Africa is the world's second largest river basin. Centrally located and with the greatest water resources in Africa, the basin is a vital resource for water and energy supply for a continent with increasing needs for safe water and energy. The Congo Basin's streams and rivers could be impacted by human activities in the region, notably by land cover and land use change (LCLUC) considering the strong interactions between hydrology and ecosystem processes in the humid tropics. It could impact flow discharge downstream Congo River and hydropower potential at the Inga hydroelectric site, the largest such installation in Africa, located 150km upstream from the river's mouth. The seasonal rainfall regime, to which the Congo River owes its regular flow regime, play an important role in mediating freshwater resources. An improvement to our baseline information on the Congo's rainfall and streamflow

dynamics allows for a greater quantitative understanding of the basin's hydrology, necessary for the current and future management of Congo Basin water resources. The hydrometeorological observation network in the Congo Basin is very limited, and this environment of scarce ground data necessitates the use of remotely-sensed data for hydrological modeling.

This dissertation reports the use of hydrological modeling supported by remotely-sensed data to 1) characterize precipitation and climate in the Congo Basin, 2) characterize daily streamflow across the basin, 3) assess the hydrological response to LCLUC, including the additional response caused by climatic feedbacks following LCLUC. The study uses rainfall gauge data within the Democratic Republic of Congo (DRC) to re-calibrate a TRMM science product. It then describes a physically-based parameterization of a semi-distributed hydrological model, augmented with a spatially-distributed calibration that enables the model to simulate hydrologic processes in the Congo Basin, including the slowing effect of the basin's central wetlands, the *Cuvette Centrale*. Model simulations included scenarios of 25% to 100% conversion of the Basins forest cover to agricultural mosaic and compared simulated flows to those of the current baseline conditions. The dissertation also reports on the estimated impacts of the hydrological response to LCLUC on the river's hydropower potential.

Re-calibration of TRMM improved rainfall accuracy at the gauges by 15% and correctly captured important rainfall patterns such as the ones representative of the highland climate. Model calibration of daily streamflow resulted in a model with high predictive power (Nash-Sutcliffe coefficient of efficiency of 0.70) when compared to Kinshasa gauge downstream Congo River, near its outlet. Model shows realistic seasonal and spatial patterns that can be explained by the ITCZ-driven rainfall patterns in the Congo Basin.

Models of the direct effects alone of 25% to 100% forest conversion produce increases in peak flows of 7% to 8%, respectively, relative to the baseline, and decreases in low flow of 1% and 6%, for 75% and 100% forest conversion respectively, relative to the baseline. However, 25% and 50% forest conversion produce increases in low flows of 3% and 1% respectively indicating a possible sensitivity of the hydrological response to the spatial variability of forest conversion. Models of the combined direct and indirect effects of 25% to 100% conversion produce decreases in peak flows of 7% to 5% respectively and decreases in low flow of 8% to 11% respectively. Model estimates of the impacts on hydropower potential range from 11% decrease during dry season to 10% increase during rainy season, with greater impacts (year-round decrease) for increasing LCLUC models including indirect effect. The modeled loss in hydropower potential during dry season reaches -5,797 MW corresponding to the hydropower potential of countries such as Zambia or Angola and of grand projects such as the Grand Ethiopian Renaissance Dam. The dissertation has showed the adequacy of TRMM precipitation products for Congo Basin rainfall regime representation and daily flow estimation particularly in capturing the timing and the seasonality of the flow. The results of these modeling efforts can be useful in research and decision-making contexts and validate the application of satellite-based hydrologic models driven for large, data-scarce river systems such as the Congo Basin by producing reliable baseline information.

We recommend a prioritization of further data collection and more gauges installation required to enable further satellite-derived data calibration and models simulations. Likewise, the results from LCLUC analysis support the need for field campaigns to better understand sub-watersheds responses and to improve the calibration of currently used simulation models.

CHARACTERIZING HYDROLOGICAL PROCESSES WITHIN THE DATA-  
SCARCE ENVIRONMENT OF THE CONGO BASIN

by

Yolande A. Munzimi

Dissertation submitted to the Faculty of the Graduate School of the  
University of Maryland, College Park, in partial fulfillment  
of the requirements for the degree of  
Doctor of Philosophy  
2019

Advisory Committee:

Professor Matthew C. Hansen, Chair  
Professor Christopher O. Justice  
Professor Eric F. Vermote  
Professor Kwabena O. Asante  
Professor Gabriel B. Senay  
Professor Joseph H. Sullivan

© Copyright by  
Yolande A. Munzimi  
2019

## Foreword

Chapter 2-4 contain jointly authored work in which Yolande A. Munzimi is the primary author. Methods development, data processing, analysis of the findings and manuscript writing are led by Yolande A. Munzimi. The results presented in this dissertation are the outcome of Yolande A. Munzimi's work.

## Dedication

*To my family: Amadeo, Nathalie, Sandra, Patrick, Junior, Gladys & Marie-Patricia.*

*Thank you all for always being there.*

## Acknowledgements

I thank my PhD advisor, Dr. Matthew C. Hansen, for dedicating himself to supervising me. He took a chance on a project that was outside the scope of his group, guided and supported me over the years. His passion and knowledge of the Congo Basin empowered me to follow my own passion for Congo Basin waters and to get my science questions answered.

I also extend my thanks to the members of my dissertation committee, particularly to Dr. Christopher O. Justice who early on introduced me to NASA Tropical Rainfall Measuring Mission (TRMM). I did not know at the time that his initial encouragement would bring me this far. Special thanks to Dr. Kwabena O. Asante, my mentor in Surface Hydrology. He taught me everything that I know in hydrological modeling, even through his publications long before we were introduced. Dr. Kwabena O. Asante and Dr. Gabriel Senay, my other mentor in hydrology, were the ones who trusted me with this PhD opportunity. Thank you for being there from the beginning to this day. Thank you to Dr. Eric Vermote for his support and to Dr. Joseph Sullivan, the Dean's Representative, who has been very encouraging since joining the team.

I would like to thank my University of Maryland CARPE and GLAD teams in the UMD Department of Geographical Sciences: Diane Davies, Alice Altstatt, Janet Nackoney, Emma Minnis, Eddy Bongwele, Andre Mazinga, Bernard Adusei for his particular contribution to my work, Anil and Indrani Kommareddy, Qing Ying, Patrick Lola Amani, Alexandra Tyukavina, Andres, Viviana, Amy, Sam and so many more. I have benefited from our sharing of ideas and skills and the good time spent together.

I would also like to acknowledge the particular assistance of Dr. Marc Steininger for providing assistance in proofreading most of my work. Marc Steininger and Yamile Talero are the two friends that I needed, to help me cross the finish line of my race. Thank you. I do not forget the Department of Agronomic Sciences of the University of Kinshasa where my race began. That is where my passion for Congo Basin waters started out and developed under the supervision of Dr. Raymond S. Lumbuenamo and Dr. Jean-Robert B. Bwangoy. Thank you.

This research was made possible in large part by the United States Agency for International Development (USAID) Central African Programme for the Environment (CARPE). I hope that my work contributes to the CARPE legacy as the CARPE III phase reaches its conclusion. I would also like to gratefully acknowledge support from the NASA Earth System Science Fellowship awarded to me and extend many thanks to the NASA's Carbon Cycle & Ecosystems research program.

Finally, I extend enormous gratitude to my family and friends. Without their unconditional love, I would not have completed this long journey.

To you My Lord, I say Thank you. You are the Alpha and the Omega.

# Table of Contents

Foreword.....	ii
Dedication.....	iii
Acknowledgements.....	iv
Table of Contents.....	v
List of Tables.....	vii
List of Figures.....	viii
Chapter 1: Introduction.....	1
1.1. Background of the research.....	1
1.1.1. Current context.....	1
1.1.2. Remote Sensing of Congo Basin water resources: rainfall and streamflow current state of knowledge.....	4
1.1.3. Hydrological modeling.....	5
1.2. Research goals and objectives.....	7
1.3. Structure of the dissertation.....	8
Chapter 2: Characterizing Congo Basin rainfall and climate using Tropical Rainfall Measuring Mission (TRMM) satellite data and limited rain gauge.....	10
2.1. Introduction.....	10
2.2. Data.....	14
2.2.1. Precipitation Data.....	14
2.2.2. Temperature data.....	19
2.2.3. Climate data.....	19
2.3. Methods.....	20
2.3.1. Rainfall estimation.....	20
2.3.2. Climatological validation of re-calibrated TRMM data.....	21
2.3.3. Rainfall and temperature-based climate characterization.....	22
2.4. Results.....	25
2.4.1. Comparison of ground rain gauge and TRMM 3B42 data.....	25
2.4.2. TRMM re-calibration.....	27
2.4.3. Validation.....	29
2.4.4. Climate characterization.....	33
2.5. Discussion.....	36
2.5.1. Model performance.....	36
2.5.2. Climate classification.....	37
2.5.3. Application of re-calibrated TRMM in characterizing seasonal rainfall..	39

2.6. Conclusion .....	44
Chapter 3: Estimating daily streamflow in the Congo Basin using satellite-derived data and semi-distributed hydrologic model.....	46
3.1. Introduction.....	46
3.2. Data.....	51
3.3. The Geospatial Streamflow Model (GeoSFM).....	52
3.4. Methods.....	52
3.4.1. Initial Parameterization with Remote Sensing Data.....	54
3.4.2. Model calibration.....	55
3.4.3. Validation.....	58
3.5. Results and discussion.....	59
3.5.1. Calibration of the initial basin-wide model.....	59
3.5.2. Calibration of the initial regional (subbasin) model.....	65
3.5.3. Validation of the calibrated basin-wide and subbasin models.....	67
3.5.4. Model interpretation.....	74
3.6. Conclusion.....	78
Chapter 4: Assessment of streamflow response to forest conversion in the Congo Basin .....	81
4.1. Introduction.....	81
4.1.1. Congo Basin hydrology and water resources.....	81
4.1.2. Congo Basin land cover change.....	82
4.1.3. Hydrological dynamics and land cover change.....	83
4.1.4. Hydrological dynamics and land cover change.....	87
4.1.5. Purpose.....	90
4.2. Data and Methods.....	91
4.2.1. Data.....	91
4.2.2. Direct effects.....	94
4.2.3. Indirect effects.....	96
4.2.4. Hydropower potential.....	97
4.3. Results.....	98
4.3.1. Flow discharge.....	98
4.3.2. Surface runoff.....	99
4.3.3. Hydropower potential.....	100
4.4. Discussion.....	105
4.5. Conclusion.....	111
Chapter 5: Summary of findings, significance and future research directions .....	113
5.1. Summary.....	113
5.2. Major findings and contributions.....	114
5.3. Future research directions.....	121
Bibliography .....	125

## List of Tables

Table 2.1 Key Description of Köppen climate symbols and defining criteria - Adapted from Kottek et al. (2006) and Peel et al. (2007) for the Central African region.....	24
Table 2.2 Basin wide standard errors of the estimate (STEYX), coefficients of determination and bias, mean bias error (MBE) in mm and root mean square error (RMSE) in mm for TRMM 3B42 (o), re-calibrated TRMM (r) and TRMM 3B43 (3b), in comparison to WORLDCLIM monthly precipitation totals. Best performing products per statistical measure are shown in bold.....	31
Table 2.3 Classification results by area (km <sup>2</sup> ) and as a percentage of total Congo Basin area (3,700,000 km <sup>2</sup> ). Climate class totals of climate maps derived from TRMM 3B42, re-calibrated TRMM and TRMM 3B43 products and the map of Peel et al. (2007)...	35
Table 3.1 Data inputs to the basin model.....	53
Table 3.2 Comparison of satellite-derived model inputs from the current study (1998-2012) to published estimates for the Congo Basin.....	63
Table 3.3 Validation statistics of daily flow for gauge sites in Kinshasa, Ouesso and Bangui. ‘O’ is gauge station observation, ‘S’ is model simulation, ‘StdDev’ is standard deviation, ‘R <sup>2</sup> ’ is linear regression coefficient of determination, and ‘NSE’ is Nash-Sutcliffe model efficiency coefficient.....	69
Table 3.4 Means, 25 <sup>th</sup> percentiles and 75 <sup>th</sup> percentiles of daily low flow (Low), centroid of flow (Cent) and peak flow (Peak) for the observed (O), initial un-calibrated (U) and calibrated flow (C) of the Congo River at Kinshasa, Sangha River at Ouesso and Ubangi River at Bangui. These are the percentiles in the inter-annual variation and the dates of the occurrences of their annual minimum, maximum and mean. Flow magnitude is in m <sup>3</sup> /s. Model improvements are shown in boldface type.....	70
Table 3.5 Validation statistics of monthly mean flow for gauge sites in Ilebo, Kutu-Moke, Ubundu, Chembe-Ferry, Ouesso and Bangui. ‘O’ is gauge station observation, ‘S’ is model simulation, ‘StdDev’ is standard deviation, ‘R <sup>2</sup> ’ is linear regression coefficient of determination, and ‘NSE’ is Nash-Sutcliffe model efficiency coefficient.....	71
Table 4.1 Change in annual runoff volume/depth induced by LUC without and with climatic feedback.....	102
Table 4.2 Maximum (peak) and minimum (low) flow magnitude and percent of flow decrease/increase under the eight scenarios with no climatic feedback and with climatic feedback.....	103

## List of Figures

Figure 1.1 Structure of the dissertation.....	9
Figure 2.1 The Congo Basin with GPCC gridded precipitation gauge stations locations.....	17
Figure 2.2 Annual Total Precipitation at Kinshasa/N'djili Station (1961 - 2006).....	19
Figure 2.3 TRMM 3B42 Version 6 monthly rainfall accumulation of 10 years (1998 - 2007) compared with concurrent observed in situ data from gauges.....	26
Figure 2.4 Rainfall regime monthly averages for the Congo Basin.....	28
Figure 2.5 Monthly fractional augmentation of TRMM 3B42 Version 6.....	29
Figure 2.6 Mean precipitation for the 12 months of the year and annually.....	32
Figure 2.7 Köppen–Geiger climate classifications for the Congo Basin.....	34
Figure 2.8 a) Month of maximum precipitation for re-calibrated TRMM data; b) Ratio of big to small dry season precipitation minima.....	41
Figure 2.9 Plots of monthly precipitation.....	42
Figure 2.10 Re-calibrated TRMM Congo Basin monthly precipitation and Congo River mean streamflow discharge at Kinshasa.....	43
Figure 3.1 Stations locations and corresponding watersheds.....	48
Figure 3.2 Daily observed flow discharge at Kinshasa (1998 - 2010). Data are from the Régie des Voies Fluviales (RVF), Democratic Republic of the Congo.....	49
Figure 3.3 Final sequence applied for the basin-wide and regional calibration process. Basin-wide calibration is to the Congo River flow at its core, downstream from the Cuvette Centrale. Regional calibration is to Congo Basin sub-watersheds upstream from the Cuvette Centrale.....	59
Figure 3.4 (a) Daily observed flow discharge and (b) daily initial flow estimate discharge prior to calibration at the Congo River at Kinshasa.....	61
Figure 3.5 Multi-year average 1998 - 2010 of observed daily flow discharge and initial daily flow estimate discharge prior to calibration at the Congo River at Kinshasa.....	62

Figure 3.6 Comparison of 15 years (1998 - 2012) of daily discharge on Congo River at Kinshasa from basin-wide calibration. Blue is estimated flow from the calibrated model and red is gauge observations. The dashed line separates calibration and validation periods.....64

Figure 3.7 Monthly-mean of observed flow vs. simulated flow from regional calibration with no bias correction at Bangui (blue) and Ouesso (pink).....65

Figure 3.8 Comparison of 15 years (1998 - 2012) of daily discharge on Sangha River at Ouesso from regional calibration. Blue is estimated flow from the calibrated model and red is gauge observations. The dashed line separates calibration and validation periods.....66

Figure 3.9 Daily calibrated flow discharge over 15 years (1998 - 2012) on Congo River at Kinshasa from basin-wide calibration, and on the Sangha River at Ouesso and Ubangi River at Bangui from regional calibration compared to the un-calibrated estimates and observed flows.....67

Figure 3.10 Multi-year average of daily observed flow, initial estimate, estimate from basin-wide calibration at the Congo River at Kinshasa (2006 - 2010) and regional estimate at Sangha River at Ouesso (2006 - 2011) and Ubangi River at Bangui (2003 - 2007). The estimate from basin-wide calibration is the calibrated estimate at Kinshasa gauge while the regional estimate is the calibrated estimate at the Ouesso and Bangui gauges.....68

Figure 3.11 Monthly mean of observed flow, initial estimate, estimate from basin-wide calibration and regional estimate at the four Global River Discharge Database (GRDC) stations and at Bangui and Ouesso.....72

Figure 3.12 Spatial distribution of calibrated daily (a) high, (b) mean and (c) low flow magnitude over the 15 years of study (1998 - 2012) per subbasin. In each subbasin the flow condition (magnitude) of the corresponding river reach is represented.....76

Figure 3.13 Spatial distribution of calibrated day of (a) lowest flow and (b) peak flow, based on the modeled daily mean flow averaged over 1998 - 2012.....77

Figure 4.1 Fifteen years of observed (red) and simulated (blue) daily flow discharge of Congo River at Kinshasa from Munzimi et al, 2018. As shown for each year there are two peak flows and two low flows, which are also featured/found at Inga, denoting a bimodal flow regime. The bimodal flow exhibits a peak in December timeframe and a secondary peak in May that is approximately 50% of the December streamflow. The two low-flow periods occur in March and July (Munzimi et al, 2018).....88

Figure 4.2 Satellite-derived estimates of bioclimatic data inputs used in the GeoSFM model: a) current annual precipitation and b) evapotranspiration. See main text for data sources.....	91
Figure 4.3 Land cover classes used in the GeoSFM model: a) at full resolution compiled from a suite of existing, satellite-derived data products and b) majority values assigned to sub-basin units of the model. See main text for data sources.....	92
Figure 4.4 Definition of four scenarios of land-cover change where a) 25%, b) 50%, c) 75% and d) 100% of forest is converted to rural complex and the resulting majority land-cover class is assigned to each sub-basin polygon.....	93
Figure 4.5 Daily average hydrograph at the Congo River at Inga under four scenarios (25, 50, 75% and all forest conversion to rural complex) with and without consideration to climatic feedback. With forest conversion to rural complex, the rising limb get steeper, the rise time get slightly shorter and the peak discharge get higher. In red, current daily average hydrograph. Increase of runoff contribute to a higher peak flow. Yet, the increase of runoff occurs at the cost of groundwater recharge and other losses, impacting low flow by a noticeable decrease.....	100
Figure 4.6 Daily mean precipitation (1998-2012) in the overall Congo Basin.....	101
Figure 4.7 Change in annual runoff volume/depth induced by LUC without and with climatic feedback.....	101

# Chapter 1: Introduction

## **1.1. Background of the research**

### 1.1.1. Current context

Our understanding of the Congo Basin's hydrology is very limited by a lack of quantitative data and models, although it is essential for efficient management, present and future, of the basin's water resources. The Congo Basin is the world's second largest river basin, with a drainage area of over 3.5 million square kilometers, notable for its large internal bowl-shaped depression, referred to as the *Cuvette Centrale*, which lies in the center of the basin.

Centrally located and with the greatest water resources in Africa, the basin is a vital resource for a continent with increasing needs for safe water and energy (Mandelli, S et al, 2014). The rainfall regime of the Congo Basin, to whom the Congo River owes its regular regime year-round, is a major component of the water cycle, being a source of freshwater, defining conditions for diverse ecosystems, and enabling economic activities such as rainfed agriculture.

The drainage basin of the Congo River includes parts or the whole of ten countries: The Democratic Republic of the Congo, the Central African Republic, the Republic of Congo, Angola, Zambia, Tanzania, Cameroon, Burundi, Rwanda and South Sudan. All of 10 of Congo Basin countries are developing countries, a paradox considering the availability of water resources and their importance in socio-economic development.

In spite of the abundance of water, these countries face serious water-related issues such as limited access to safe drinking water, energy poverty and economic vulnerability. The last is based on the instability of and the significant dependence on agricultural production. Yet, in a region where water availability is not a limiting factor, its proper management would favor economic development principally by augmenting the primary and secondary sectors, production and transformation of raw material. However, with Africa being the most vulnerable continent to climate change, Congo Basin countries are exposed to and defenseless against natural disasters caused by water such as flood or erosion.

The Congo Basin streams and rivers are susceptible to human activities in the region, most notably by the ongoing loss of forest cover. The interactions between hydrology and the ecosystem are particularly very strong in the humid tropics. The distribution of vegetation influences the flow of water, while the presence of water makes the very existence of the ecosystem possible (Brauman et al. 2007). Forest conversion to rural complex, a characteristic mosaic of forest, plantations and rural human settlement (Molinario et al, 2017), could significantly impact downstream flow discharge and hydropower potential. While deforestation and conversion to agriculture have been linked to increasing flow magnitude and hydropower potential, model studies of the Amazon Basin, a basin of comparable size to the Congo Basin, suggest reasons for concern of the effects of large-scale forest loss on the Congo Basin. Stickler et al (2012) wrote, “Tropical rainforest regions have large hydropower generation potential that figures prominently in many nations’ energy growth strategies. Feasibility studies of hydropower plants typically ignore the effect of future

deforestation or assume that deforestation will have a positive effect on river discharge and energy generation resulting from declines in evapotranspiration (ET) associated with forest conversion. Forest loss can also reduce river discharge, however, by inhibiting rainfall”. This could be the case in the Congo Basin. Alteration, decrease or increase, of the streamflow regime could be detrimental to existing infrastructure, including the Inga hydropower facility downstream Congo River, a hydroelectric site located 150 km upstream from the Congo River’s mouth in the western Democratic Republic of the Congo (DRC). The facility is part of the Inga hydroelectric site, the largest such installation in Africa, which has a proposed expansion to add the Grand Inga dam.

The Congo Basin thus faces conflicting interests: the development of agriculture inducing the intrusion of the rural complex within the forest domain and the conservation of the integrity of water resources by keeping the forest cover intact. These conflicting interests must be acknowledged by the public and acted upon by decision-makers in charge of Congo Basin water and forest resources, particularly in the context of regional expansion of hydropower production with the Grand Inga dam. As the considerable availability of Congo Basin surface water and its tremendous hydropower potential are yet to be exploited, information on the Congo Basin rainfall and streamflow regimes are of crucial importance. Quantitative baseline information would enable a greater understanding of the basin’s hydrology, which is necessary for the current and future management of Africa’s water resources.

To monitor rainfall and streamflow discharge over an area, timely information on precipitation dynamics and timely information on flow regime are measured and

distributed by meteorological station networks and by hydrological station networks respectively. In the Congo Basin, the hydrometeorological observation network is limited. In cases such as these where ground data are scarce, the application of remotely-sensed data for hydrological modeling is required. In data scarce environment, remote sensing of water resources combined with modeling has significantly contributed to research and operational applications such as precipitation estimation for forecasting, soil moisture for irrigation programming and estimation of inundated areas for floodplain management. It has thus advanced the quantitative understanding of hydrographic basins worldwide such as the Amazon, the Yangtze, the Nile and others and helped solve some of the most challenging water-related problems. However, the Congo Basin is one of the least studied major river basins (Alsdorf et al 2016).

#### 1.1.2. Remote Sensing of Congo Basin water resources: rainfall and streamflow current state of knowledge

The Congo Basin has been investigated as a part of continental and sub-continental studies of Africa and the Central Africa region. These previous studies provide some information for use in studies specifically of the Congo Basin.

For rainfall, meteorological stations are poorly distributed across Africa. As a result, rainfall regimes in Africa have not been sufficiently quantified due to the lack of ground information. Several researchers, such as Nicholson (2000), Dinku et al. (2007) and others, have used historical ground station information to characterize rainfall regime and seasonality at the continental scale, a challenging task in the context of a sparse and deteriorating gauge network. Alternatively, satellite rainfall estimates are being

used extensively to replace or augment ground data, thanks to their temporal continuity and full spatial coverage. Satellite-based estimates of rainfall from the joint NASA/JAXA Tropical Rainfall Measuring Mission (TRMM) are one of those data. Validation studies of TRMM precipitation data within Africa present a reasonable level of accuracy, although they also suggest an underestimation in areas with few rainfall gauges such as the Congo Basin (Huffman et al 2014; Bitew and Gebremichael 2011). Nicholson et al (2019) has evaluated 10 different satellite-derived precipitation products over the Congo Basin. They found that the gauge-calibrated products' performance was notably poorer in recent years (1998–2010), when the station network was sparse, than during the period 1983–1994, when the dense station network provided more reliable estimates of rainfall. They concluded that gauge data have a strong impact on the various satellite-derived products and that there is a need to have access to such gauge data, in order to produce reliable rainfall estimates from satellites for the Congo Basin.

For surface water, recent remote-sensing studies of the Congo Basin's hydrology include various wetland characterization products, historical streamflow modeling as well as impact assessment of future climate changes on Congo River major tributaries. Producing high-resolution models of current daily streamflow capturing flow seasonality, timing and magnitude is challenging, although it is possible as well as providing statistical evaluation of model outputs.

### 1.1.3. Hydrological modeling

Integrating remote sensing and hydrological modeling particularly for ungauged catchments has offered great opportunities for better management of water resources

but also for research, due to the need for fine-scale spatial and temporal information. This has been verified for a wide range of applications including mitigation of hydrometeorological hazards and extremes (Nikolaos et al 2019), navigation operation (Fernandez et al 2010), irrigation programming (Al-Abed et al 2002), operational implementation in major basins of Africa and Asia for Famine Early Warning Systems (Verdin et al 2005) and others.

Hydrological models may be statistical, physically based or conceptual. Statistical models are based on associations between hydrological variables using long-term records. They describe the data and the form and strength of the relationships between variables. Physically based hydrologic models are based on known scientific principles of energy and water fluxes, while conceptual models are based on conceptual estimates of storages and other model parameters that require calibration, without explicitly considering fluxes (Islam 2011). Physically based distributed hydrologic models are meant to minimize the deficiencies of the conceptual models, although they might also require calibration. Hejazi and Moglen (2008) summarized their review of physically based models findings by stating: “Continuous streamflow models may be used to better understand the hydrologic response of a watershed to changing conditions in climate and land use. Such models are driven by weather data time series such as precipitation, temperature, and soil moisture. The models can be calibrated to achieve an agreement between simulated and observed flows for some selected hydrologic input values. Once calibrated, climate and/or land use may be varied to study their effects on streamflows”.

A data-scarce system such as the Congo Basin one would benefit from modeling efforts leading to accurate representation of its hydrological processes.

### **1.2. Research goals and objectives**

This research seeks to characterize two major hydrological processes in the Congo Basin, rainfall precipitation and streamflow, as well as hydrological responses to Land Cover Land Use Change (LCLUC) using remotely-sensed data. The methods and findings resulting from the work can contribute directly to the characterization of hydrological processes in data-scarce environment, as well as to the quantification of regional and global and regional water cycles. The research tests and reports the use of limited rainfall gauge data within the Democratic Republic of Congo (DRC) to recalibrate a TRMM science product (TRMM 3B42, version 6) in characterizing precipitation and climate in the Congo Basin.

The research applies remotely-sensed data in hydrological modeling of the Congo Basin streamflow. Physically-based parameterization is augmented with a spatially-distributed calibration that enables the USGS Geospatial Streamflow Model (GeoSFM), a semi-distributed hydrologic model, to simulate hydrologic processes in the Congo Basin. A particular aspect is the slowing effect on flow of the *Cuvette Centrale*, the low lying bowl-shaped depression in the center of the basin, which gradually release water downstream through a diffuse channel. This research assesses the hydrological response to land cover and land use change (LCLUC) in the Congo Basin and to the climatic feedback induced by LCLUC. It also investigates the resulting impact of this hydrological response on Congo River hydropower potential.

The major research objectives are the following:

- 1) Re-calibrate a TRMM science product (TRMM 3B42, version 6) on a monthly scale by using rainfall gauge data from 12 gauges within the Democratic Republic of Congo (DRC) and a statistical model, in this case a regression-tree algorithm, to characterize rainfall regime and climate in the Congo Basin.
- 2) Produce a quantitative baseline of contemporary daily-flow discharge using a physically-based hydrological model driven by satellite-derived data.
- 3) Build from the physically-based modeling effort (objective 2) to simulate the impact of LCLUC scenarios on daily flow at the Congo River at Inga.

### ***1.3. Structure of the dissertation***

This dissertation consists of three research components which are detailed in Chapters 2-4. Although these chapters were originally written in a self-contained format prepared for journal submission, they have been condensed in the dissertation to avoid redundancy. Chapter 5 summarizes the findings, provides a discussion of the overall conclusions, and suggests directions for future research.

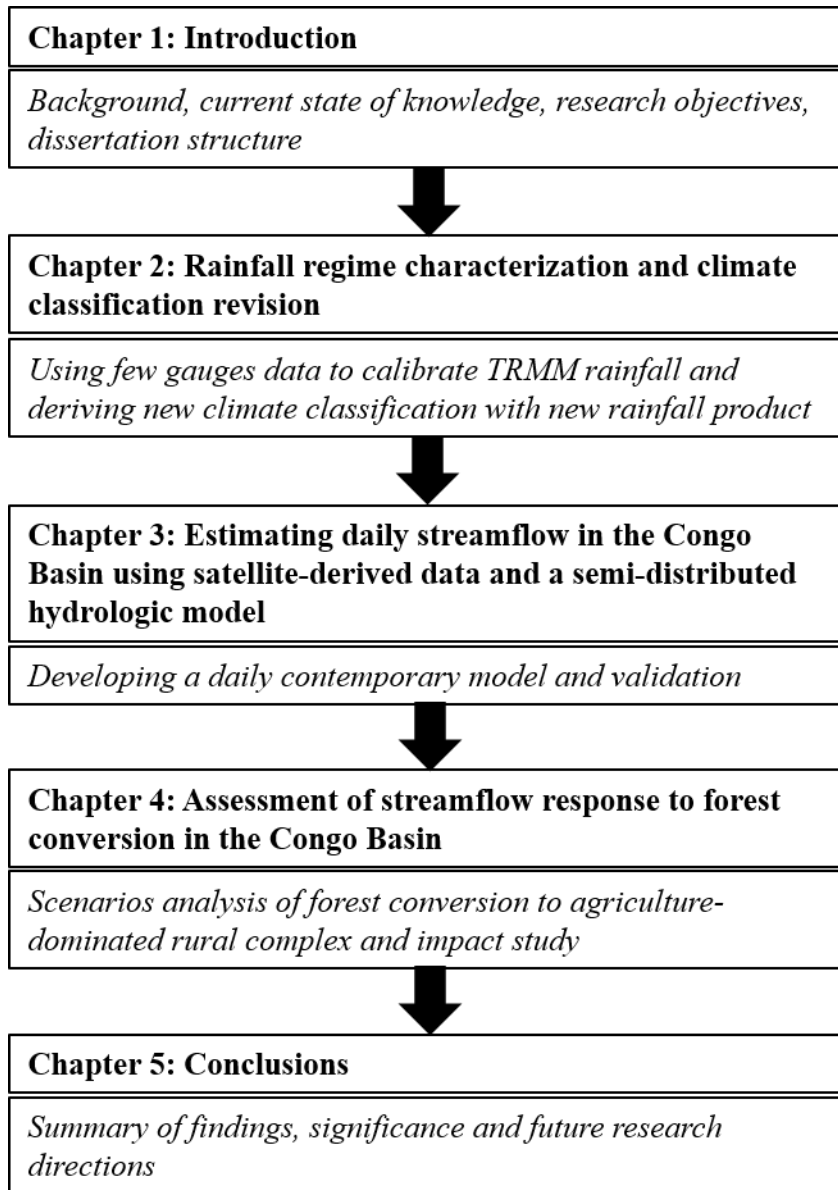


**Figure 1.1** Structure of the dissertation

## Chapter 2: Characterizing Congo Basin rainfall and climate using Tropical Rainfall Measuring Mission (TRMM) satellite data and limited rain gauge

### **2.1. Introduction**

Rainfall plays many important roles in the earth system, including being the primary source of fresh water, defining conditions for diverse ecosystems, and enabling economic activities such as agriculture. As such, rainfall information from any given hydrological system is of crucial importance. To monitor rainfall over an area, timely information on precipitation dynamics are measured and distributed by meteorological station networks. Unfortunately, many of these networks are poorly distributed across the globe in general and across Africa in particular. As a result, rainfall regimes in Africa have not been sufficiently quantified due to a lack of ground rainfall data. Few authors, such as Nicholson (2000), have used historical ground station information to characterize rainfall regimes and seasons at the continental scale. However, with station data being sparse, not covering concurrent time periods, and having incomplete time series, achieving consistency is a challenge. Speaking particularly about Africa, Dinku et al. (2007) wrote: “The number of rain gauges throughout Africa is small and unevenly distributed, and the gauge network is deteriorating. Satellite rainfall estimates are being used widely in place of gauge observations or to supplement gauge observations.” The lack of ground observations has led to the necessity of exploring

alternative solutions such as satellite rainfall estimates to replace or augment ground data.

The extensive data records of gridded, satellite-based rainfall estimates at a variety of spatial resolutions provide improved means for the continental-scale mapping of rainfall regimes (Herrmann and Mohr, 2011). This fact has motivated recent advances in rainfall characterization with satellite precipitation products. Rainfall classifications such as Dinku et al.'s (2007, 2008 and 2010) or Herrmann and Mohr's (2011) offer improved rainfall products for Africa. They have higher spatial resolutions than ground-based products and are generated from data with temporal continuity.

The Congo Basin in Central Africa is one of the river systems where ground data availability is a limiting factor to rainfall regime characterization. In such cases, satellite-based estimates of rainfall can be used to quantify rainfall patterns. Data from the joint NASA/JAXA Tropical Rainfall Measuring Mission (TRMM), operational since January 1998, are one such example. Throughout the last decade, validation studies performed using TRMM precipitation data within Africa present a reasonable level of accuracy (Adeyewa and Nakamura, 2003; Nicholson et al., 2003; Dinku et al., 2007, 2010; Roca et al. 2010). However, these studies of TRMM products also suggest a slight underestimation of monthly mean rainfall and increased uncertainties for some areas. TRMM science products such as the monthly TRMM 3B43 Version 7 dataset (Huffman and Bolvin, 2014) have been found to have limited accuracy even though they are calibrated using rain gauge data from the Global Precipitation Climatology Centre (GPCC) (Rudolf, 1993; Rudolf et al., 1994; Huffman et al., 1997; Huffman and

Bolvin, 2012), specifically Version 6 Full GPCC Data reanalysis (Huffman and Bolvin, 2014). A reason adduced for this is the sparseness of GPCC gauge locations. The Congo Basin is one such region lacking GPCC gauge locations for the period of study (from 1998 to 2007) due to their absence in the Democratic Republic of Congo (DRC), which covers 60% of the Congo Basin watershed. Because most of the GPCC gauges are concentrated in more seasonal regions adjacent to the Congo Basin, there is reason to believe that algorithms developed to calibrate TRMM science products in Africa likely favor the arid influence of these stations. As such, it is worth investigating the performance of TRMM 3B43 products over the Congo Basin.

Regarding deficiencies in current gauge-calibrated analyses of Africa, Huffman et al. (2014) reported that it will continue to be the case that some underdeveloped areas, such as Central Africa, will have greater uncertainty due to a lack of gauge inputs (Huffman and al., 2014). Bitew and Gebremichael (2011) demonstrated that gauge-calibrated products likely have low accuracy for regions lacking rain gauge data. After comparing integrated satellite-gauge rainfall products to satellite-only products for the Nile Basin, they suggested that users forego the conventional notion that satellite rainfall products that incorporate GPCC rain gauge data have higher accuracies than satellite-only products (Bitew and Gebremichael, 2011). The mentioned limitation has also been attributed to the deficiency in gauge observations. A limited number of gauges in sparse regions have been reported to be unsuitable for Huffman et al's (1997) merging analysis for TRMM science products. Given these findings, alternative methods for gauge-sparse regions are warranted.

The purpose of this chapter is to test a calibration that uses limited/sparse in situ gauge data for Congo Basin precipitation characterization. A generic feature space, or set of independent variables, is used to extrapolate the limited gauge data to the Basin-scale using TRMM 3B42 Version 6 inputs and a regression tree algorithm.

We re-calibrate TRMM 3B42 Version 6 satellite-derived rainfall data for the Congo Basin using concurrent ground data from rain gauges located in the DRC. The 3B42 daily rainfall data are derived from 3-hourly observations as part of the TRMM Multi-satellite Precipitation Analysis. These data consist of merged microwave, infrared and spaceborne radar inputs and incorporate gauge data where feasible from the Global Precipitation Climatology Centre (GPCC) and from the Climate Assessment and Monitoring System (CAMS) (more details on the gauge analysis in Huffman et al. 2007). In the absence of Basin-wide rainfall data concurrent to TRMM 3B42 Version 6 to evaluate the output, we compare the re-calibrated TRMM rainfall data with WORLDCLIM isohyets derived from longer-term historical records (Hijmans et al., 2005). We also include a comparison of our modeled monthly precipitation estimates and WORLDCLIM data with the latest TRMM gauge-calibrated standard monthly product, the Version 7 TRMM 3B43 data set.

In a region where the climate is principally driven by precipitation, accurate rainfall data are required to characterize regional climates. We therefore propose a classification of the Congo Basin climate using our re-calibrated TRMM data and temperature grids and compare it with climates derived using the TRMM 3B43 Version 7 and the TRMM 3B42 Version 6 data. Finally, we discuss seasonal rainfall patterns across the Basin and relate monthly rainfall estimates to stream gauge data. Our goal

is to assess standard and regionally-calibrated TRMM products for future Basin-scale hydrological modeling of the Congo Basin that will employ the improved rainfall data in characterizing Basin streamflows. A climate classification will be used as the basis for grouping rivers and streams by climate type within the Congo Basin in order to facilitate comparisons of runoff characteristics.

## **2.2. Data**

### 2.2.1. Precipitation Data

#### *2.1.1.1 TRMM Precipitation Data and data limitations for the Congo Basin precipitation system*

We wanted to select the most accurate and most uniformly processed TRMM precipitation products for the time frame coincident with available recent in situ gauge data (1998-2007). When comparing Versions 6 and 7 TRMM Multi-satellite Precipitation Analysis (TMPA) precipitation products, TRMM data producers Huffman and Bolvin (2014) reported that products series for Version 7 were retrospectively processed back to 2000 and not before. More relevant to our purpose is the need to maximize the record's length coincident with available gauge data for the DRC. Version 6 of the TRMM science product 3B42 (Huffman, 2013) was consistently produced from 1998 to 2007. We consider the extra years valuable for model calibration and chose to employ the Version 6 of TRMM 3B42 product as our model inputs. These inputs are employed to estimate precipitation at a 3-hour temporal resolution and a 0.25° by 0.25° spatial resolution in a global belt extending from 50°S

to 50°N latitude. Daily accumulations of the data are processed and hosted at USGS EROS. The 0.25° TRMM 3B42 Version 6 product has complete spatial coverage for Africa. The daily grids from 1998 to 2007 were summed to a monthly interval. These monthly aggregate 3B42 data (hereafter “TRMM 3B42”) are used as inputs for re-calibration by monthly local gauge data and are made comparable to the TRMM 3B43 monthly product. For the purposes of comparison, we chose to use the most recent version of the GPCP gauge-calibrated TRMM 3B43 standard science product (Version 7).

Limitations of TRMM real-time products and science products have been documented in detail and include underestimation of convective and stratiform rain regimes. Huffman et al. (2007) quantified gaps in 3-hour combined microwave precipitation estimates that can omit convective precipitation events in TRMM 3B42 Version 6 product. There is also a lack of sensitivity to light precipitation that results in regionally dependent underestimation of rainfall in the TRMM 3B42 archive (Huffman and Bolvin, 2012). Comparing TRMM Real Time estimates from heavy, convective warm-season regimes and light, stratiform, cool-season regimes, Ebert et al. (2007) found convective rain better quantified by TRMM Real Time data.

These TRMM product limitations have a direct impact on rainfall regime estimation in the Congo Basin. Due to the Congo Basin’s location straddling the equator, convective and convergence systems are predominant. They are controlled by the northward and southward movement of the Intertropical Convergence Zone and by the eastward and westward movement of the Congo Air Boundary (Tierney et al., 2011). Convective systems are fast moving, of small extent and short duration and are characterized by

thunderstorms and squall lines. Stratiform or frontal rainfall generated by convergence systems is usually slow moving, of large extent and low intensity. For the entire tropics however, Houze (1997) has suggested that even though most precipitation in the tropics appears to be convective, the tropics show large radar echoes composed of convective rain alongside stratiform precipitation, with the stratiform echoes covering large areas and accounting for a large portion of tropical rainfall. However, even if a significant portion of tropical rainfall is stratiform, Schumacher and Houze (2003) cited Central Africa as one of the areas where convective rain amounts are high and stratiform rain fractions low (20%-30%).

#### *2.1.1.2 Ground Precipitation Data*

For this chapter, data on precipitation regime were obtained from 12 meteorological stations within the Democratic Republic of the Congo (DRC) and managed by the DRC meteorological agency, Agence Nationale de Météorologie et de Télédétection par Satellite (*METTELSAT*). The ground precipitation data reported in this nationally-held dataset are concurrent with TRMM observations. The limited number of operational stations represents a sparse and unevenly distributed rainfall gauge network within the DRC. Concerns of non-representativeness of the stations sample can be legitimately raised. However, it has been demonstrated that the general spatio-temporal variation of rainfall over Africa can be described using time series from a few selected regions (Nicholson, 2000). While such an approach has limitations over large areas, it is posited here that the different rainfall regimes of the Congo Basin can be described with the available ground measurements. In addition, the proposed method generalizes

the relationship between the ground data and TRMM 3B42 inputs using a geographic and time-insensitive feature space (see Methods). Figure 2.1 shows the extent of the Congo Basin and the locations of available time-series precipitation data from ground gauge measurements vs. GPCC gridded precipitation gauge stations locations for year 2005.

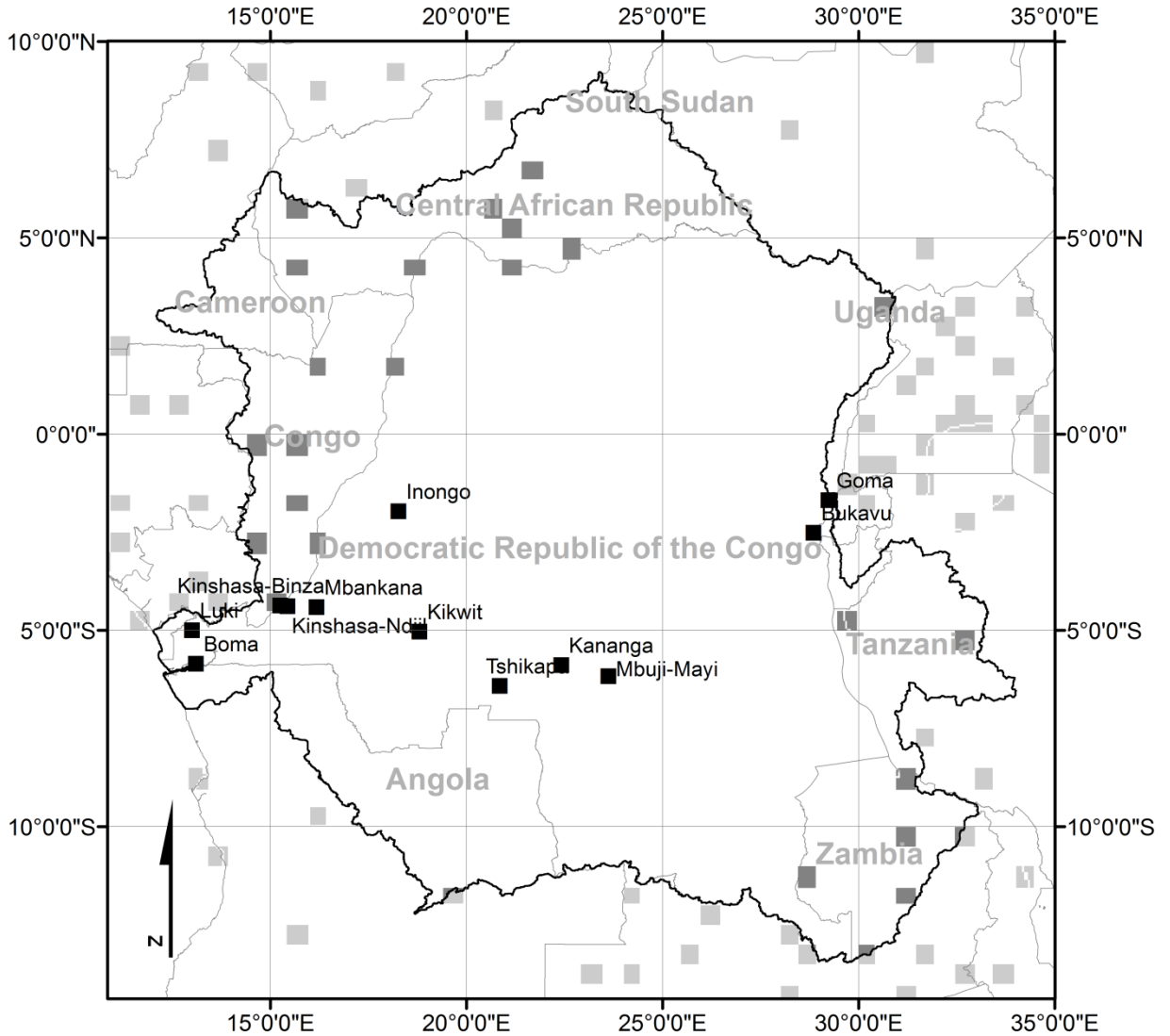


**Figure 2.1** The Congo Basin with GPCC gridded precipitation gauge stations locations (dark gray squares for the ones in the Basin and light gray squares for those outside the Basin) for year 2005 available via the Visualizer from <http://kunden.dwd.de/GPCC/Visualizer>. In black squares, the 12 precipitation gauge stations locations used in this chapter.

### *2.1.1.3 WORLDCLIM Climatological Precipitation Data*

The independent validation dataset used for this chapter is the WORLDCLIM precipitation model of Hijmans et al. (2005). WORLDCLIM data are used to validate the monthly mean re-calibrated TRMM product averaged over the 10 years of study (1998-2007). WORLDCLIM interpolated grids have been developed for global land areas at a spatial resolution of 30 arcs second (1 km). In Hijmans study, WORLDCLIM monthly mean rainfall were averaged over 10 years for the Congo Basin with most of the records preceding 1960 for the Democratic Republic of the Congo. Hijmans et al. (2005) aggregated WORLDCLIM monthly mean precipitation data from historical records collected during the colonial period in the Congo Basin, meaning WORLDCLIM monthly mean data are not concurrent to the timeframe of the present chapter (1998 - 2007). However, despite the difference between the time periods of the datasets, the Basin-wide coverage of WORLDCLIM affords a valuable basis for intercomparison, assuming no significant recent climate change within the region.

In the absence of ground information concurrent to TRMM, long-term averaged observed rainfall data have been used extensively to perform climatological validation of TRMM products (in West-Africa by Nicholson et al., 2003; in Cyprus by Gabella et al., 2006, 2008 and many others). In addition, a long-term record of 45 years (1960-2005) available for one station of the Congo Basin at Kinshasa (Figure 2.2) shows a relatively steady, even slightly upward trend of the annual rainfall over these years. A more recent study (Zhou et al, 2014), quantified a more recent decline in Basin-wide precipitation for selected months. Our decadal-scale approach should be less sensitive

to such variations. However, reservations could be raised concerning the comparison of dated WORLDCLIM and more recent TRMM precipitation estimates.

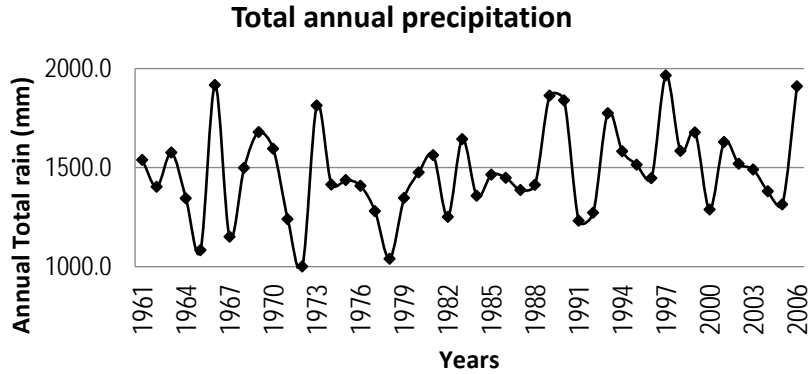


**Figure 2.2** Annual Total Precipitation (mm) at Kinshasa/N'djili Station (1961 - 2006).

### 2.2.2. Temperature data

WORLDCLIM mean temperature grids are used in combination with TRMM 3B42 and re-calibrated TRMM as well as TRMM 3B43 data to map new climate classifications for the Congo Basin with respect to rules from the Köppen–Geiger climate classification system (Köppen, 1918, see also 1884 republished in 2011; Kottek et al., 2006; Peel et al., 2007). The climate in the Congo Basin is principally driven by the rainfall with slight influences of temperature. There are no thermal seasons with the temperature representing a uniform picture and low annual range. Only the high altitudes of the eastern and southern fringes of the Basin have a maximum of 4° annual temperature range.

### 2.2.3. Climate data

Updated Köppen-Geiger Climate data (Peel et al., 2007) were used for spatial comparison with TRMM-derived climate classification products in the Congo Basin.

The updated Köppen-Geiger (K-G) dataset has a spatial resolution of 0.1 degree lat/long. The climate system characterized by Peel et al. (2007) is based on global annual and monthly averages of interpolated temperature and precipitation data. Climate variables (temperature and precipitation) used in the K-G system were calculated at each station and interpolated between stations using a two-dimensional (latitude and longitude) thin-plate spline onto a  $0.1^{\circ} \times 0.1^{\circ}$  grid for each continent (more details on the analysis in Peel et al. 2007).

### **2.3. Methods**

#### 2.3.1. Rainfall estimation

A regression tree algorithm was used to relate TRMM 3B42 data to gauge data. Regression trees are distribution-free models that reduce the overall sum of squares for a continuous dependent variable, in this case precipitation, by recursively partitioning the data set into less varying subsets, referred to as nodes (Breiman et al, 1984). For ease and speed of implementation, we employed a bagging methodology to avoid overfitting of the model (Breiman 1996). The first step consisted of preparing 25 samples, each consisting of 10% of the population of 10 years (1998-2007) of monthly rainfall observed at the 12 gauges. The sampled data sets were used to build 25 regression trees and the median of the 25 model results was taken as the final estimate. The tree models predicted the sampled population of monthly rainfall data observed at the 12 gauges using 9 independent variables (statistics) generated from daily TRMM 3B42 observations. The variables included TRMM 3B42 monthly total, TRMM 3B42 monthly average, minimum, 10<sup>th</sup> percentile, 25<sup>th</sup> percentile, 50<sup>th</sup> percentile, 75<sup>th</sup>

percentile, 90<sup>th</sup> percentile and maximum rainfall. All input variables were created without regard to specific month or specific region, enabling the creation of a generic feature space for Basin-wide extrapolation. After model application, each grid cell over the Congo Basin was assigned a series of re-calibrated monthly precipitation values from 1998-2007. These 10 years of re-calibrated TRMM monthly total were then averaged to generate rainfall climatology or monthly rainfall records.

### 2.3.2. Climatological validation of re-calibrated TRMM data

WORLDCLIM climatological historical isohyet ranges (Hijmans et al., 2005) were compared with re-calibrated monthly and annual precipitation data to validate model outputs. The long-term isohyet data were derived from a rich, if dated, historical record. The standard error of the predicted value (STEYX) for each x in the regression, the mean bias error (MBE), the root mean square error (RMSE) and coefficients of determination ( $r^2$ ) were used to measure the correspondence of the TRMM 3B42, TRMM 3B43 and re-calibrated TRMM data to the historical precipitation record. The comparison was made for the 30072 grid cells constituting the Congo Basin. In addition, biases which express systematic differences were calculated for every month. The expression for the STEYX used for evaluation is given below:

$$STEYX = \sqrt{\frac{1}{(N-2)} \left[ \Sigma(y - \bar{y})^2 - \frac{[\Sigma(x - \bar{x})(y - \bar{y})]^2}{\Sigma(x - \bar{x})^2} \right]}$$

Where: x = WORLDCLIM rainfall values, y = satellite rainfall predicted-value,  $\bar{x}$  and  $\bar{y}$  = their corresponding means, and N = number of data pairs.

Mean bias error and root mean square error were calculated as follows:

$$MBE = \frac{[\Sigma(S - G)]}{N}$$

$$RMSE = \sqrt{\frac{[\Sigma(S - G)^2]}{N}}$$

Where: G=gauge rainfall measurement, S=satellite rainfall estimate and N=number of data pairs. MBE and RMSE are measured in millimeters.

The expression for the bias statistic used for evaluation is given below:

$$Bias = \frac{\Sigma C}{\Sigma I}$$

Where: *I*=interpolated rainfall grid and *C*=satellite rainfall estimate. Bias is dimensionless.

Note that pre-calibration, the coefficient of determination ( $r^2$ ), the mean bias error (MBE) and the root mean square error (RMSE) were also used to evaluate the performance of TRMM 3B42 satellite products in estimating the amount of the rainfall based on comparison at gauges with observed data concurrent to TRMM 3B42.

### 2.3.3. Rainfall and temperature-based climate characterization

From the precipitation products and the WORLDCLIM temperature products, spatially explicit climate maps for the Congo Basin were created following the Köppen climate classification rules shown in Table 2.1 (Köppen, 1918, 2011; Kotttek et al., 2006; Peel et al., 2007). Precipitation products were averaged to mean monthly rainfall over the period of observation (10 years for TRMM 3B42, TRMM 3B43 and re-calibrated TRMM precipitation data). A similar averaging procedure was performed by Hijmans et al. (2005) for the WORLDCLIM temperature grids.

A climate system characterized by Peel et al. (2007) based on the annual and monthly averages of interpolated temperature and precipitation data was compared to the new climate classifications, where the interpolated precipitation data were replaced by TRMM 3B42, TRMM 3B43 and re-calibrated TRMM-derived precipitation. These three maps were compared to the map of Peel et al. (2007) to quantify climate type extent and overall agreement. Quantitative agreement was assessed by comparing the reference dataset (Peel's map) with the re-calibrated TRMM-derived classified images. A confusion matrix, a common image classification accuracy assessment technique including overall, producer's and user's accuracy was employed. In the absence of a regional classification for the Congo Basin, the Peel et al. (2007) K-G climate classification is used in this chapter as the default reference.

**Table 2.1** Key Description of Köppen climate symbols and defining criteria - Adapted from Kottek et al. (2006) and Peel et al. (2007) for the Central African region.

Type 1 <sup>st</sup> 2 <sup>nd</sup> d	Description	Criterion
<b>A</b>	<b>Equatorial Climates</b>	<b>T<sub>min</sub> ≥ +18 °C</b>
Af	Equatorial rainforest, fully humid	P <sub>min</sub> ≥ 60 mm
Am	Equatorial monsoon	Not (Af) and P <sub>ann</sub> ≥ 25(100-P <sub>min</sub> )
Aw	Equatorial savannah with dry winter	Not (Af) and P <sub>min</sub> < 60 mm in winter
<b>B</b>	<b>Arid climates</b>	<b>P<sub>ann</sub> &lt; 10 P<sub>th</sub></b>
BS	Steppe climate	P <sub>ann</sub> > 5 P <sub>th</sub>
BW	Desert climate	P <sub>ann</sub> ≤ 5 P <sub>th</sub>
	h	Hot steppe / desert T <sub>ann</sub> ≥ +18 °C
	k	Cold steppe /desert T <sub>ann</sub> < +18 °C
<b>C</b>	<b>Warm temperate climates</b>	<b>-3 °C &lt; T<sub>min</sub> &lt; +18 °C</b>
Cs	Warm temperate climates with dry summer	P <sub>smin</sub> < P <sub>wmin</sub> , P <sub>wmax</sub> > 3 P <sub>smin</sub> , P <sub>smin</sub> < 40
Cw	Warm temperate climates with dry winter	P <sub>wmin</sub> < P <sub>smin</sub> and P <sub>smax</sub> > 10 P <sub>wmin</sub>
Cf	Warm temperate climates, fully humid	neither Cs nor Cw
	a	Hot summer T <sub>max</sub> ≥ +22 °C
	b	Warm summer not (a) and at least 4 T <sub>mon</sub> ≥ +10 °C
	c	Cold Summer not (b) and T <sub>min</sub> > -38 °C
<b>H</b>	<b>Highland climate</b>	<b>T<sub>max</sub> &lt; +10 °C</b>

The annual mean near-surface (2 m) temperature is denoted by  $T_{ann}$  and the monthly mean temperatures of the warmest and coldest months by  $T_{max}$  and  $T_{min}$ , respectively.  $P_{ann}$  is the accumulated annual precipitation and  $P_{min}$  is the precipitation of the driest month. Additionally  $P_{smin}$ ,  $P_{smax}$ ,  $P_{wmin}$  and  $P_{wmax}$  are defined as the lowest and highest monthly precipitation values for the summer and winter half-years on the hemisphere considered. All temperatures are given in °C, monthly precipitations in mm/month and  $P_{ann}$  in mm/year. In addition to these temperature and precipitation values, a dryness threshold  $P_{th}$  in mm is introduced for the arid climates (B), which depends on  $\{T_{ann}\}$ , the absolute measure of the annual mean temperature in °C, and on the annual cycle of precipitation.  $P_{th}$  varies according to the following rules (if 70% of  $P_{ann}$  occurs in winter then  $P_{th} = 2 \times T_{ann}$ , if 70% of  $P_{ann}$  occurs in summer then  $P_{th} = 2 \times T_{ann} + 28$ , otherwise  $P_{th} = 2 \times T_{ann} + 14$ ). Summer (winter) is defined as the warmer (cooler) six month period of ONDJFM and AMJJAS.  $T_{mon}$  denotes the mean monthly temperature in °C. A third letter (2<sup>nd</sup> column) is included to indicate temperature.

## **2.4. Results**

### 2.4.1. Comparison of ground rain gauge and TRMM 3B42 data

TRMM precipitation data from the Version 6 3B42 product used in this chapter were compared to within-region rain gauge data. Monthly precipitation data for four gauges from the 12 total used for calibration are shown plotted against concurrent TRMM 3B42 data (Figure 2.3). The graphs illustrate the strong seasonal rainfall patterns within the Congo Basin. During the rainy season months, an increase in rainfall can be observed, with a corresponding minimum rainfall during the dry season months. The plots of Figure 2.3 also show in most cases a tendency towards underestimation of monthly rainfall, most noticeably during the rainy season. The underestimation varies from station to station with mean bias error (MBE) having mostly negative values ranging from -57 to -3 mm. The relatively poor performance exhibited by the product varies from station to station, with low coefficients of determination  $r^2$  of the monthly rainfall ranging from 0.15 to 0.70 and by relatively high root mean square errors (RMSE) ranging from 56 to 112 mm.

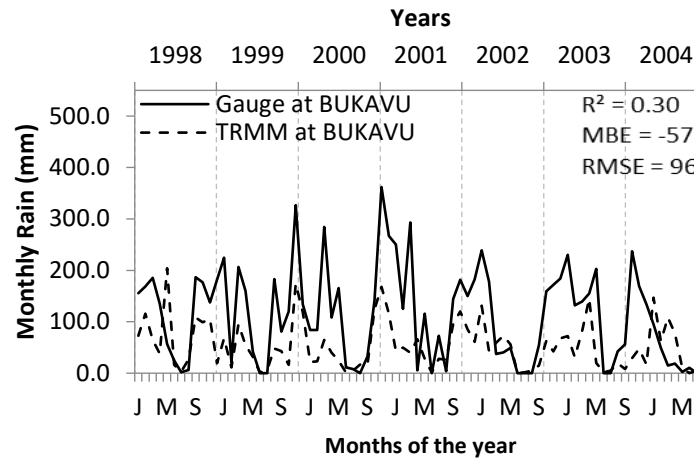
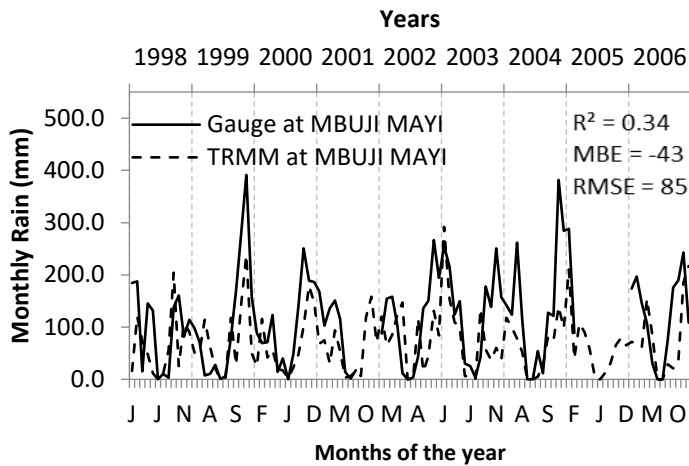
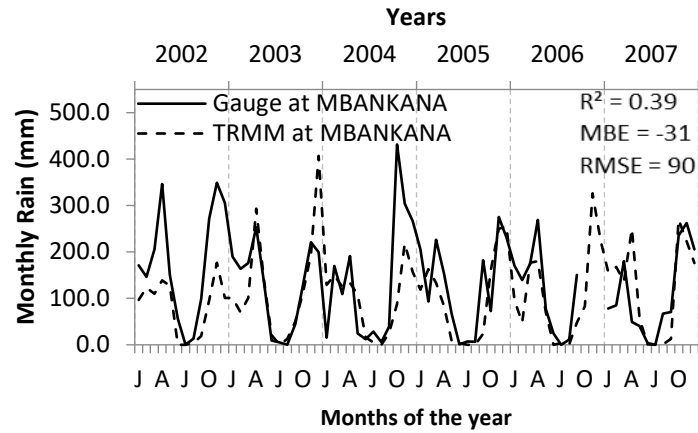
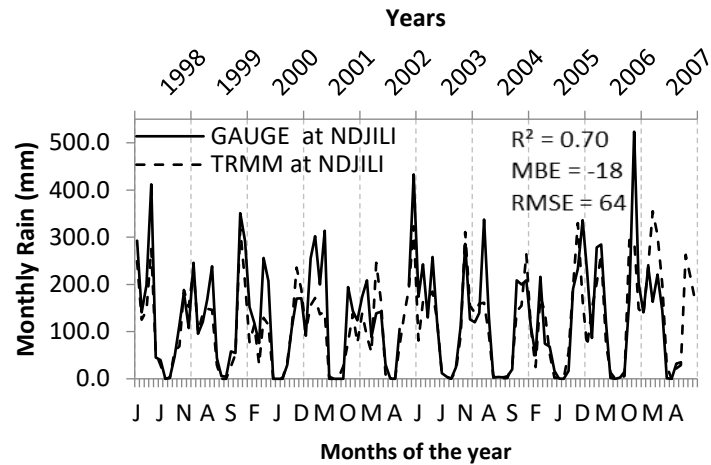


**Figure 2.3** TRMM 3B42 Version 6 monthly rainfall accumulation (mm) of 10 years (1998 - 2007) compared with concurrent observed in situ data from gauges. MBE and RMSE are in mm.

#### 2.4.2. TRMM re-calibration

The differences in monthly precipitation totals for the 3B42, 3B43 science product and re-calibrated TRMM data for the entire Basin are shown in Figure 2.4. When compared to WORLDCLIM climatological data, TRMM 3B42 data underestimates rainfall totals by 12% Basin-wide. The 3B43 and re-calibrated rainfall estimates add 13% and 15% more precipitation to the total annual rainfall, respectively, compared with TRMM 3B42 estimates. Figure 2.5 shows the fractional augmentation of precipitation by month of the 3B43 product and the re-calibration of this chapter. All months gain precipitation with dry season months (i.e. November to March in the Northern hemisphere and May to September in the Southern hemisphere) receiving proportionally greater augmentations. The largest proportional disagreement can be seen in the southern hemisphere dry season, where the 3B43 product adds less rainfall proportionally than the re-calibration of this chapter. Results of these data sets are compared with TRMM 3B42 and WORLDCLIM data in Figure 2.6. In all products, the seasonal rainfall regime is evident. The position of the basin across the Equator subjects the Congo Basin to an alternating seasonal pattern between the southern and northern hemispheres. The passage of the Intertropical Convergence Zone (ITCZ) results in two local rainy and dry seasons of varying length and intensity.

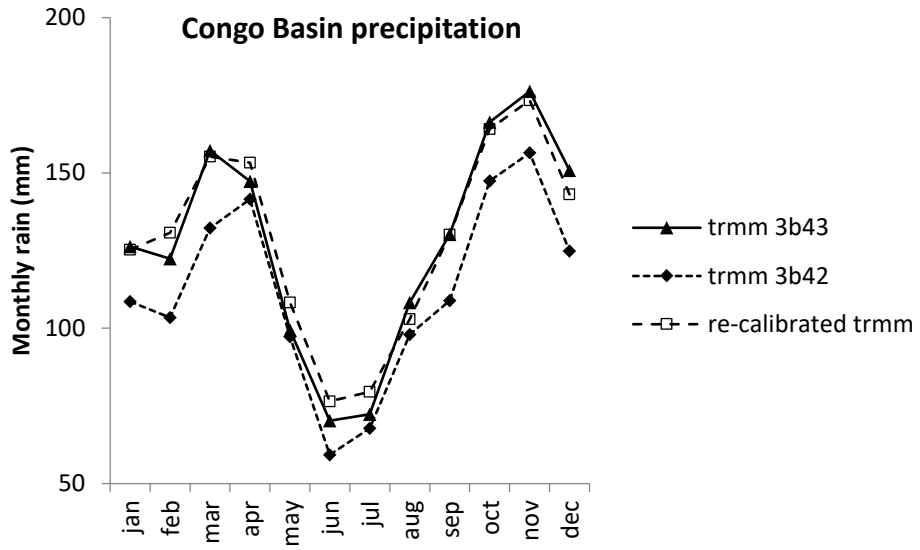


**Figure 2.4** Rainfall regime monthly averages for the Congo Basin.

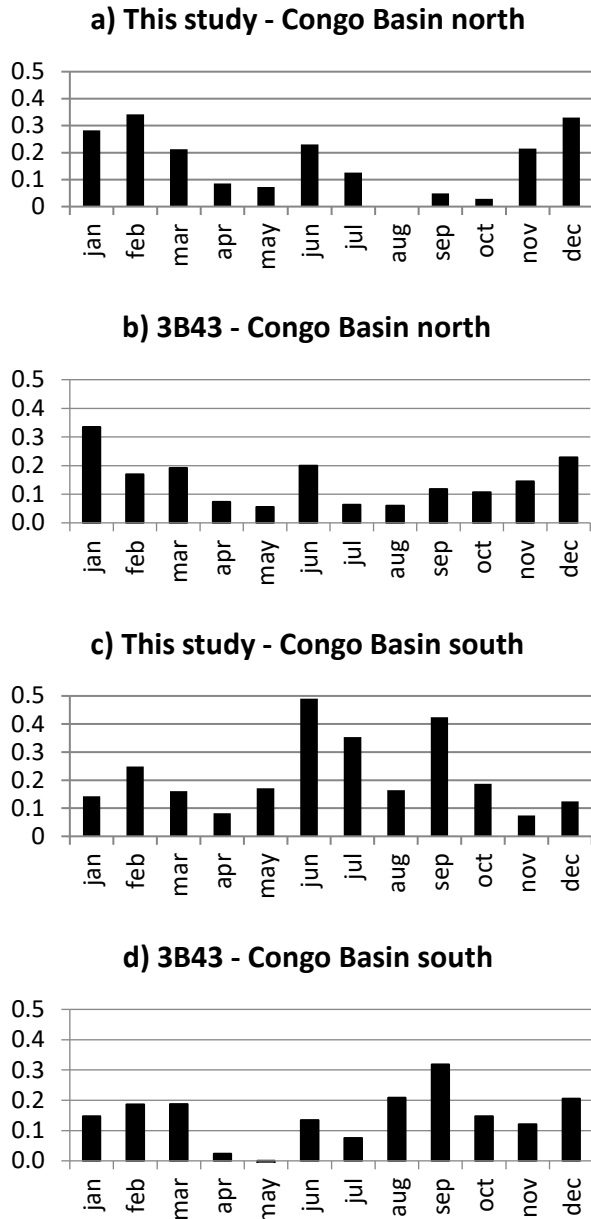


**Figure 2.5** Monthly fractional augmentation of TRMM 3B42 Version 6, average per grid cell for a) re-calibrated TRMM with DRC gauge data for the Congo Basin north of the equator and b) TRMM 3B43 Version 7 data for the Congo Basin north of the equator, c) re-calibrated TRMM with DRC gauge data for the Congo Basin south of the equator and d) TRMM 3B43 Version 7 data for the Congo Basin south of the equator.

#### 2.4.3. Validation

The WORLDCLIM precipitation data of Hijmans et al. (2005) are used as the basis of comparison for validating the re-calibrated TRMM data. The re-calibrated TRMM data

result in uniformly decreasing standard errors of the estimate and root mean square errors and corresponding increasing  $r^2$  values (Table 2.2). Significance tests revealed that all reported correlations are highly significant with  $p < 0.01$  for 30072 observations. The general improvements validate the regression tree model in the re-calibration of TRMM data. In addition, with values closer to 1, bias measures show improvements made for every month but July and August which correspond to the months with lowest rainfall totals for the entire Congo Basin (Table 2.2 and 2.6).

The same comparison was done for the 3B43 and WORLDCLIM precipitation data. Results in Table 2.2 demonstrate that STEYX of this product is generally greater than the re-calibrated TRMM one, and even greater than the TRMM 3B42 in some cases. Re-calibrated TRMM's  $r^2$  and TRMM 3B43  $r^2$  are generally similar except in some cases where the re-calibrated TRMM have a stronger correlation to WORLDCLIM precipitation data. Both TRMM 3B43 and re-calibrated TRMM have similar biases with values mostly close to 1, with the 3B43 showing less bias for a majority of the monthly values. MBE values are also generally better using the 3B43 data compared to the re-calibrated model of this chapter. Overall, the re-calibrated TRMM and TRMM 3B43 are comparable, indicating that the 3B43 extrapolation from the edges of the Basin to its interior in the DRC was successfully performed. As well, the sparse data-driven model from limited DRC gauge data performed well in Basin-wide extrapolation.

**Table 2.2** Basin wide standard errors of the estimate (STEYX), coefficients of determination and bias, mean bias error (MBE) in mm and root mean square error (RMSE) in mm for TRMM 3B42 (o), re-calibrated TRMM (r) and TRMM 3B43 (3b), in comparison to WORLDCLIM monthly precipitation totals. Best performing products per statistical measure are shown in bold.

	STEYX -(o)	STEYX -(r)	STEYX -(3b)	$r^2$ -(o)	$r^2$ -(r)	$r^2$ -(3b)	<i>bias</i> - (o)	<i>bias</i> - (r)	<i>bias</i> - (3b)	MBE- (o)	MBE- (r)	MBE- (3b)	RMSE -(o)	RMSE -(r)	RMSE -(3b)
JAN	28	<b>25</b>	30	0.85	<b>0.89</b>	0.88	0.86	0.99	<b>1.00</b>	-18.06	-1.30	<b>-0.31</b>	33.86	<b>24.87</b>	30.25
FEB	27	<b>24</b>	25	0.73	<b>0.84</b>	<b>0.84</b>	0.83	1.05	<b>0.99</b>	-20.57	6.70	<b>-1.61</b>	36.57	24.69	<b>24.67</b>
MAR	27	<b>22</b>	29	0.63	<b>0.74</b>	0.72	0.79	0.93	<b>0.94</b>	-35.08	-12.13	<b>-10.15</b>	45.75	<b>26.85</b>	30.83
APR	30	<b>21</b>	29	0.63	<b>0.71</b>	0.66	0.90	<b>0.98</b>	0.94	-15.11	<b>-3.31</b>	-9.29	34.18	<b>24.12</b>	30.83
MAY	24	<b>20</b>	28	0.86	<b>0.91</b>	0.84	0.91	<b>1.01</b>	0.93	-9.82	<b>1.26</b>	-7.60	27.25	<b>20.72</b>	28.90
JUN	<b>18</b>	<b>18</b>	<b>18</b>	0.91	0.93	<b>0.94</b>	0.85	1.10	<b>1.01</b>	-10.19	7.03	<b>0.78</b>	25.94	19.71	<b>17.84</b>
JUL	24	<b>20</b>	<b>20</b>	0.89	<b>0.93</b>	0.93	0.97	1.14	<b>1.03</b>	<b>-2.04</b>	9.68	2.44	25.57	22.57	<b>20.91</b>
AUG	31	<b>22</b>	27	0.87	<b>0.92</b>	0.91	<b>1.04</b>	1.09	1.15	<b>3.76</b>	8.72	14.07	31.93	<b>25.28</b>	30.52
SEP	25	<b>19</b>	25	0.89	<b>0.93</b>	0.91	0.85	<b>1.02</b>	<b>1.02</b>	-18.73	<b>2.52</b>	2.60	32.59	<b>23.21</b>	25.02
OCT	28	<b>20</b>	28	0.84	<b>0.87</b>	0.85	0.90	<b>0.99</b>	<b>1.01</b>	-17.07	<b>-0.44</b>	1.85	33.32	<b>26.77</b>	28.18
NOV	32	<b>22</b>	33	0.74	<b>0.81</b>	0.74	0.92	<b>1.02</b>	1.04	-12.89	<b>4.08</b>	6.93	34.86	<b>25.86</b>	34.05
DEC	34	<b>26</b>	29	0.79	<b>0.89</b>	0.89	0.83	0.96	<b>1.00</b>	-24.79	-6.51	<b>1.20</b>	44.01	<b>27.45</b>	29.86
ANNUAL	188	<b>143</b>	199	0.58	<b>0.70</b>	0.54	0.88	1.01	<b>1.00</b>	-177.78	20.75	<b>5.34</b>	268.30	<b>162.37</b>	212.07

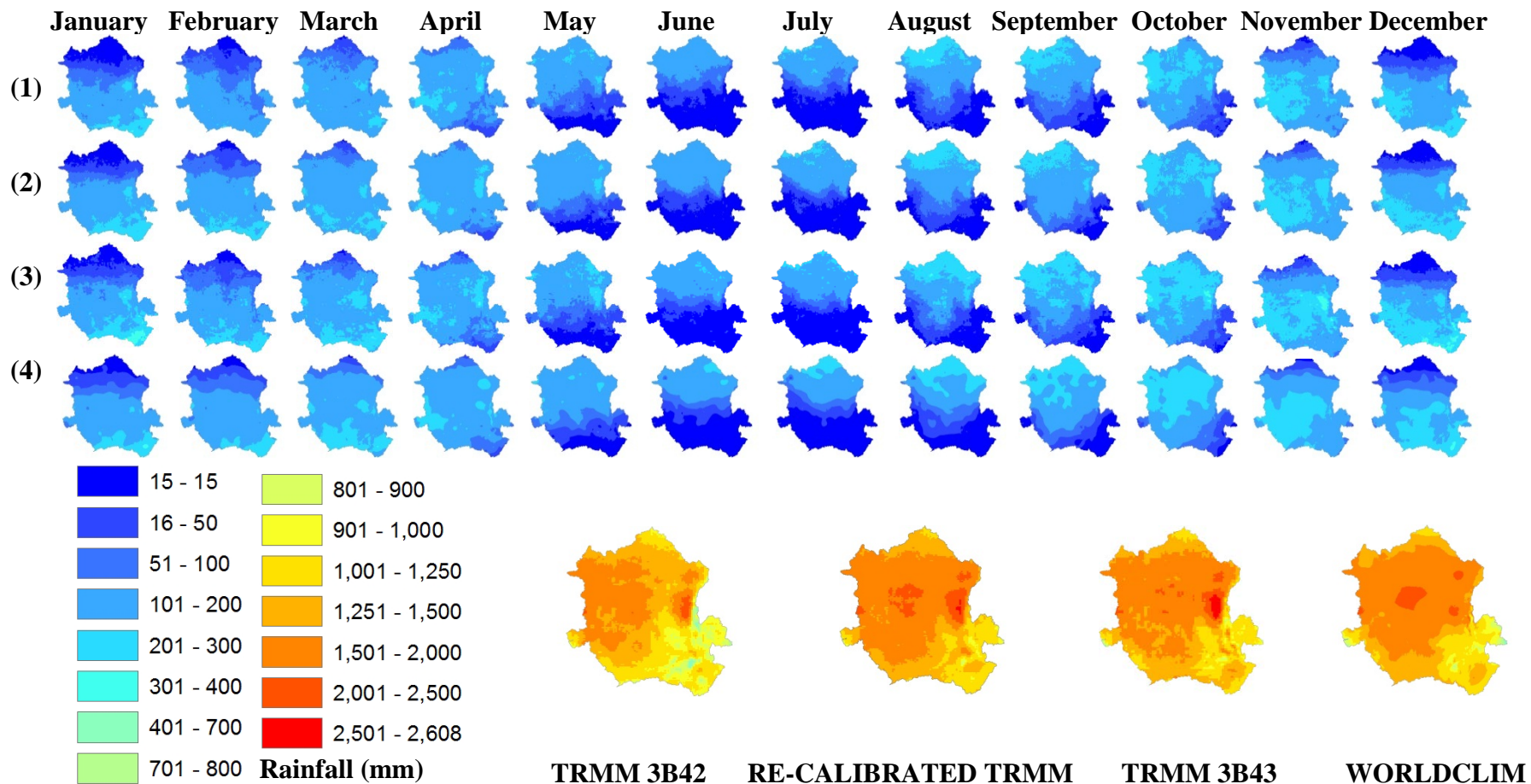


**Figure 2.6** Mean precipitation for the 12 months of the year and annually; monthly mean of TRMM 3B42 Version 6 (1), monthly mean of re-calibrated TRMM (2) and monthly mean of TRMM 3B43 Version 7 (3) are compared against monthly mean of WORLDCLIM precipitation data (4). The 10 year time series of TRMM 3B42 Version 6, re-calibrated TRMM and TRMM 3B43 Version 7 monthly data were averaged to depict the Basin-scale rainfall regime. The position of the basin across the Equator subjects the Congo Basin to an alternate seasonal pattern between the southern and northern hemispheres.

#### 2.4.4. Climate characterization

Using TRMM 3B43, TRMM 3B42 and re-calibrated TRMM precipitation data and WORLDCLIM temperature data grids (Hijmans et al., 2005), digital climate classification maps for the Congo Basin were generated, valid for the 10 years of TRMM presently studied (1998-2007). With the three TRMM data sets, we quantified a Köppen-Geiger map of 7 climate types at a resolution of 0.1 degree lat/long. The map and climate type area totals are shown in Figure 2.7 and Table 2.3, respectively. The most common climate type by land area is Aw (Tropical savannah) followed by Af (Tropical Rain forest), Am (Tropical Monsoon), Cwa (Humid Subtropical), Cwb (Temperate), H (Highland) and Bsh (Hot semi-arid). For all products, the tropical rainforest climate borders the equator and is surrounded by the tropical monsoon climate which in turn is surrounded by the tropical savanna climate. The temperate-defined climates are mostly located in the east and south-east highland areas. When using the TRMM 3B42 data to derive a climate classification, a zone of hot semi-arid climate (Bsh) in the east and south-east of the Basin is erroneously depicted. In addition, the TRMM 3B42 data depict a much narrower band of tropical rain forest and monsoon climate domains. This is indicative of the lower monthly and seasonal rainfall totals of the TRMM 3B42.

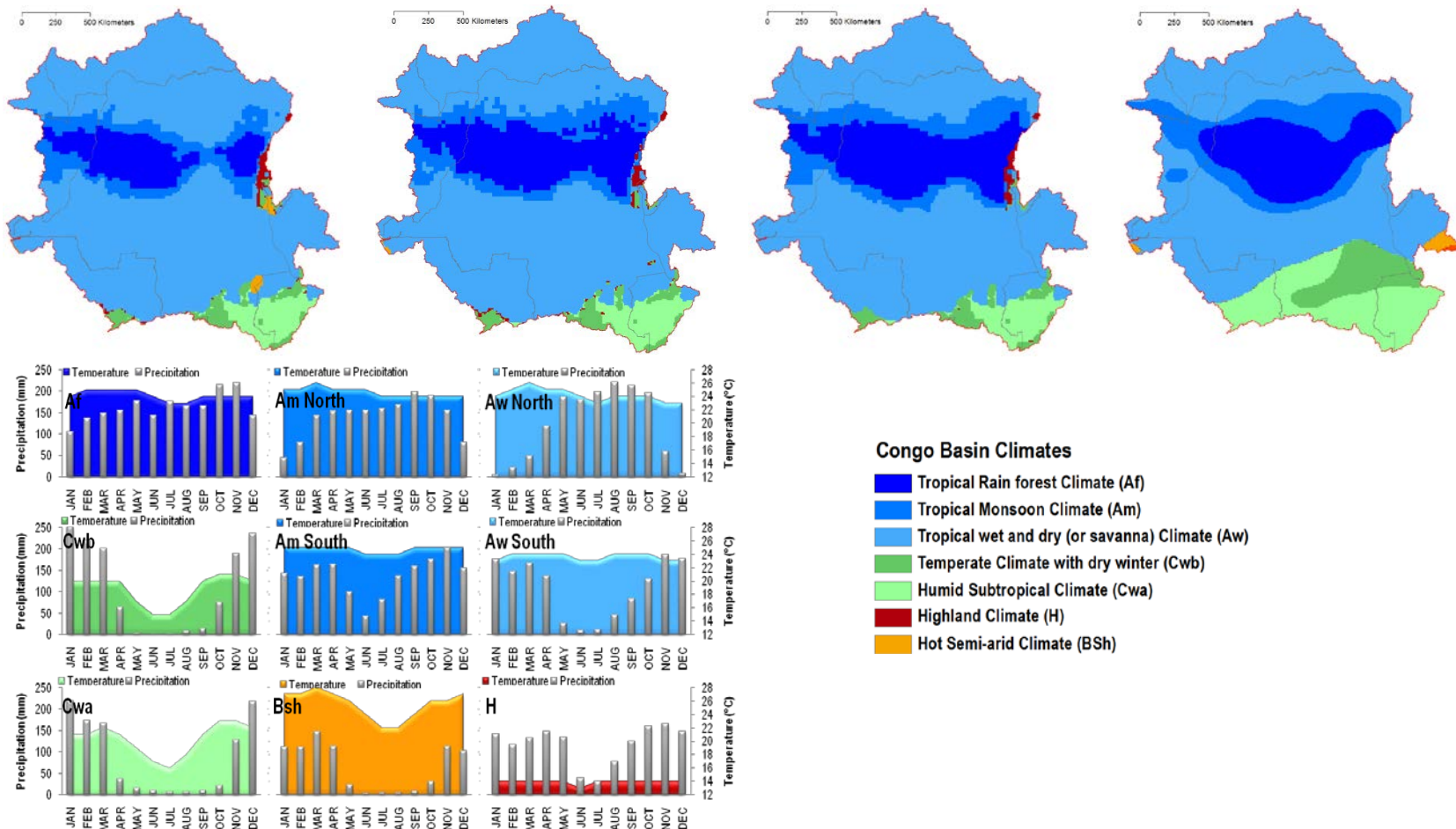


**Figure 2.7** Köppen–Geiger climate classifications for the Congo Basin using TRMM 3B42 Version 6 precipitation data with WORLDCLIM temperature data (left), using TRMM 3B43 Version 7 precipitation data with WORLDCLIM temperature data (center left), using re-calibrated TRMM precipitation data with WORLDCLIM temperature data (center right), and that of Peel et al. (2007) (right). The graphs illustrate the re-calibrated TRMM monthly mean precipitation and WORLDCLIM monthly mean temperature for representative sites in the re-calibrated TRMM-derived climate map (center).

**Table 2.3** Classification results by area (km<sup>2</sup>) and as a percentage of total Congo Basin area (3,700,000 km<sup>2</sup>). Climate class totals of climate maps derived from TRMM 3B42, re-calibrated TRMM and TRMM 3B43 products and the map of Peel et al. (2007).

Climate class	TRMM 3B42-derived climate map (1000 km <sup>2</sup> )	Re-calibrated TRMM-derived climate map (1000 km <sup>2</sup> )	TRMM 3B43 derived climate map (1000 km <sup>2</sup> )	Peel's climate map (1000 km <sup>2</sup> )
Tropical Rain forest (Af)	369 (10%)	627 (17%)	574 (16%)	559 (15%)
Tropical Monsoon (Am)	361 (10%)	403 (11%)	406 (11%)	474 (13%)
Tropical wet and dry (Aw)	2689 (72%)	2393 (65%)	2447 (66%)	1932 (52%)
Temperate (Cwb)	109 (3%)	108 (3%)	98 (3%)	227 (6%)
Humid Subtropical (Cwa)	153 (4%)	148 (4%)	151 (4%)	482 (13%)
Highland (H)	28 (1%)	21 (1%)	25 (1%)	0

## **2.5. Discussion**

### 2.5.1. Model performance

Contemporary ground data from rain gauges were used to re-calibrate TRMM data with the resulting modeled precipitation agreeing with WORLCLIM data. In general, the model was differentially additive in augmenting monthly TRMM 3B42 data (Figure 2.5). The 75<sup>th</sup> percentile and the 90<sup>th</sup> percentile monthly TRMM metrics derived from the daily 3B42 data were the most significant variables among all inputs in predicting gauge-measured monthly rainfall totals. These two variables accounted for 44% and 19% of the reduction of overall sum of squares, respectively. The first split in the bagged trees employed the 75<sup>th</sup> percentile 16 times with a mean threshold of 1.2mm of precipitation. Less than this value resulted in an average child node of 30mm of monthly precipitation, greater than this and the average estimated monthly precipitation equaled 172mm. Another six trees employed the 90<sup>th</sup> percentile with a mean threshold of 3.7mm of precipitation and child nodes of 25mm and 176mm of precipitation. Subsequent splits further refined the estimates beyond these initial thresholds. Generally, if 10 to 25 percent of the daily rainfall per month was greater than 1.2 to 3.7mm, that month had mean gauge-measured precipitation greater than 170mm. If the frequency of such rains was less than this, the mean gauge-measured precipitation was less than 30mm. After these two percentile metrics came the monthly 3B42 totals, which explained 12% of the model's reduction in sum of squares. Results illustrate the value of statistical derivatives of the daily data in predicting monthly precipitation. However, the generalized bagged regression tree model does not fit well to outliers and

there was no sensitivity to monthly rainfall greater than 300mm. This could be due to the limited number of high monthly input observations coupled with a lack of separability of these months in the statistical feature space.

The general deficit observed by the TRMM 3B42 inputs could be explained by omitted rainfall events, specifically a lack of sensitivity to different types of rain by TRMM sensors. TRMM 3B42 data are known to omit rainy season convective storms, leading to possible rainy season underestimation of precipitation. TRMM 3B42 data are also insensitive to light rain events; such light rain events, characteristic of stratiform rain in the region, are more frequent during the Congo Basin dry season. These two sources of rain event omission (missing rainy season convective and missing dry season stratiform rain events) could explain the general underestimation of rainfall throughout the year.

#### 2.5.2. Climate classification

Both the 3B43 and re-calibrated TRMM-derived climate maps compare favorably to the updated world map of the Köppen–Geiger climate classification of Peel et al. (2007) (Figure 2.7 and Table 2.3). However, the temperate and humid subtropical climates are significantly more represented in Peel's map. Peel et al. (2007) explained a source of uncertainty for these two classes by reporting: "The low density of temperature stations in Africa resulted in some climate types extending further than expected, which could not be corrected due to lack of data. The regions where this is most evident are the temperate regions in the Eastern Rift Valley. In these regions the temperature stations are at high elevation and experience a temperate climate type. However, due to the lack of nearby lower elevation temperature stations, the temperate influence of these high

elevation stations extends well beyond their immediate location and large regions of temperate climate type result in regions that are more likely to be tropical” (Peel et al., 2007). The WORLDCLIM temperature data used for this chapter have the slight advantage of having fewer spatial data gaps than the temperature data used by Peel et al. (2007), resulting in a reduced extent of continental climate types (Cwb and Cwa) for all TRMM-derived climate maps (Figure 2.7).

Table 2.3 compares the different areas of climate classes between the four products. Class membership as a percentage of the overall study area varied greatly. At 72%, 65%, 66% and 52% of the TRMM 3B42 derived climate map, re-calibrated TRMM derived climate map, TRMM 3B43 derived climate map, and Peel’s climate map, respectively, the tropical wet and dry climate class (Aw) is by far the most abundant in Congo Basin. The tropical rain forest class (Af) is the next most plentiful at 10%, 17%, 16% and 15% of the four respective maps. In the TRMM 3B42 derived climate map, the tropical monsoon class (Am) extent equals that of tropical rain forest.

The derived climate map from 3B43 and from re-calibrated product of this chapter have high agreement (91%). Overall agreement with Peel et al. was 63% when employing the climate classification with TRMM 3B42 inputs. Agreement rose to 69% and to 70% when using TRMM 3B43 and the re-calibrated TRMM inputs respectively. The tropical rain forest class (Af) agreement increased by 70% and the tropical monsoon (Am) class agreement increased by 111% for the re-calibrated product. While Peel’s map cannot be taken as truth, the intercomparison points out some strengths of the TRMM-derived climate map using gauge-calibrated product of the present chapter. First, the tropical rain forest and monsoon climates are more accurately depicted.

Second, the hot semi-arid climate and the hot desert climate are not characterized at all. Third, the highland climate is captured. The overall performance of the re-calibrated TRMM-derived climate classifier is promising, although its application in other regions would most likely require local TRMM re-calibration with appropriate ground data.

### 2.5.3. Application of re-calibrated TRMM in characterizing seasonal rainfall

Waliser and Gauthier (1993) quantified the annual cycle of ITCZ migration and its occurrence in the African continent. As described by McGregor and Nieuwolt (1998), a zone of maximum rainfall related to the African ITCZ follows the solar declination with a delay of about 1 month. The ITCZ passes through the Southern hemisphere from October to April and the Northern hemisphere from April to October. Our results show April and October to be the peak rainfall months for both hemispheres. This is consistent with Waliser and Gauthier's model that places the ITCZ position near the equator during these two months. Tsuneaki (2011) explained the driving forces of the seasonal variation of the ITCZ, and found that the origin of the water vapor fluxes feeding the ITCZ varied by season. In April, the water vapor flux is mostly derived from the Indian Ocean via Tanzania. In October, the water vapor flux is supplied from within the Congo Basin. Varying sources of water vapor could explain the difference between the two peak rainfall months (April and October) observed across the Basin. The bi-modal pattern of precipitation in the Congo Basin is illustrated in Figure 2.4. The larger rainy season occurs after the autumnal equinox, as the ITCZ returns from the north and crosses the Congo Basin. The peak Basin-wide rainfall total of November reflects this. The return of the ITCZ from the south does not result in a similar

magnitude of rainfall. This intraannual variation in Congo Basin rainfall is present in all products. Given this fact, we now examine seasonality using the re-calibrated TRMM data of this chapter. Figure 2.8a shows the month of maximum rainfall and the fact that the ITCZ migration from north to south from August through January represents the peak precipitation totals across the Basin. While there is a bi-modal seasonality, it is not ‘mirrored’ or proportional between the two rainy season peaks. All areas of the Basin likewise experience two dry seasons. The farther from the equator, the more different the dry seasons are in terms of length and precipitation totals. As the ITCZ heads south or north, it leaves the Congo Basin and for all regions of the Basin, a dry season occurs. For regions on the same side of the equator as the ITCZ during a solstice, this period is often referred to as the “little” dry season. The period when the ITCZ is at its farthest distance from any locality falls within the time of the local “big” dry season. Figure 2.8b shows the ratio of the big dry season’s minimum rainfall compared to the little dry season’s minimum rainfall. The actual equator is very close to this “precipitation” equator, as only a very small band of area near/south of the actual equator features balanced dry season minima.

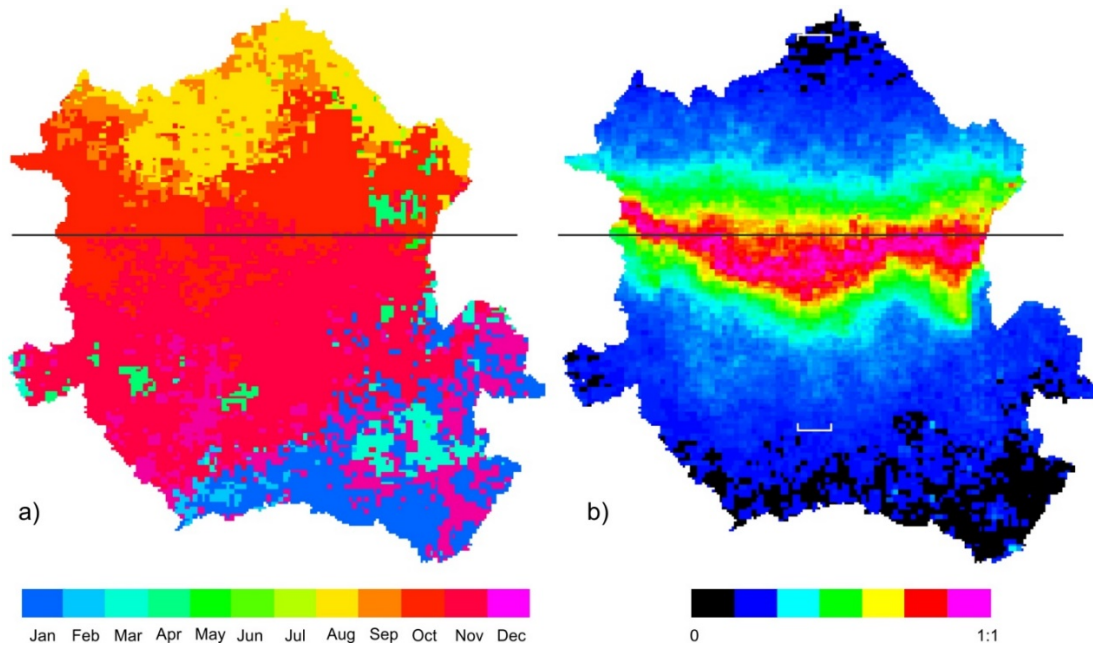


**Figure 2.8** a) Month of maximum precipitation for re-calibrated TRMM data; b) Ratio of big to small dry season precipitation minima.

The white brackets in Figure 2.8b delimit a north-south transect displayed graphically in Figure 2.9. The plot depicts the set of mean monthly precipitation values for 1 degree squares from 0 to 8 degrees north and south, along a transect from 22 to 23 degrees east in the middle of the Basin. Post-equinoxes, there is high rainfall across all latitudes within the Basin. Pre-equinoxes, there is a wider range of precipitation across all latitudes within the Basin. This plot is a sample across latitudes and confirms that per unit area, the Congo Basin receives more rain in the August to December time-frame than the mirrored period of year of February to June. Again, the southward movement of the ITCZ is the dominant rain mechanism over the Basin.

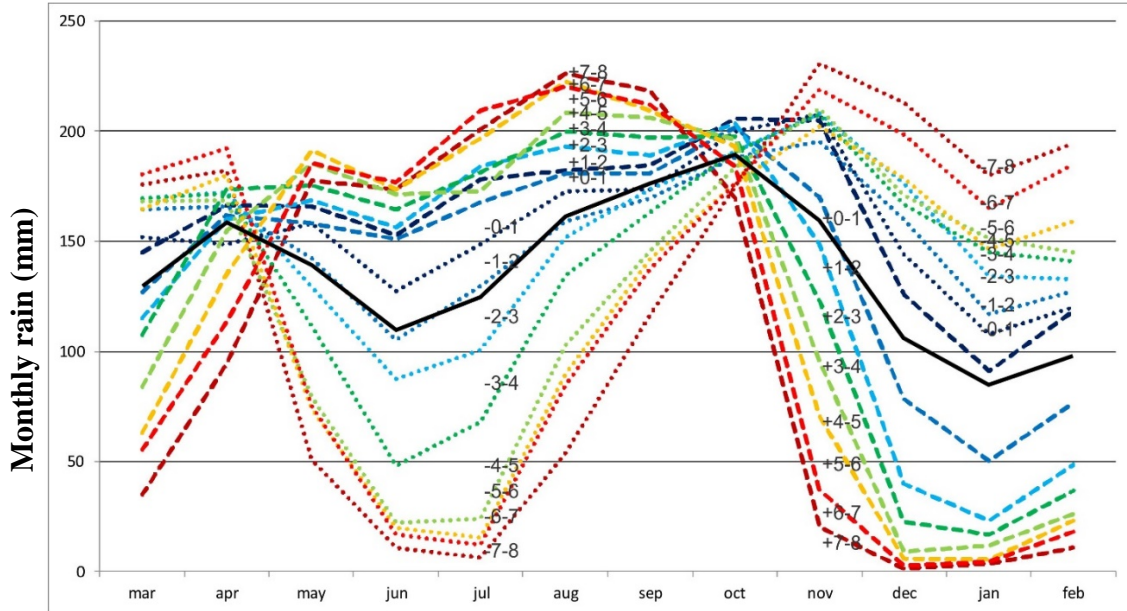


**Figure 2.9** Plots of monthly precipitation for 1 degree blocks from +8 degrees latitude to -8 degrees latitude, for the transect along 22 to 23 degrees longitude east (brackets of Figure 2.9b show the area). Dashed lines are latitudes north of the equator and dotted lines are latitudes south of the equator. Colors correspond to latitudinal increments of one degree and are labeled. The black line is the transect monthly means.

Assuming a conceptual model where there is no difference in the rainfall amounts associated with the twice yearly passing of the ITCZ and equal areas of catchment north and south of the equator, mirrored or symmetrical intraannual precipitation would be expected on each side of the equator. This is clearly not the case and the asymmetry is due to two principal factors. First, the Basin extends nearly twice as far to the south of the equator as to the north; the southern portion accounts for two-thirds of the overall catchment area. The ITCZ's proportionally greater presence in the south leads to a corresponding proportional increase in rainfall associated with the periods of ITCZ passage. Another cause is the greater rainfall associated with the southern movement of the ITCZ compared to its northern movement, as documented in the preceding discussion. Tsuneaki (2011) identified seasonally varying water vapor fluxes for the ITCZ. The post-autumnal equinox source of the Congo Basin itself leads to greater

precipitation than the post-vernal equinox source of the Indian Ocean. The deviation from the symmetrical model can be seen as well in the stream hydrograph at Kinshasa, the capital of the Democratic Republic of the Congo. The Kinshasa gauge station is situated along the lower reaches of the Congo River, roughly 400km from the ocean. The area upstream from the gauge station (the “Area-to-Point” watershed) encompasses more than 90% of the Congo Basin drainage area. Figure 2.11 shows two peaks of high streamflow, with one in the November timeframe constituting a clear maximum annual flow. The secondary peak is in April, the expected symmetrical counterpart. However, the streamflow of April is roughly 50 to 80% of the November streamflow. Testing the three monthly TRMM precipitation products against the stream gauge data of Kinshasa, including time lags, the highest correlation of 0.81 was found for the re-calibrated TRMM model with a one month lag (Figure 2.10).

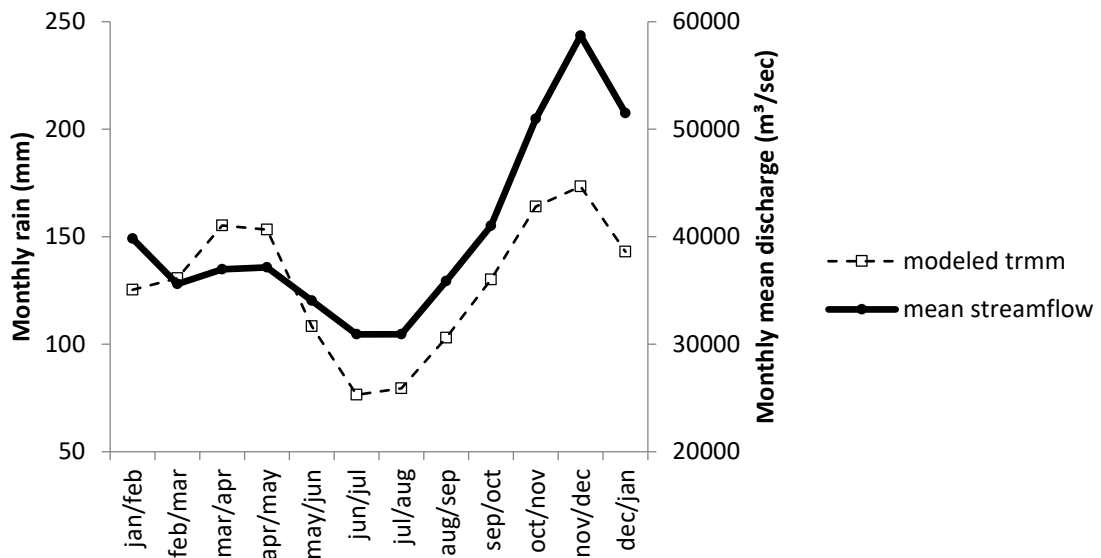


**Figure 2.10.** Re-calibrated/modeled TRMM Congo Basin monthly precipitation and Congo River mean streamflow discharge at Kinshasa from 2000 to 2007 (Data from the DRC waterway public company, Régie des voies fluviales (RVF)). Congo River streamflow is offset by one month from the precipitation data, for example jan/feb represents January rainfall and February streamflow at Kinshasa.

## **2.6. Conclusion**

The present chapter indicates that TRMM 3B42 Version 6 data are appropriate for quantifying Congo Basin rainfall regimes and for deriving climate maps when calibrated by ground gauge data sets from within the region. Two products, the TRMM 3B43 Version 7, calibrated by ground data located largely at the periphery of the Congo Basin, and a new product calibrated using ground data within the central Congo Basin, both yielded viable precipitation and climate characterizations. Despite having no ground calibration sites within the DRC, the TRMM 3B43 Version 7 product accurately depicted Congo Basin precipitation without bias. The sparse data model employed in this chapter also compared well with ancillary data. The generalized statistical feature space derived from daily accumulations of TRMM 3B42 Version 6 observations enabled the extrapolation of monthly-re-calibrated rainfall from only 12 gauge stations. Re-calibration of TRMM data resulted in a general augmentation of rainfall for both local rainy and dry seasons and a slight bias compared to the TRMM 3B43 Version 7 science product. While the new model was insensitive to high precipitation events, the general depiction at mean annual and monthly time scales also agreed well with WORLCLIM data, although exhibiting a slight bias. Added rainfall was absolutely higher during rainy season months and relatively higher during dry season months. These results indicate that both warm, convective-driven and cool, stratiform-driven rain regimes were underestimated by the TRMM 3B42 Version 6 estimates. All products were consistent in the depiction of intraannual variation (Figure 2.4); the dominance of post-autumnal equinox rainfall was captured in observed downstream Congo River hydrographs, pointing the way forward for more substantive modeling of

streamflow using TRMM, either the standard 3B43 or new products such as the one presented here. Climate characterizations using the 3B43 Version 7 and re-calibrated results of this chapter resulted in nearly equal areas for the climate types found within the Congo Basin. The chapter serves as a demonstration of an alternative approach to processing TRMM data in characterizing regional precipitation regimes, as well as a validation of TRMM 3B43 Version 7 science product for a poorly covered region of Africa.

## Chapter 3: Estimating daily streamflow in the Congo Basin using satellite-derived data and semi-distributed hydrologic model

### **3.1. Introduction**

Quantification of global and regional water cycles is required for hydrological research, and model improvement, especially in data-poor contexts, is critical. The Congo Basin in Africa is the world's second largest river basin, with a drainage area of 3 689 550 km<sup>2</sup>. Centrally located and with the greatest water resources in Africa, the basin is a vital resource for water and energy supply for a continent with increasing needs for safe water and energy (Mandelli *et al.* 2014). A greater quantitative understanding of the basin's hydrology is necessary for the current and future management of Africa's water resources.

The major river systems of Africa share distinctive morphological characteristics, including inland deltas that re-orient tributaries that empty through rapids near their coastal effluent (Goudie 2005). The Congo Basin is notable for its large internal drainage basin, referred to as the Cuvette Centrale, the remains of an ancient lake bed from the Tertiary period. This internal basin delineates an ancient lake which contains the relic lakes Mai-Ndombe and Tumba and swamp forests that dominate much of the flatter terrain (Bwangoy *et al.* 2010). It is believed that as the Congo Basin's internal drainage evolved, it was captured by a short stream draining to the coast, cutting through the high ground at the continental margin on the western rim of the basin. The modern Congo River has a narrow exit to the sea, notable for cataracts

between Kinshasa and the coast that link the Congo Basin to the Atlantic (Goudie 2005).

The Cuvette Centrale is a low lying, bowl-shaped depression which lies in the center of the basin and extends in all directions along the arc of the Congo River (Figure 3.1). Inputs to the Cuvette Centrale form a branching pattern where most of the major Congo River tributaries point towards the Cuvette rather than the Basin's outlet (Summerfield 1991, Goudie 2005). Wetlands such as the inland drainage of the Cuvette Centrale have a substantial impact on river basin flow rates, as wetland water depths are shallow within a diffuse channel geometry (Betbeder *et al.* 2014, Alsdorf 2016). Approximately 70 % of the Congo Basin's water volume accumulates in the Cuvette, and its gradual release plays a critical role in regulating downstream flows (Thieme *et al.* 2005, Partow 2011). Flows of the Congo River's main stem downstream from the Cuvette, such as at Kinshasa, are expected to exhibit different dynamics than those that flow into the Cuvette.

The flow regime at the Kinshasa gauge is representative of the overall basin as 98 % of the basin is upstream of it (Figure 3.1). The Congo River hydrograph observed at Kinshasa from 1998 to 2010 shows for each year two peaks of high streamflow denoting a bimodal flow regime (Figure 3.2). The peak in November-December constitutes an annual maximum and the one in April-May a secondary peak. The April-May peak is 49 % (1999) to 83 % (2010) of the November-December peak, per the 13-year data record (1998 - 2010). The hydrograph at Kinshasa depicts large inter- and intra-annual variations in streamflow that are driven by rainfall seasonality (Munzimi *et al.* 2015). This seasonality is consistent in wet and dry years; during drier than usual

years, for example in 2004, 2005 and 2006, a decline in both high and low flows is observed at Kinshasa.

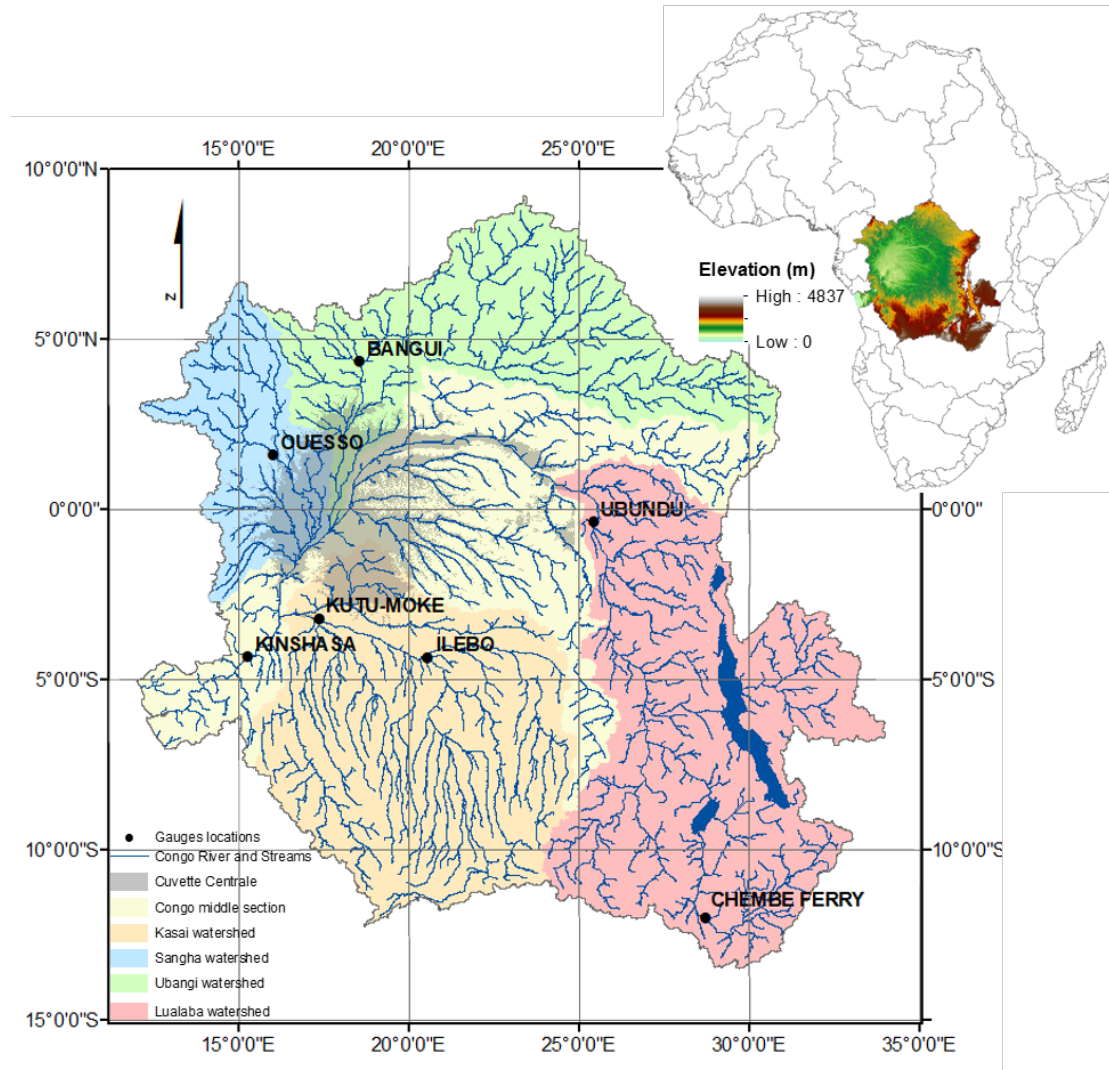


**Figure 3.1** Stations locations and corresponding watersheds

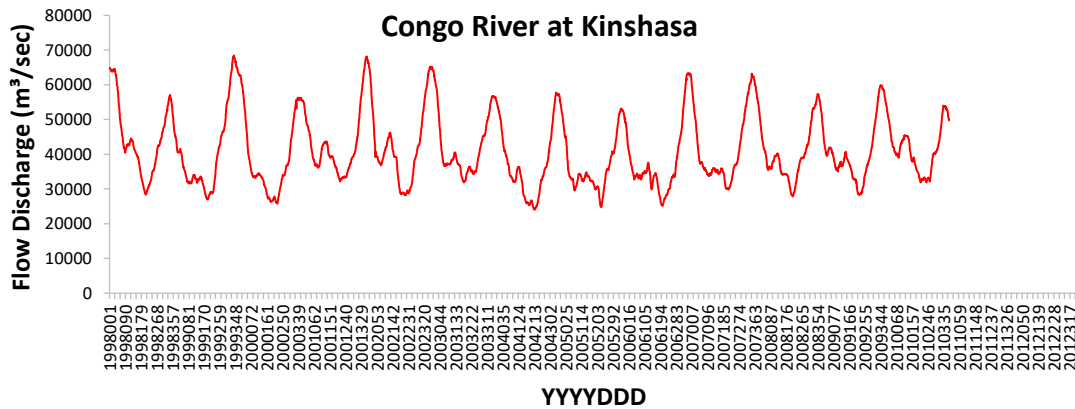


**Figure 3.2** Daily observed flow discharge at Kinshasa (1998 - 2010). Data are from the Régie des Voies Fluviales (RVF), Democratic Republic of the Congo

Our understanding of the basin’s hydrology is severely limited by the paucity of ground-based hydrometeorological data. Hydrological models of ungauged catchments can potentially provide reliable information, especially if they can incorporate satellite observations and derived data products. Recent remote-sensing studies of the Congo Basin’s hydrology include mapping of wetland extent using Landsat, the Phased Array type L-band Synthetic Aperture Radar (PALSAR) and Shuttle Radar Topography Mission (SRTM) data (Bwangoy *et al.* 2010); estimation of wetland dynamics using PALSAR, Light Detection and Ranging (LIDAR) data and temporal vegetation indices from the Moderate Resolution Imaging Spectroradiometer (MODIS) (Betbeder *et al.* 2014); and estimation of seasonal variations in wetland water storage using estimates of inundation from various data sources and data from the Gravity Recovery and Climate Experiment (GRACE) (Lee *et al.* 2011). Several studies have also modeled historical streamflow within major tributaries of the Congo River using various satellite-data inputs (Asante *et al.* 2008, Munzimi 2008, Tshimanga *et al.* 2011, Tshimanga and Hughes 2014), and some have assessed the impact of future climate changes on tributaries (Tshimanga and Hughes 2012, Aloysius and Saiers

2017). Beighley *et al.* (2011) reviewed the applicability of various satellite-derived precipitation datasets in the Congo Basin. While these studies have advanced models of the Congo Basin's hydrology, a contemporary, high-resolution model of daily streamflow is lacking and remains a need for operational decision-making across the basin (Reitsma 1996).

Operational decisions of interest in the Congo Basin include short-range forecasting of reservoir inflows, releases and hydropower operations at the Inga dam, the largest such installation in Africa; evaluation of hydropower generation at numerous potential sites on upstream tributaries; and forecasting of flood risk near population centers, roads and other infrastructure throughout the basin. Drainage areas, which experience significant deforestation due to timber harvesting, agricultural expansion and increased human settlement, could also cause significant hydrologic changes downstream with consequences for hydropower and flood risk. Daily streamflow models are therefore required for simulating historical, current and future flows, and for making short-term management, monitoring and planning decisions in the Congo Basin.

The chapter reported here improves our understanding of Congo Basin hydrology by estimating daily streamflow along the main stem of the Congo River and within smaller river reaches throughout the basin using a hydrologic model. The chapter also improves our understanding of the opportunities and limitations of a physically-based model using interactive calibration and limited gauge data augmented with satellite-derived products in simulating daily hydrologic processes of a large and complex basin.

### **3.2. Data**

We drive the USGS Geospatial Streamflow Model (GeoSFM) (Asante *et al.* 2007a,b, Artan *et al.* 2007a,b) with satellite-derived and terrestrial data to estimate daily streamflow in the Congo Basin. Input data are: 1) daily rainfall derived from the joint NASA/JAXA Tropical Rainfall Measuring Mission (TRMM) 3B42 product, 2) daily evapotranspiration from NOAA Global Daily Reference Evapotranspiration product (GDET), 3) soil type and texture from the UN Food and Agriculture Organization (FAO), 4) topography from NASA SRTM, 5) land cover from Landsat-derived maps (Potapov *et al.* 2012), and 6) wetlands extent from Landsat/MODIS-derived maps (Bwangoy *et al.* 2010) (Table 3.1). Topography was resampled from 90 m to 180 m to enhance the model's computation efficiency.

The monthly re-calibrated TRMM estimates from chapter 2 are not used to drive our daily flow model in this chapter. A re-calibration of daily rainfall or any temporal downscaling procedure of re-calibrated monthly rainfall was not possible since daily gauge data were not available. Considering the importance of the daily time step of input rainfall, we forgo the use of adjusted monthly data, and use instead the original TRMM daily data.

Ground-based gauge data are from the Régie des Voies Fluviales (RVF), Democratic Republic of the Congo (DRC); daily data exist for the main stem of Congo River at Kinshasa from 1998 to 2010, for the Ubangi River at Bangui from 1998 to 2007 and for the Sangha River at Ouesso from 1999 to 2011. In addition, the World Meteorological Organization's (WMO) Global Runoff Data Centre (GRDC) (Coe and Olejniczak 1999) provides monthly mean data for Kutu-Moke, Chembe-Ferry, Ilebo

and Ubundu; while these data pre-date the timeframe of our study (1998 - 2012), they provide useful information on general flow patterns in locations with no current daily or monthly flow.

### **3.3. The Geospatial Streamflow Model (GeoSFM)**

GeoSFM is a semi-distributed hydrologic model for research and operational monitoring applicable in data-scarce environments. GeoSFM has been implemented in a wide range of applications in diverse regions of the world (e.g. Asante *et al.* 2007b, Brown *et al.* 2014, Cole *et al.* 2014, Dessu *et al.* 2016) and has been applied operationally by the Famine Early Warning Systems Network (<http://earlywarning.usgs.gov/fews/>). GeoSFM includes GIS-based preprocessing, subbasin options for modeling soil moisture, routing of flow using either a diffusion-analog or the Muskingum-Cunge formula, and tools for calibration, sensitivity analysis, and post-processing for analysis. (Asante *et al.* 2007a, Artan *et al.* 2007a).

### **3.4. Methods**

We parameterized the GeoSFM model to simulate daily streamflow of the main stem and tributaries of the Congo Basin. We then attempted to improve model performance using interactive model adjustment. The overall approach is initial model parameterization for basin-wide daily flow, basin-level calibration for the Congo River at Kinshasa, and subbasin level calibration for the upstream gauge sites.

The parameter set to minimize error in flow at Kinshasa was deduced from prior studies (Artan *et al.* 2007a, Kiluva *et al.* 2011, Agunbiade and Jimoh 2013, Tshimanga and Hughes 2014, Dessu *et al.* 2016). Parameter values were adjusted until minimal error was reached from the Kinshasa gauge.

**Table 3.1** Data inputs to the basin model.

Data sets	Input data sources	Spatial and temporal resolution	Data coverage	References
<b>Hydrological data</b>				
TRMM 3B42	Geo-IR, SSMI, AMSU, TRMM, AMSR, Gauges	0.25°, three-hourly *	50°S-50°N 1998 to present	Huffman <i>et al.</i> 2007
Global Daily Reference Evapotranspiration (GDET)	GDAS six-hourly operational meteorological data	1°, daily	Global 2001 to present	Senay <i>et al.</i> 2008
<b>Terrestrial data</b>				
Soil data	FAO/UNESCO Digital Soil Map of the World	1 - kilometer	Global	FAO, 1995, FAO, 1971 - 1981
SRTM DEM	Radar	90 - meter	60°S-60°N near-global	Van Zyl, 2001, Rodriguez <i>et al.</i> 2006
Land Cover data set	Landsat 57 m, MODIS 250 m, VCF 500 m, Landsat Congo Wetlands 57 m, MERIS 300 m	57 - meter	Congo Basin	Potapov <i>et al.</i> 2012, Bwangoy <i>et al.</i> 2010, Clevers <i>et al.</i> 2004

\*Daily accumulations of this data set are processed at USGS EROS

Regional disaggregation followed, calibrating subbasin streamflows using discharge data from the Ubangi and Sangha rivers. For all three gauges, the first half (1998 - 2004 for Kinshasa, 1998 - 2002 for Bangui and 1999 - 2004 for Ouesso) of the time series was used for calibration and the second half (2004 - 2010 for Kinshasa, 2003 - 2007 for Bangui and 2005 - 2011 for Ouesso) was retained for validation. Additional validation was performed using the GRDC's historical monthly gauge data from Kutu-Moke, Chembe-Ferry, Ilebo and Ubundu.

#### 3.4.1. Initial Parameterization with Remote Sensing Data

Terrain analysis was performed on the DEM to delineate subbasins and streams, constrained to a minimum drainage area of 324 km<sup>2</sup> (10 000 cells), yielding 2950 subbasins and river reaches with a median area of 1501 km<sup>2</sup> and a median length of 41 km respectively. This catchment threshold provides sufficient spatial detail for most needs of operational hydrological monitoring of the Congo Basin. The land-cover map indicates that the basin is 59 % forest and woodland, 11 % wetland, 7 % water bodies, and the remainder savannah and human settlements. Soils in the basin are 31 % clay, 26 % sandy soil, 22 % water, 14 % sandy clay loam and 6 % loam. Runoff curve numbers computed for the subbasins with these mapped inputs range from 52 to 98 with a basin-wide average of 76. Unit hydrographs computed yield daily estimates of 29 %, 25 %, 17 %, 9 %, 6 %, 4 %, and 2 %, respectively, of total runoff over the first seven days following a rainfall event. Runoff discharged from an event gradually approaches zero within three weeks. The model was then used to simulate daily streamflow for each stream segment in the basin. Subbasin averaged daily soil moisture

was estimated from gridded rainfall and evapotranspiration. Daily runoff from saturated soils was routed to the subbasin outlet and from there routed through the river network using the Muskingum-Cunge method until it reached the basin outlet beyond the river gauge at Kinshasa.

### 3.4.2. Model calibration

Previous studies have successfully simulated seasonal anomalies associated with major floods in several basins, including the Congo Basin, using the GeoSFM model with initial parameterization and without calibration (Asante *et al.* 2005, 2007b, 2008, Artan *et al.* 2007b, Blanc and Strobl 2013). However, some parameter calibration is required to achieve accurate estimates of flow volumes and timing, particularly for applications requiring daily hydrographs. Inaccuracies in initial parameter estimates may arise from differences in the scale and quality of the input data or from the model itself (Gupta *et al.* 1999, Wijesundera *et al.* 2012, Blanc and Strobl 2013). Parameter adjustment can reduce such effects (Sahoo *et al.* 2006).

#### 3.4.2.1. Basin-wide Calibration

Simulated flow was initially calibrated and validated against measured streamflow at Kinshasa. Estimates of the percentage adjustments required to achieve accuracy in basin water-balance components (i.e. surface runoff, precipitation and evapotranspiration) and horizontal timing of median flows were computed. Adjustments were made by scaling the spatially-distributed parameters, based on differences between the modeled and observed flows at Kinshasa, iteratively until a

difference of less than 5 % is achieved. Based on previous research (Asante *et al.* 2007a, Artan *et al.* 2007a, Kiluva *et al.* 2011, Agunbiade and Jimoh 2013, Tshimanga and Hughes 2014, Dessu *et al.* 2016), we limited parameter adjustment to the following variables: residence time for interflow reservoir, river loss factor, river floodplain loss factor and kinematic wave celerity. Adjustments were confined to ranges of parameter values that retain physical meaning. The identified parameters were used to calibrate the model for daily flow magnitude and timing at the Kinshasa gauge. To account for the attenuation of flows in the Cuvette Centrale, semi-lumped and semi-distributed calibrations (Ajami *et al.* 2004, Khakbaz *et al.* 2012) were used during basin-level parameters adjustments. The semi-lumped calibration was used to adjust residence time for interflow reservoir, river loss factor and river floodplain loss factor. These three parameters were set to be identical among subbasins, e.g. the new value of the residence time for interflow reservoir corresponds to the maximum possible number of days, which maximizes flow attenuation, and was applied to all subbasins at the end of the calibration procedure. This optimal parameter set was applied to all the subbasins in the semi-distributed structure of GeoSFM model in order to simulate the streamflow. Basin-level calibration also included spatially-distributed forcing aggregated over each subbasin.

The semi-distributed calibration was used to adjust the kinematic wave celerity to further slow the Congo River hydrograph. Adjustments of the parameter were uniformly and proportionally applied across subbasins, keeping final values within realistic ranges. To further handle delays caused by the Cuvette Centrale wetlands, GeoSFM was adjusted by increasing the number of days for subbasin response.

### *3.4.2.2. Regional Calibration*

The basin-wide, calibrated flow model is not expected to perform well for tributaries upstream of the Cuvette Centrale, since they are not impacted by its dispersive effect. For upstream watersheds, we performed a regional calibration using observations of gauge locations at Bangui and at Ouesso. For regional calibration of subbasins, a different set of adjustments was applied to the residence time for interflow reservoir, river loss factor, and river floodplain loss factor parameters. No adjustment was made to kinematic wave celerity, which largely served to slow the Kinshasa hydrograph downstream of the Cuvette Centrale for the global calibration.

Regional calibration employing the Bangui and Ouesso gauge data focused on the accurate capture of flow timing and flow seasonality, with considerable residual bias in total volume estimates. Their respective  $R^2$  values were high (0.74 and 0.82), denoting a strong relative correlation. To adjust model overestimation, a simple bias correction was made. The over-predicted estimates were divided by the value of the average slope derived from the linear regression fit of the monthly mean flow data (modeled versus observed, aggregated from current averages) for Bangui and Ouesso. The simple bias correction is a recognition of the limitations of available gauge data in executing a more robust calibration. The adjustment was applied to subbasins and compared to four gauges for which monthly mean data were available. The final sequence of the entire calibration process resulting from these evaluations are summarized in Figure 3.3.

### 3.4.3. Validation

Validation was performed using the set aside half of the time-series observations from Kinshasa (2004 - 2010), Bangui (2003 - 2007) and Ouesso (2005 - 2011). Comparisons were performed at three temporal levels. First, the modeled flow at each gauge station averaged over the entire validation period was evaluated by comparing with gauge-data means and standard deviations. Second, daily flows were evaluated via Nash-Sutcliffe model efficiency coefficient and linear regression of all daily observations over the validation period against daily gauge data at the three stations. A bias of simulated and observed flow, presented as a percentage, was also calculated as:

$$P_{\text{bias}} = 100 \frac{\sum_{i=1}^n (S_i - O_i)}{\sum_{i=1}^n (O_i)}$$

where  $S_i$  and  $O_i$  are the simulated and observed flows. Third, seasonal trends were evaluated by comparing modeled versus observed estimates of the 25<sup>th</sup> and 75<sup>th</sup> percentiles of magnitude and date of flows at the three gauge stations, as percentiles are characterizations of flow inter-annual variability. The 25th and 75th percentiles of all daily data in the validation periods for each site are valuable indicators for streamflow discharge based on daily flow data by avoiding outliers in the datasets. In addition, results of the modeled hydrographs before and after calibration were compared graphically to the gauge-based hydrographs. Further evaluation was conducted at the monthly level by comparing modeled hydrographs with the current monthly averages from the Ubangi River at Bangui and the Sangha River at Ouesso and with the historical monthly averages from the four GRDC gauges at the Kasai River at Ilebo, the Kasai River at Kutu-Moke, the Congo River at Ubundu, and the Luapula River at Chembe Ferry.

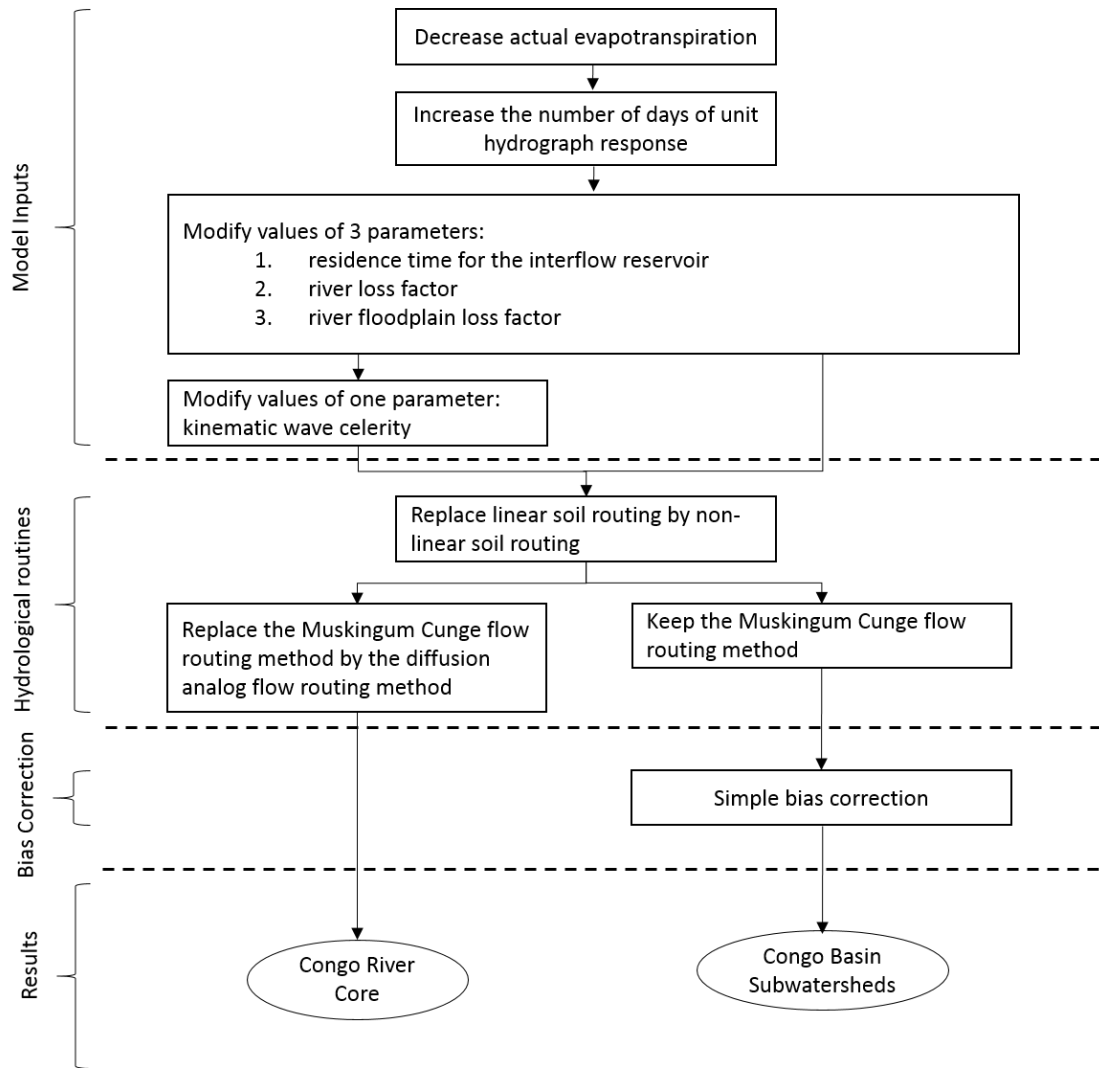


**Figure 3.3** Final sequence applied for the basin-wide and regional calibration process. Basin-wide calibration is to the Congo River flow at its core, downstream from the Cuvette Centrale. Regional calibration is to Congo Basin sub-watersheds upstream from the Cuvette Centrale.

### 3.5. Results and discussion

#### 3.5.1. Calibration of the initial basin-wide model

Results of the initial run are averaged into daily means of flow discharge over the 13-year period (1998 - 2010) and compared to observed flow at Kinshasa (Figures 3.4, 3.5). Modeled flow is bimodal, although it differs in magnitude and timing from the gauge data. Component analysis indicated that these differences were a function of the

four most sensitive model parameters, but also to two other main components, the water balance and the response generated by the model. Model adjustments related to timing focused on the months leading to peak flow over the August-February period. A time shift of the August-February portion of the hydrograph was applied as well as an adjustment of the mass balance simulations to correct runoff volume and streamflow magnitude.

Water balance adjustment could include increasing precipitation or decreasing evapotranspiration. Basin-wide annual rainfall volume from TRMM's 3B42 is 4427 km<sup>3</sup>/year which is significantly lower than corresponding estimates from WORLDCLIM isohyets derived from long-term historical gauge records (Hijmans *et al.* 2005), at 5678 km<sup>3</sup>/year. The pattern of rainfall underestimation in the basin is spatially and seasonally variable, and gauge data are inadequate for performing spatial and temporal corrections on a daily scale. However, considering the low spatio-temporal variability of evapotranspiration, we chose to decrease evapotranspiration for this adjustment. GeoSFM contains procedures for ingesting potential evapotranspiration grids and computing actual daily evapotranspiration based on antecedent soil moisture conditions (Asante *et al.* 2007a).

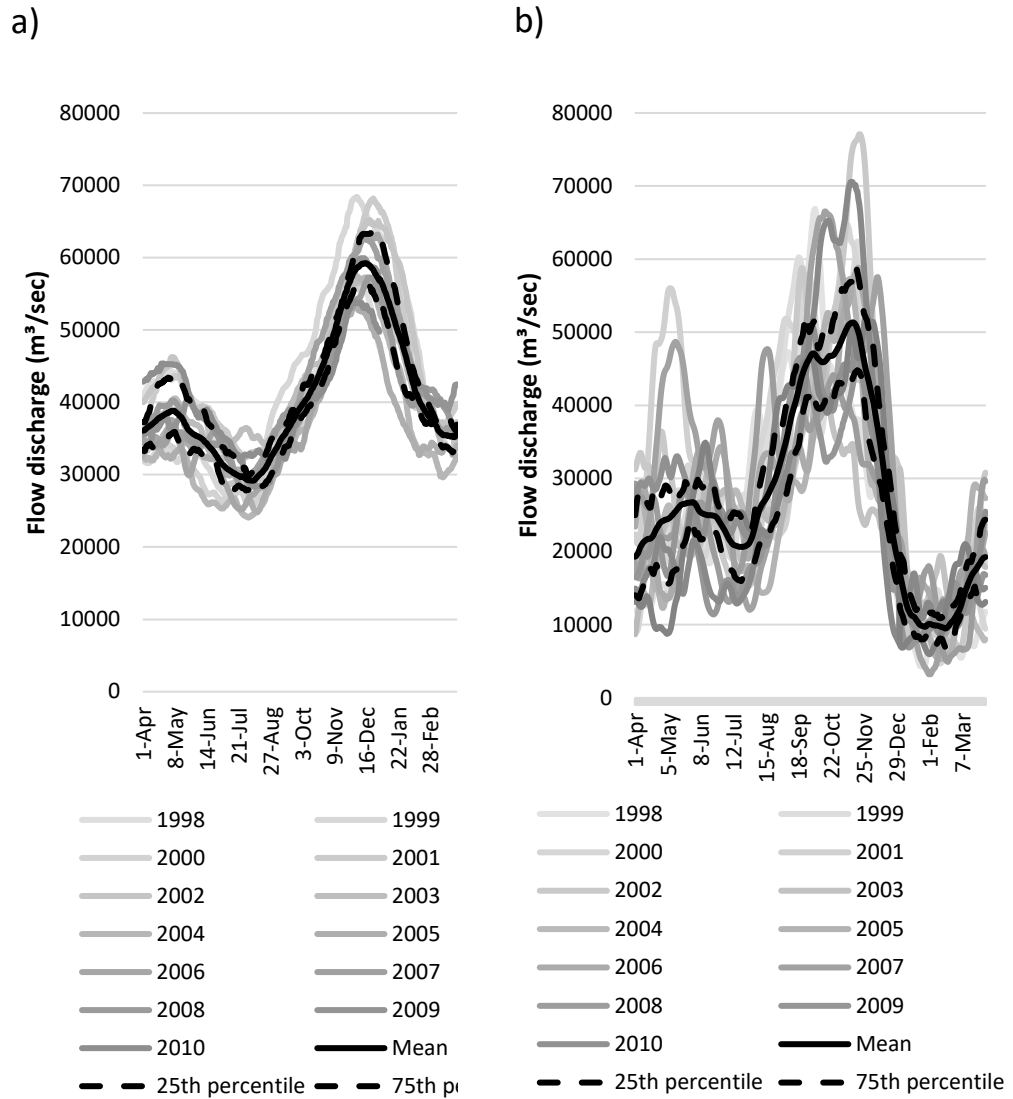


**Figure 3.4** (a) Daily observed flow discharge and (b) daily initial flow estimate discharge prior to calibration at the Congo River at Kinshasa

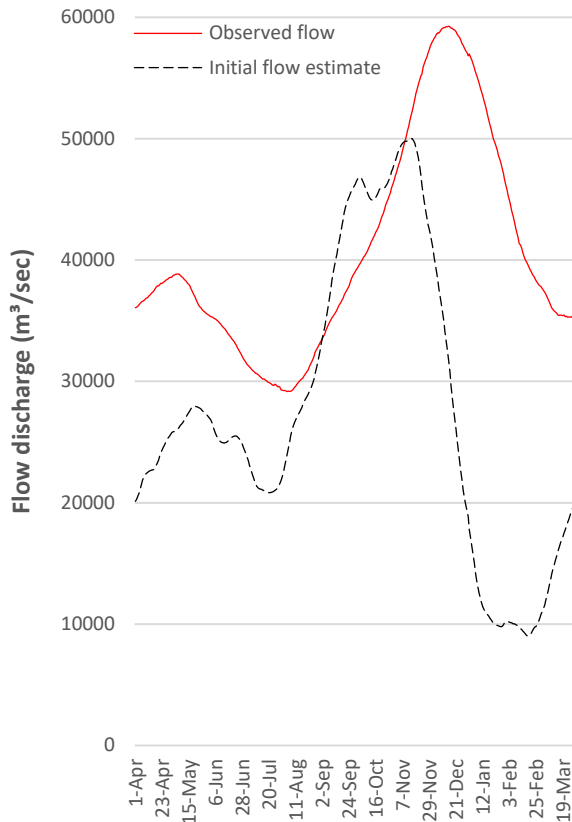


**Figure 3.5** Multi-year average 1998 - 2010 of observed daily flow discharge and initial daily flow estimate discharge prior to calibration at the Congo River at Kinshasa

Initial model runs significantly underestimated the basinwide water balance, yielding 129 mm/year from 1200 mm/year of precipitation and 1071 mm/year of actual evapotranspiration ( $ET_a$ ). We evaluated reducing the  $ET_a$  using multiplier scaling factors. A multiplier of 0.3 yielded the best result, increasing the basinwide water balance generated to 424 mm/year (Table 3.2). Discharge from the model (derived from daily calibrated modeled flow) at the basin outlet was estimated at 302 mm/year while in-stream modeled losses including floodplains losses make up the balance of 122 mm/year. The in-stream losses are incurred in the rivers and floodplains where there is also an extended storage of rainfall. While, the river and floodplain losses reported in Table 3.2 explain the difference between water balance and runoff, more accurate

estimation of the magnitude of the losses would probably require a focused study, likely with a field campaign to accurately capture the extent, evaporation rates and other losses from the floodplains.

**Table 3.2** Comparison of satellite-derived model inputs from the current study (1998-2012) to published estimates for the Congo Basin.

	Current Study	Other Published Data	Source for Other Data
<b>Area (km<sup>2</sup>)</b>	3689550	3700000 - 4100000	Campbell (2005) - Crowley et al. (2006)
<b>P (mm/year)</b>	1200	1900	Alsdorf et al. (2016)
<b>ET<sub>o</sub> (mm/year)</b>	1339	1300	Shiklomanov (2009)
<b>Initial Model ET<sub>a</sub> (mm/year)</b>	1071	1098	Chishugi et al. (2009)
<b>Initial Model P-ET<sub>a</sub> (mm/year)</b>	129		
<b>Adjusted Model ET<sub>a</sub> (mm/year)</b>	776	1098	Chishugi et al. (2009)
<b>Adjusted Model P-ET<sub>a</sub> (mm/year)</b>	424		
<b>R (mm/year) at Basin Outlet</b>	302	342	Chishugi et al. (2009)
<b>Model in-stream Losses (mm/year)</b>	122		

Rainfall flux (P), actual and potential evapotranspiration (ET<sub>a</sub>, ET<sub>o</sub>) fluxes and calibrated model runoff discharged (R).

The observed peaks at Kinshasa in November-December and April-May are driven by the November and March rainfall peaks with about a month lag, and these rainfall timing are accurately estimated by the TRMM product, as found in Munzimi *et al.* (2015). The temporal connection between precipitation and streamflow has been related to the temporal connection between P-ET runoff (precipitation – evapotranspiration runoff) and wetland filling and draining in the central portion of the Congo Basin i.e. the Cuvette Centrale (Lee *et al.* 2011). The temporal shift in modeled flow was likely due to the response structure related to the filling and emptying of the wetlands of the Cuvette Centrale. The one-month shift of simulated flow of the

November peak for the Kinshasa gauge (Figure 3.4) suggested that the hydrograph response needed to be slowed by increasing its number of days for the rise and the recession of the curve. As the calibration was done near the Congo Basin's outlet, all upstream subbasins were subjected to this adjustment. Subbasin responses originally generated in the initial preprocessing module had a median of 21 days for runoff from rainfall events to completely drain out of a subbasin. To account for detention of water in the floodplain, the median number of days for full drainage was extended to 97 days by applying a simple diffusion equation to the initial subbasin responses. Thus, the new unit hydrographs stored in the new response file gave a better simulation of the typical response of each catchment to rainfall. The initial unit hydrograph was developed for each catchment during the model preprocessing phase, prior to any flow routing. The amplitude and timing of modeled hydrograph following basin-wide calibration display a much better counterpart to data from the Congo River gauge at Kinshasa (Figures 3.6).

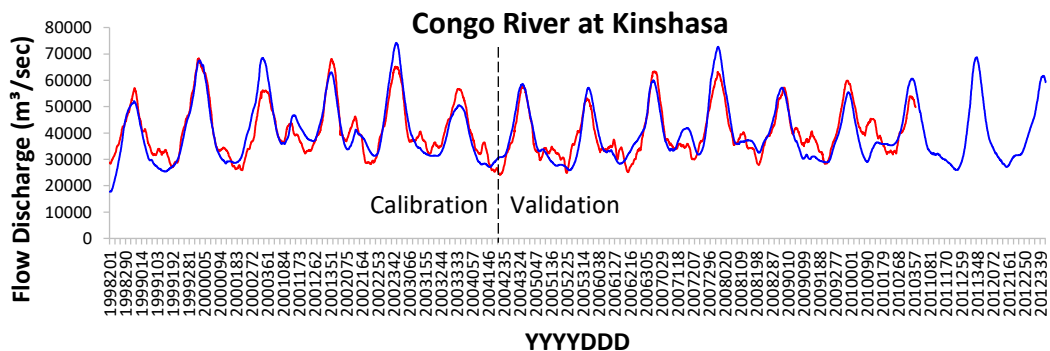


**Figure 3.6** Comparison of 15 years (1998 - 2012) of daily discharge on Congo River at Kinshasa from basin-wide calibration. Blue is estimated flow from the calibrated model and red is gauge observations. The dashed line separates calibration and validation periods

### 3.5.2. Calibration of the initial regional (subbasin) model

Parameter adjustment for calibrating the regional model to Bangui and Ouesso daily flow data yielded strong agreement in terms of timing and seasonality. However, the model yielded considerable overestimation of the amplitude of the seasonal cycle for these gauges (Figure 3.7), requiring a bias adjustment. A simple correction based on the average slope of the two linear regression fits to monthly mean flow data (modeled versus observed, aggregated from current averages at Bangui and Ouesso) yielded a value of 2.5 (average of 3.8 and 1.2). This value was used to adjust the over-predicted daily flow of the entire series for all subbasins. As intended, the bias correction offsets the general model's over-prediction. However, the amplitude of modeled hydrographs following this regional calibration display a better counterpart to data from the Sangha River at Ouesso than from the Ubangi River at Bangui where the flow is still substantially over-predicted after bias correction (Figures 3.8). The performance at the GRDC gauges (Table 3.5) provides some confidence in the performance of the model in basins other than Ubangi and Sangha. Regardless, the single-value bias correction is a limiting factor of the regional calibration effort in improving flow magnitude at subbasin level.

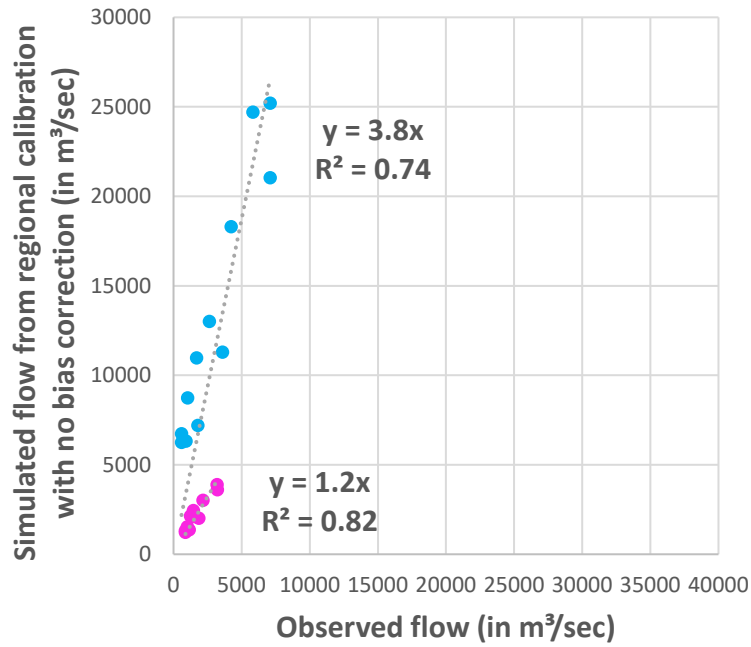


**Figure 3.7** Monthly-mean of observed flow vs. simulated flow from regional calibration with no bias correction at Bangui (blue) and Ouesso (pink).

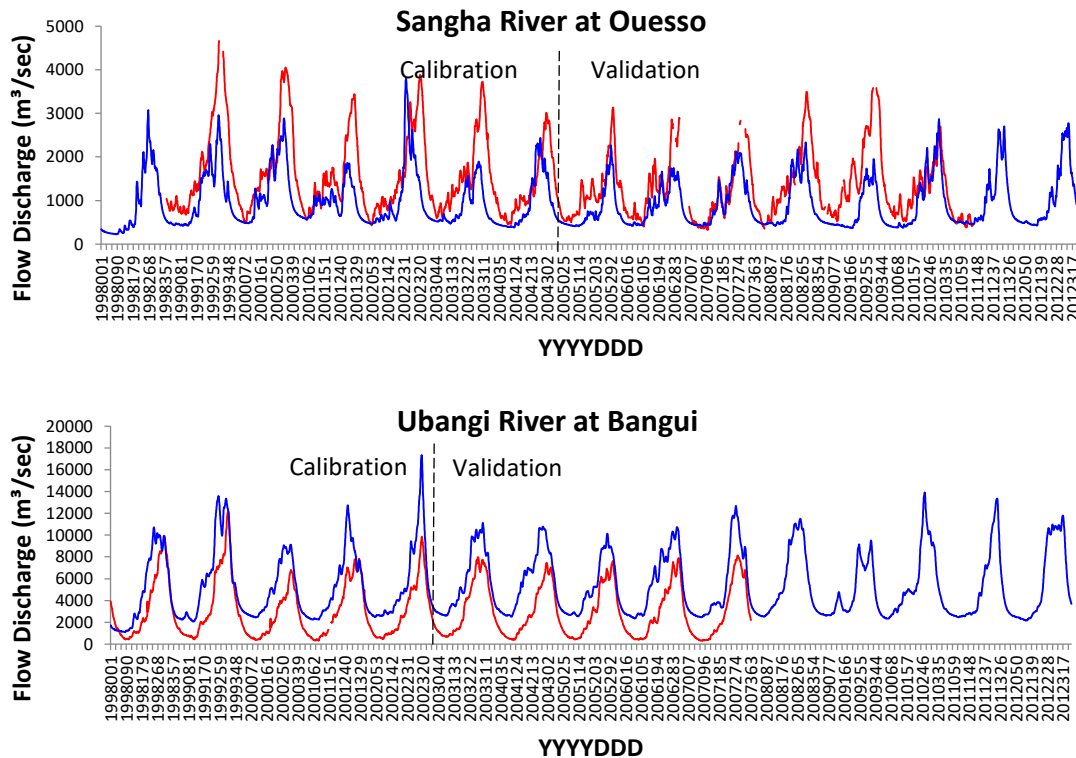


**Figure 3.8** Comparison of 15 years (1998 - 2012) of daily discharge on Sangha River at Ouesso and Ubangi River at Bangui from regional calibration. Blue is estimated flow from the calibrated model and red is gauge observations. The dashed line separates calibration and validation periods

### 3.5.3. Validation of the calibrated basin-wide and subbasin models

The amplitude and timing of modeled hydrographs following calibration display a better counterpart to data from the three gauge sites (Figures 3.9). Average discharge at Kinshasa from the calibrated model captures 99 % of the observed average, compared to 67 % for that from the un-calibrated model. Simulations track observed data in both drier years (2004, 2005 and 2006) and wetter years (1999, 2001, 2002, 2007 and 2008). Daily means over the validation period closely track the observed means at Kinshasa for the basin-wide model, while evidencing residual bias for Ouesso (underestimate) and Bangui (overestimate) for the subbasin model (Figure 3.10).

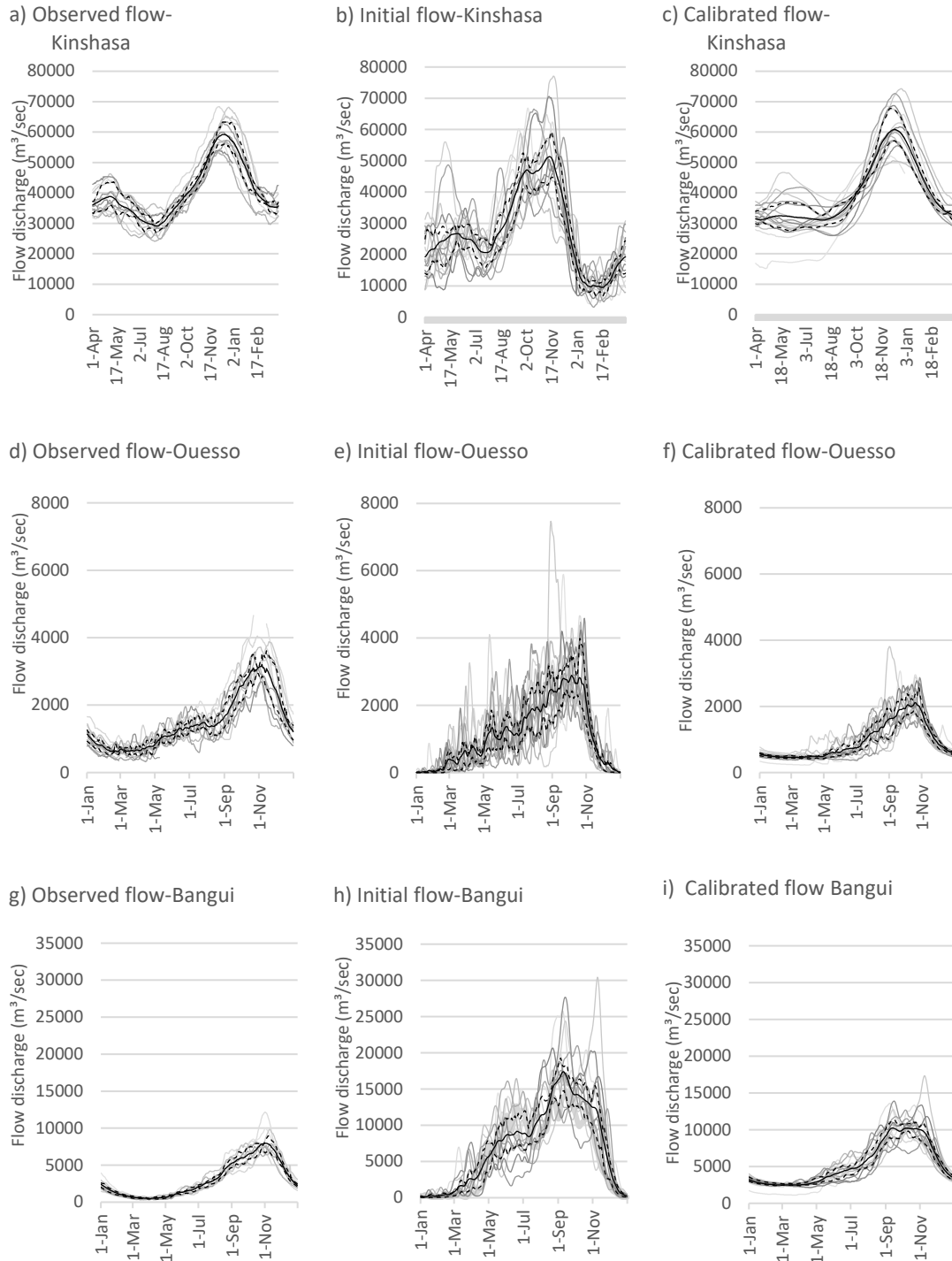
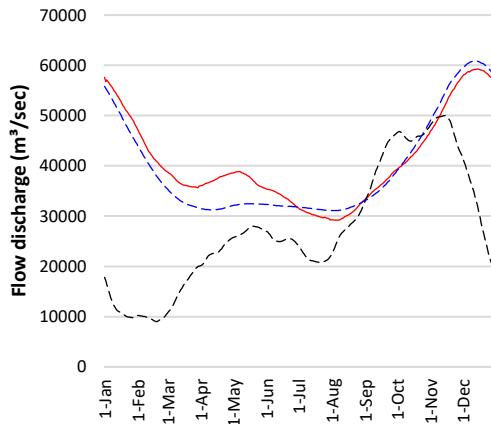
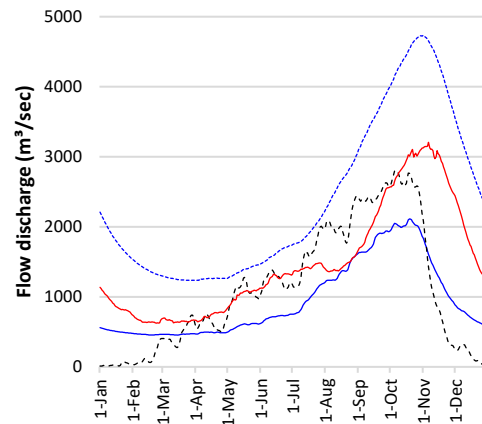


**Figure 3.9** Daily calibrated flow discharge over 15 years (1998 - 2012) on Congo River at Kinshasa from basin-wide calibration, and on the Sangha River at Ouesso and Ubangi River at Bangui from regional calibration compared to the un-calibrated estimates and observed flows

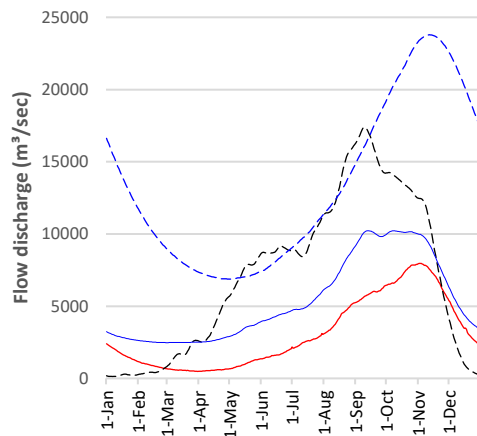
**Congo River at Kinshasa**  
 $R^2 = .93$



**Sangha River at Ouesso**  
 $R^2 = .71$



**Ubangi River at Bangui**  
 $R^2 = .91$



- Observation
- - - - Initial estimate
- - - - Estimate from basin-wide calibration
- Regional estimate

**Figure 3.10** Multi-year average of daily observed flow, initial estimate, estimate from basin-wide calibration at the Congo River at Kinshasa (2004 - 2010) and regional estimate at Sangha River at Ouesso (2005 - 2011) and Ubangi River at Bangui (2003 - 2007). The estimate from basin-wide calibration is the calibrated estimate at Kinshasa gauge while the regional estimate is the calibrated estimate at the Ouesso and Bangui gauges

At the daily level, regressions of modeled versus observed flow yield coefficients of determination ( $R^2$ ) of 0.76, 0.87, and 0.58 and Nash-Sutcliffe coefficients (NSE) of 0.70, -0.31, and 0.23 for Kinshasa, Bangui and Ouesso,

respectively (Table 3.3). Comparing the means, 25<sup>th</sup> percentiles and 75<sup>th</sup> percentiles of daily low flow, centroid of flow and peak flow from the un-calibrated and calibrated models to the observed data from the three validation sites further demonstrates the model improvements from calibration (Table 3.4). Un-calibrated estimates differ from the observations by up to over 100%, while most of the calibrated estimates are within 28% of the observations. Comparison of monthly mean flow modeled over the study period to historical monthly flows from the GRDC stations further indicate confidence in the estimated timing of peaks and lows, although magnitudes and overall values across months show disagreement and agreement comparable to the three contemporaneous validation sites (Figure 3.11 and Table 3.5).

**Table 3.3** Validation statistics of daily flow for gauge sites in Kinshasa, Ouesso and Bangui. ‘O’ is gauge station observation, ‘S’ is model simulation, ‘StdDev’ is standard deviation, ‘R<sup>2</sup>’ is linear regression coefficient of determination, and ‘NSE’ is Nash-Sutcliffe model efficiency coefficient

	<u>Region/City</u>	<u>Kinshasa</u>	<u>Ouesso</u>	<u>Bangui</u>
Gauge	River	Congo	Sangha	Ubangi
Details	Location	Kinshasa	Ouesso	Bangui
	Country	Dem. Rep. Congo	Rep. of Congo	C. A. Rep.
6 to 7 validation - year daily average	Mean (O) m <sup>3</sup> /s	40638	1258	2994
	Mean (S) m <sup>3</sup> /s	40631	859	5486
	StdDev (O) m <sup>3</sup> /s	8981	714	2363
	StdDev (S) m <sup>3</sup> /s	10028	518	2781
Daily-level regression	R <sup>2</sup> %	76	58	87
Other statistics	NSE	0.70	0.23	-.31
	P <sub>bias</sub> %	0	-33	83

**Table 3.4** Means, 25<sup>th</sup> percentiles and 75<sup>th</sup> percentiles of daily low flow (Low), centroid of flow (Cent) and peak flow (Peak) for the observed (*O*), initial un-calibrated (*U*) and calibrated flow (*C*) of the Congo River at Kinshasa, Sangha River at Ouesso and Ubangi River at Bangui. These are the percentiles in the inter-annual variation and the dates of the occurrences of their annual minimum, maximum and mean. Flow magnitude is in m<sup>3</sup>/s. Model improvements are shown in boldface type.

		<u>25th percentile</u>			<u>Mean</u>			<u>75th percentile</u>					
		Magnitude			Date			Magnitude			Date		
		<i>O</i>	<i>U</i>	<i>C</i>	<i>O</i>	<i>U</i>	<i>C</i>	<i>O</i>	<i>U</i>	<i>C</i>	<i>O</i>	<i>U</i>	<i>C</i>
<u>Kinshasa</u>	<b>Low</b>	26949	6765	<b>27626</b>	3-Aug	18-Feb	<b>5-Jun</b>	29178	9511	<b>30834</b>	6-Aug	18-Feb	<b>3-Aug</b>
	<b>Cent</b>	27821	21466	<b>28727</b>	9-Jul	15-Aug	<b>13-Jul</b>	30865	26542	<b>31283</b>	7-Jul	11-Aug	<b>13-Jul</b>
	<b>Peak</b>	56164	44824	<b>57136</b>	16-Dec	18-Nov	<b>11-Dec</b>	59267	51363	<b>61417</b>	15-Dec	13-Nov	<b>12-Dec</b>
<u>Ouesso</u>	<b>Low</b>	480	0	<b>415</b>	3-Apr	9-Jan	<b>2-Apr</b>	625	8	<b>453</b>	25-Feb	9-Jan	<b>15-Mar</b>
	<b>Cent</b>	1096	<b>1231</b>	941	17-Aug	22-Aug	9-Aug	1420	1892	<b>1244</b>	17-Aug	13-Aug	11-Aug
	<b>Peak</b>	2960	<b>2444</b>	1881	28-Oct	27-Sep	<b>17-Oct</b>	3207	<b>2890</b>	2113	6-Nov	5-Oct	<b>19-Oct</b>
<u>Bangui</u>	<b>Low</b>	424	<b>12</b>	2370	31-Mar	15-Jan	<b>4-Apr</b>	482	<b>132</b>	2473	31-Mar	7-Jan	<b>1-Mar</b>
	<b>Cent</b>	5105	12953	<b>5638</b>	8-Sep	19-Aug	11-Aug	5423	13217	<b>6848</b>	5-Sep	16-Aug	12-Aug
	<b>Peak</b>	7210	14798	<b>9823</b>	26-Oct	11-Sep	<b>11-Oct</b>	7961	17394	<b>10218</b>	2-Nov	10-Sep	<b>8-Oct</b>

**Table 3.5** Validation statistics of monthly mean flow for gauge sites in Ilebo, Kutu-Moke, Ubundu, Chembe-Ferry, Ouessou and Bangui. ‘*O*’ is gauge station observation, ‘*S*’ is model simulation, ‘StdDev’ is standard deviation, ‘*R*<sup>2</sup>’ is linear regression coefficient of determination, and ‘NSE’ is Nash-Sutcliffe model efficiency coefficient

	<u>Region/City</u>	<u>Ilebo</u>	<u>Kutu-Moke</u>	<u>Ubundu</u>	<u>Chembe-Ferry</u>	<u>Ouessou</u>	<u>Bangui</u>
Gauge	River	Kasai tributary	Kasai	Congo	Luapula	Sangha	Ubangi
Details	Location	Ilebo	Kutu-Moke	Ubundu	Chembe-Ferry	Ouessou	Bangui
	Country	D. R. Congo	D. R. Congo	D. R. Congo	D. R. Congo	Rep. of Congo	C. A. Rep.
Monthly average	Mean ( <i>O</i> ) m <sup>3</sup> /s	2114	8059	7477	515	1662	3089
	Mean ( <i>S</i> ) m <sup>3</sup> /s	1852	5109	6585	444	896	5325
	StdDev ( <i>O</i> ) m <sup>3</sup> /s	787	2750	1590	304	852	2574
	StdDev ( <i>S</i> ) m <sup>3</sup> /s	761	2304	1613	359	350	2869
Monthly-level regression	<i>R</i> <sup>2</sup> %	93	90	50	56	90	91
Other statistics	NSE	0.80	-0.43	0.04	0.31	-0.33	0
	<i>P</i> <sub>bias</sub> %	-12.4	-36.6	-11.9	-13.7	-46.1	72

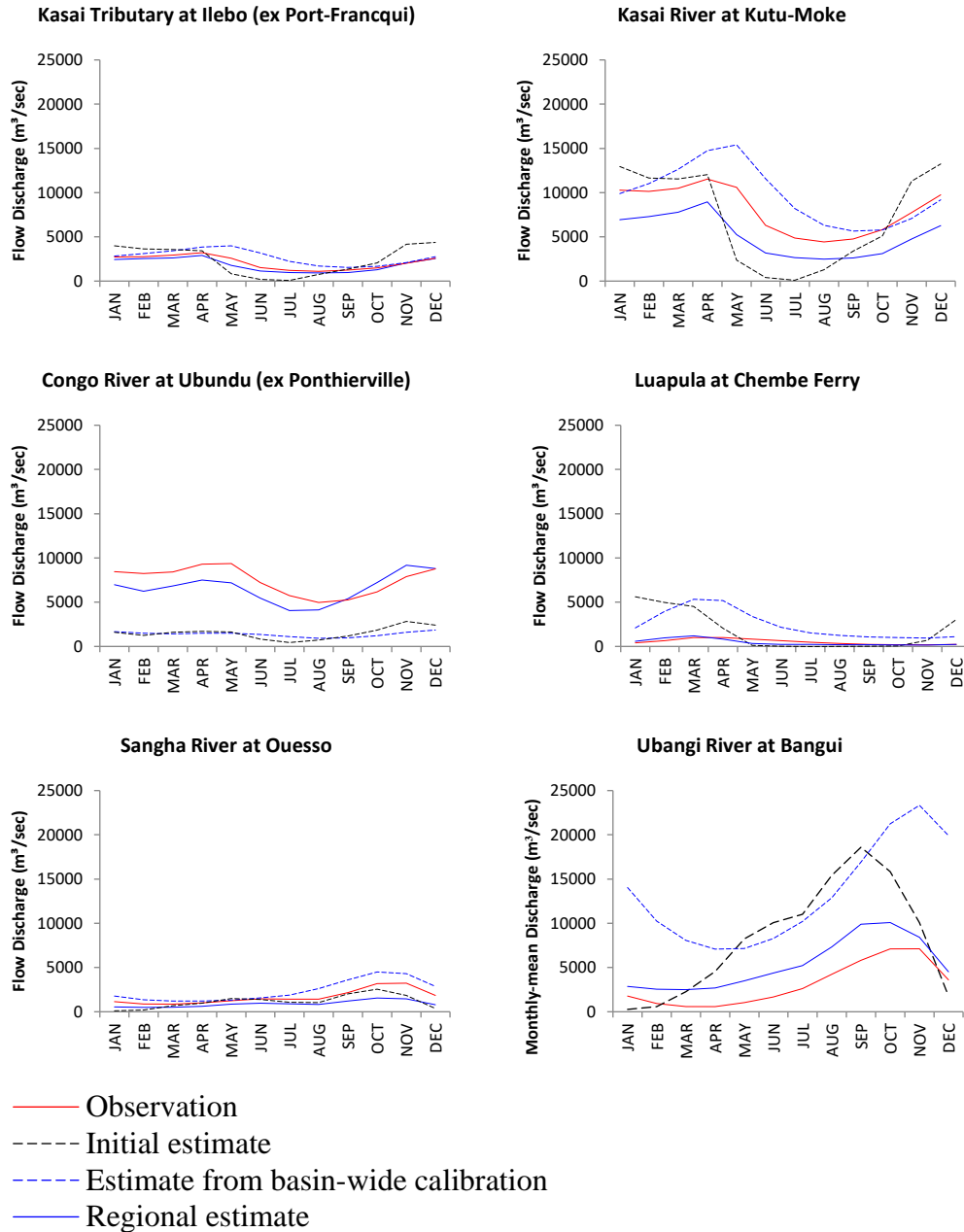


**Figure 3.11** Monthly mean of observed flow, initial estimate, estimate from basin-wide calibration and regional estimate at the four Global River Discharge Database (GRDC) stations and at Bangui and Ouesso

#### 3.5.4. Model interpretation

Time series of daily flow from the calibrated model are consistent with results from analyses made of various satellite-derived precipitation datasets in the Congo Basin (Beighley *et al.* 2011). For example, rainfall data show that 2007 and 2008 were generally wetter than 2003 through 2006, and the present model accurately captures this difference.

Modeled daily streamflow at Bangui shows an over-prediction of low and peak flows during the dry and rainy seasons of all years, affecting the NSE statistic, which is particularly sensitive to the extreme flows (Table 3.3). Nonetheless, the basin-wide level and subbasin wide calibrations successfully account for the majority of the spatial and temporal hydrological patterns of the Congo Basin when evaluated over the entire validation period. More challenging is capturing temporal patterns (timing and shape of seasonal cycle) at the daily level, and here the range of  $R^2$  values from regressing modeled versus observed daily flows are encouraging, particularly at Bangui (0.87). However, even though temporal patterns are well captured, the significant bias and the poor NSE are consistent with the systematic over-prediction of flow magnitude at Bangui.

Despite the difference between the time periods of the data sets, the four GRDC stations provide a valuable additional data source for inter-comparison. Using these data requires the assumption that there has been no significant recent streamflow regime change within the region over recent decades, and we acknowledge that reservations could be raised about the comparison of dated GRDC data and more recent streamflow discharge estimates. The evaluation of model results at the monthly-level for these sites further demonstrates the benefits of model outputs. For example, all four locations exhibit strong agreement in the timing of peak and low flow and in the magnitude of peak and low flows at Ilebo and Chembe Ferry (Figure 3.11). While the timing of

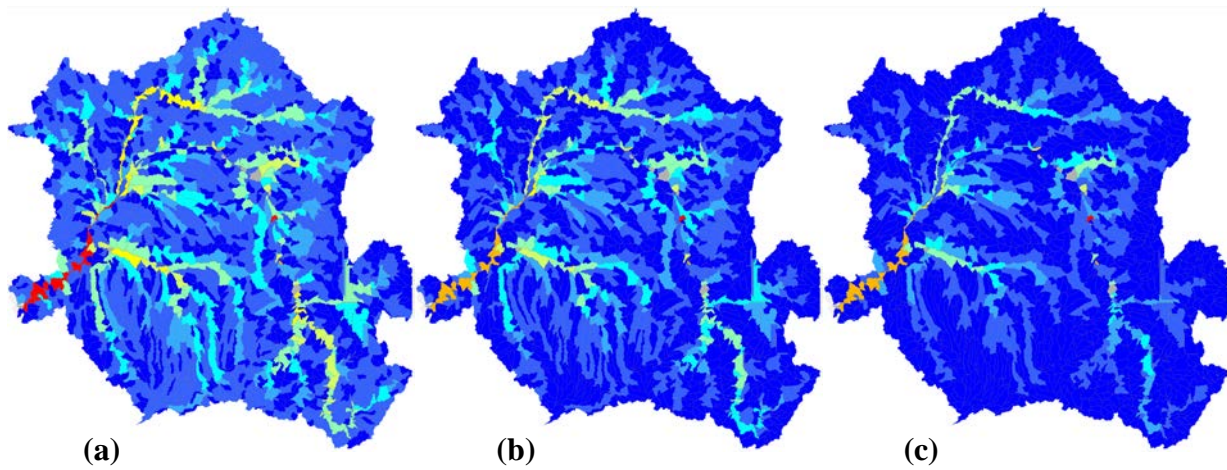
the peak and low flows is accurately estimated for the Kasai River at Kutu-Moke, the magnitude of the flow is overestimated. For the Congo River at Ubundu, the first mode of the bimodal flow regime is underestimated, while the second mode is overestimated. These under-estimates and over-estimates suggest that the regional calibration could be significantly improved. While flow seasonality and timing are successfully captured at all locations, discrepancies in magnitude of the seasonal cycle at some locations suggest that flow discharge may still be biased for some streams across the basin.

The Congo Basin lies in both the Northern and Southern Hemisphere, such that it receives year-round rainfall from the migration of the inter-tropical convergence zone (ITCZ). The passage of ITCZ drives rainy and dry seasons in the Congo Basin (Munzimi *et al.* 2015), and the seasonal progression of the ITCZ influences surface waters of the basin. The geographical distributions of the daily peak, mean and low flow magnitude for the period 1998 - 2012 of calibrated streamflow are mapped in Figure 3.12, and that of the day of minimum and peak flow is mapped in Figure 3.13. Day of minimum flow trends southward from the from early February to late October, with the exception of the northern-most part of the Basin where it occurs in April-May. The trend is reversed for day of peak flow that progresses northward from early February to late October. From July to August, peaks occur mostly in the northern-most part of the Basin. In addition, the equatorial belt is dominated by flows peaking in November and December.

These spatial patterns can be interpreted in the context of the different origins of the water vapor fluxes feeding the ITCZ, which varies in different seasons. In April, the water vapor flux is mostly derived from the Indian Ocean via Tanzania (Suzuki 2011). This is a possible explanation for why the northern-most part of the basin receives much less water than the rest of the basin in this month. In October, the water vapor flux is supplied from within the Congo Basin and brings more water

than the April flux (Suzuki 2011). This is a possible explanation for why the equatorial belt is dominated by flows peaking in November-December. The varying sources of water vapor could also explain the difference between the two peak rainfall days and months in April and October, which consequently drive the high streamflow of the Congo River in November and December, benefiting from the larger volume of water brought in by the ITCZ in October (Munzimi *et al.* 2015). This can be seen in the hydrograph at Kinshasa close to the basin outlet (Figure 3.6, 3.9). To corroborate this point, Lee *et al.* (2011) were able to correlate ITCZ to the spatial pattern of the storage changes in the Congo Basin's seasonally flooded wetlands and floodplains, which agree with the spatial patterns from our model, as an attenuation of flows is driven by the wetlands of the Cuvette.

Beighley *et al.* (2011) reported that as a result of the annual south–north migration of the ITCZ, the equatorial location of the Congo Basin results in two peaks per year, whereas non-equatorial rivers basins have only one peak flow annually. The streamflow model captures this difference (Figures 3.10, 3.11). Streamflows are illustrated by subbasin for daily maximum, mean, and minimum volumes in Figure 3.12.



Daily flow in m<sup>3</sup>/sec

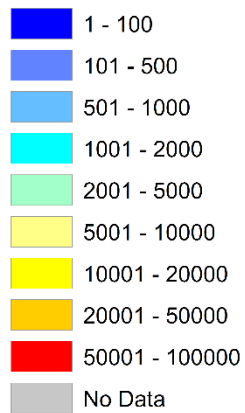


**Figure 3.12** Spatial distribution of calibrated daily (a) high, (b) mean and (c) low flow magnitude over the 15 years of study (1998 - 2012) per subbasin. In each subbasin the flow condition (magnitude) of the corresponding river reach is represented

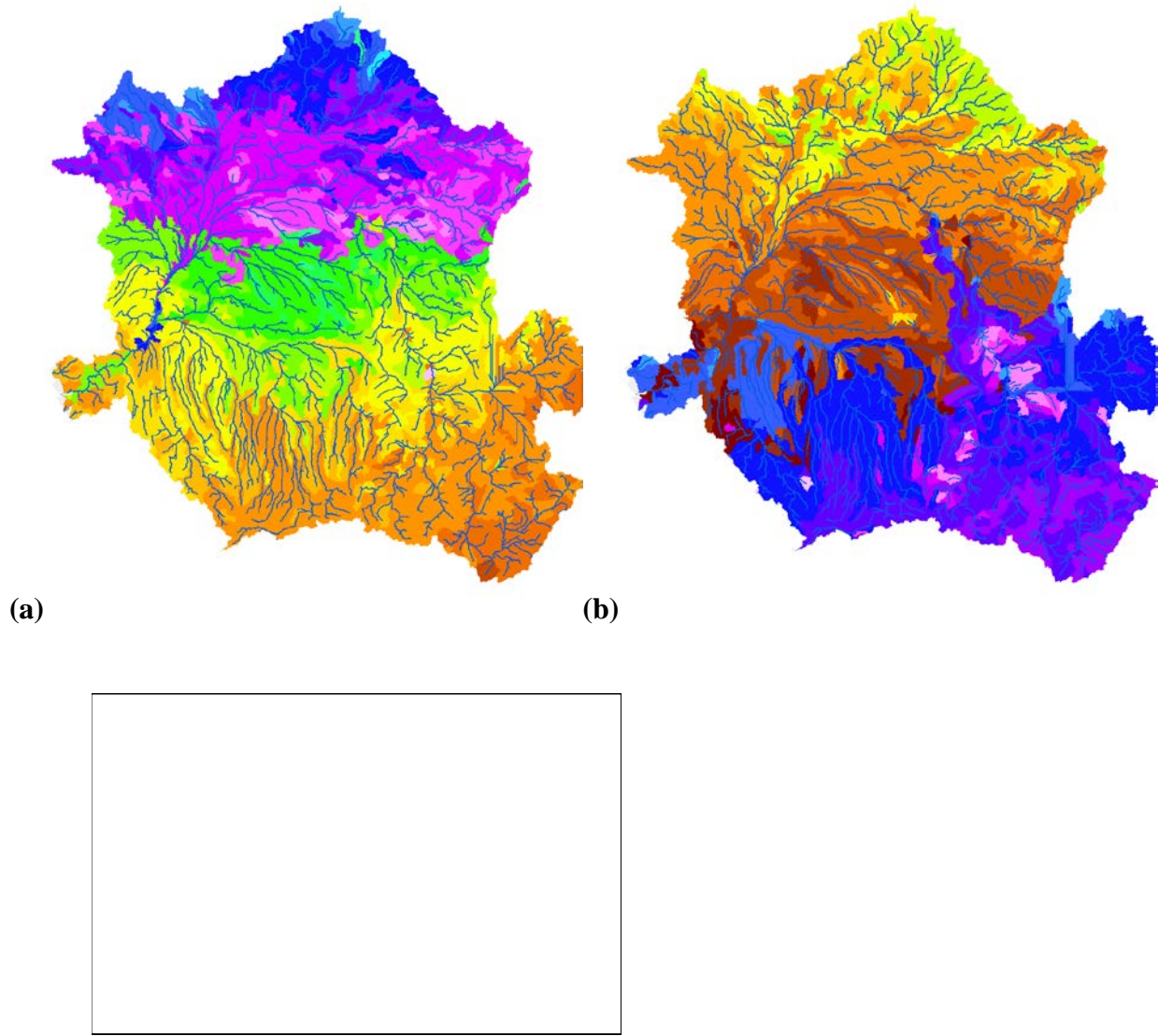


**Figure 3.13** Spatial distribution of calibrated day of (a) lowest flow and (b) peak flow, based on the modeled daily mean flow averaged over 1998 – 2012

**3.6. Conclusion**

The Congo River Basin has been modeled to capture the spatial and temporal variations in streamflow using a basin-wide and subbasin ensemble model. The two-step approach to the model and its calibration was required mainly due to the presence of a large interior basin, the Cuvette Centrale, which slows downstream flow. Basin-wide calibration involved input data adjustment

and selection of appropriate model routines and parameters to slow the flow of water across the basin; regional calibration involved a different set of adjustments and a simple bias correction to adjust flow of river subbasins. Agreement with *in situ* data is markedly improved following model calibration, compared with default initial parameterization (Table 3.5), including for set-aside validation data. While flow seasonality and timing are successfully captured at all locations, discrepancies in estimated and actual discharge at sites suggest that results are likely biased for many streams across the basin.

Previous studies have shown that hydrological mechanisms in the Congo Basin, including the effects of the Cuvette Centrale, are not well understood due to a scarcity of gauge data. Time-series remote sensing data can leverage sparse *in situ* measurements to enable improved understanding of flow dynamics through the use of semi-distributed hydrological models. The GeoSFM semi-distributed hydrological model characterizes the geospatially explicit timing and magnitude of flow across large basins such as the Congo River. Results from this chapter using GeoSFM demonstrate an acceptable level of performance of the model in estimating timing and seasonality of flow in the Congo Basin, with considerable bias in estimates of flow volumes for subbasins. Flow characterization at Kinshasa is robust for both timing and volume, with implications for its use in assessing hydropotential downstream from Kinshasa, one of the river reaches with the greatest potential for hydroelectric development. By definition, more gauge data distributed widely geographically would reduce model uncertainties across the Congo Basin.

The Congo Basin is the site of increasing human populations and land cover change, including deforestation, which is expected to alter the Basin's hydrology. The humid tropical forests of the Congo Basin are also some of the more seasonal and overall drier such forest in the equatorial tropics (Malhi *et al.* 2013), making them potentially especially susceptible to climate

change. Models such as the one presented here can help to establish baseline information on flows throughout the Congo Basin and provide a basis for assessing future hydrologic changes caused by changes in land cover and climate. Results could be used to support operational short-term management, monitoring and planning decisions in the Congo Basin.

While numerous studies of land cover and land use change (LCLUC) in the Congo Basin exist (e.g. Zhang *et al.* 2006, Hansen *et al.* 2008, Defourny *et al.* 2011, Ernst *et al.* 2013, Molinario *et al.* 2015, Ickowitz *et al.* 2015), studies of the hydrological responses to climate change, seasonal variability and LCLUC could benefit from improved daily streamflow models. Model of the effects of climate change on streamflow require knowledge of the flow characteristics of the river basin in question in order to estimate which watersheds are sensitive to temperature and which watersheds are dominated by the amount and timing of precipitation (Smith *et al.* 1998, Washington *et al.* 2013). A rainfall-based climate classification, derived from TRMM or similar products, of the Congo Basin, could serve as a starting point (Munzimi *et al.* 2015). A climate classification could be used as the basis for grouping rivers and streams within the basin by climate type to facilitate comparisons of runoff characteristics. Finally, the improved estimates of streamflows from this chapter can support more reliable assessments of possible future scenarios, including those accounting for the effects of the El Niño Southern Oscillation (ENSO) and other climatic cycles (e.g. Amarasekera *et al.* 1997) and the effects of land-use change on the Congo Basin's hydrology

## Chapter 4: Assessment of streamflow response to forest conversion in the Congo Basin

### **4.1. Introduction**

#### 4.1.1. Congo Basin hydrology and water resources

One major possible future scenario requiring assessment is the one accounting for the effects of land use land cover change on the Congo Basin's hydrology. The improved estimates of streamflows from the previous chapter could support a more reliable assessment of the mentioned change. Considering regional demands (Mandelli et al, 2014), the Congo Basin is seen as a vital resource for water and energy, the later which has mostly yet to be exploited. Hydropower is an important renewable energy alternative that could potentially support the regional economy while facilitating reductions in greenhouse gas (GHG) emissions, including via reducing deforestation. Various initiatives for small- to large-scale hydropower generation have been proposed throughout the basin, yet few include careful consideration of limiting factors, a major one being the dependence of water flows on the distribution of vegetation and potential impacts of forest conversion.

The greatest interest is in the region around the Inga Falls, the world's largest waterfall, located 150 km upstream from the Congo River's mouth in the western Democratic Republic of the Congo (DRC). There currently are two hydroelectric dams, Inga I and Inga II. Hydropower production at Inga is mainly regulated by run-of-the-river power plants that depend directly on the water-discharge regime, in contrast to reservoir-based plants that can compensate for river-flow variation (Beniston and Stoffel, 2014).

Planning is underway for a third Inga dam as well as a mega-dam, the Grand Inga to power multiple African countries (Sambo, 2008; Green, N et al, 2015; Taliotis, C et al, 2014). A non-storage, “run-of-the-river” design is also planned for the Grand Inga hydroelectric project, in which only a relatively small reservoir would be created to back up the power of the river's flow (Showers 2011). The DRC had set October 2015 as the date for the launch of the first phase of this largest hydroelectric plant in the world (DRC press release, 2013), making this the main hub of Africa’s hydroelectric potential (Sofreco et al., 2011). However, on July 2016 the World Bank withdrew its funding following disagreements over the project. The proposed Inga dams have an estimated potential of between 39,000 and 44,000 MW, more than twice the equivalent of the power of the world's current largest dam, the Three Gorges in China. However, only a small portion, roughly 1,700 MW, of this potential is used and less than half of this is operational (Sofreco et al., 2011).

#### 4.1.2. Congo Basin land cover change

The Congo Basin forest is the world’s second largest, contiguous area of moist tropical forest. The Congo Basin’s streams and rivers are susceptible to human activities in the region, facing major threats mostly via conversion of forest to agriculture and plantations. In the basin, forest cover is mainly converted into a mosaic of agriculture, primarily in the form of traditional shifting cultivation, plantations and fallow interspersed with small roads and villages, a *rural complex*, with relatively low tree cover (Molinario et al, 2017).

Forest degradation is another form of disturbance, where trees are selectively harvested for timber products or fuelwood (Tegegne et al., 2016). With the major part of the population reliant on fuelwood, wood extraction will likely continue as an important driver of forest disturbance.

Current rates of forest cover conversion are less than those in Brazil and Indonesia, yet they are increasing (Turubanova et al 2018) and are likely to increase more rapidly in coming years given the DRC's rapid population growth (United Nations 2017) and migration further into forest (Nackoney et al 2014).

#### 4.1.3. Hydrological dynamics and land cover change

Flow dynamics of rivers are closely linked to their basins' ecosystems, with vegetation cover as a primary governing factor (Brauman et al. 2007). While the ecosystem itself does not create water, it does affect the attributes and modify the amount and the timing of water moving through the landscape by reducing available water via ET and groundwater recharge (Brauman et al. 2007). River flows can be greatly altered following significant LCLUC in a basin, with effects including altering the timing, amount, and kind of inputs of water, light, organic matter and other materials to a channel, water flow and water quality (eg. Strayer et al., 2003). Modifications of the Congo River's runoff patterns are mainly caused by agricultural encroachment into forest and pose major threats to water supply sources (Partow, 2011).

As in other regions, the Congo Basin is under increasing pressure from LCLUC that could cause increases in runoff coefficients (Calder 1998, Parida 2006) and induce stress on the hydrological systems' ability to meet the demands of growing human populations. The distribution of forest-cover in particular influences hydrologic processes through rainfall interception, evapotranspiration (ET) and land-surface roughness. These effects can be considered as both direct, accounting only for the effects after rainfall, and indirect, accounting for the vegetation's influences on the source and amount of rainfall itself.

#### *4.1.3.1. Direct effects*

Direct effects of LCLUC on river flow are primarily via the effects of surface roughness on flow rate. This is characterized by the Manning's roughness coefficient, which represents the resistance to surface flow exerted by the land surface and depends on vegetation cover (Kalyanapu et al. 2010). Change from forest to agriculture reduces resistance and thus shortens the rise time of the streamflow hydrograph, producing a greater unit hydrograph peak and increasing the frequency of high and low flows. Sangvaree et Yevjevich (1977), in a study in eight different States of the United States of America, found that unit-hydrograph peaks of a catchment with mostly agricultural cover was two to four times greater than those for mostly forested catchments. They also found that an increase in forest cover decreases the peak runoff, with a half-forested catchment having a peak flow of the unit-hydrograph about 2.4 times greater than that of a fully-forested catchment. The peak flow of the unit hydrograph of a fully-agricultural catchment was over four times greater than that for the forested catchment. In their study, they also cite two previous reports (Kar 1967, Bell 1968) that both found longer rise times for mostly forested catchments than for others.

Change from forest to agriculture can also lead to slower soil infiltration, lower soil moisture and greater surface runoff. Yimer et al. (2008), in a study in Ethiopia highlands, found that infiltration capacity and soil moisture content were 70% less in cultivated versus forested land. They attributed this to changes in soil structure caused by surface soil compaction from tillage coupled with a lower soil organic carbon content. Groundwater recharge is likely to be affected by these land surface disturbances too and should in turn affect the base flow, the portion of the streamflow delivered through groundwater seepage. Groundwater is typically primary source of

running water in a stream during dry weather. However, there is a lack of information on fundamental recharge processes in the Congo Basin at local and basin scales and how these could be affected by land use (Alsdorf et al. 2016). An improved understanding of surface water-groundwater interaction mechanisms would greatly assist basin-wide planning. Nonetheless, fundamental information from studies in other regions allow a parameterization of models sufficient for the simulation of broad effects of LCLUC on the Congo Basin's hydrology.

#### *4.1.3.2. Indirect effects*

Coe et al (2009) and Bonan (2008) argued that river discharge should increase proportionally with the area deforested in a catchment, since a decrease in landscape-level leaf area index (LAI) in any deforestation experiment results in reduced ET and increased runoff. Coe et al (2009) described large-scale observations of the response of river discharge to deforestation and conversion to agriculture: ET decreases as native vegetation is replaced with less water demanding pasture and crops, and annual discharge increases. Numerous global climate model (GCM) simulations of large-scale deforestation also showed regional precipitation decreases because of the combined influences of increased albedo, decreased surface roughness and decreased water recycling that accompany deforestation (eg. Costa, 2005; Delire et al., 2001; Dickinson and Henderson-Sellers, 1988; Malhi et al., 2008a). Coe et al (2009) concluded that since long-term discharge is the residual of the precipitation minus ET, any decrease in precipitation decreases the discharge and offsets some or all of the increase in discharge that may result from a local decrease in ET.

Bonan et al (2008) also stated that forests mediate the hydrologic cycle through ET. Their climate model simulations showed that tropical forests maintain high rates of ET, decrease surface air temperature, and increase precipitation compared with pasture land. They added that in

Amazonia surface warming arising from the low albedo of forests is offset by strong evaporative cooling. They noted that similar results are seen in tropical Africa and Asia. Large-scale human activities that involve change in land cover, such as tropical deforestation, are likely to modify climate through changes in the water cycle (Eltahir and Bras, 1996). This would be the case in the Congo Basin where a significant amount of precipitation is recycled via ET from local forests.

Eltahir and Bras (1996) also described the contribution of local ET into local precipitation, in a study for different regions. The authors described the characteristic regional-water cycle: the formation of precipitation from both locally recycled water vapor from local ET and atmospheric water vapor that is transported from outside the region. They defined the relative contribution of recycled precipitation from local ET to total precipitation as the recycling ratio. Dyer et al (2017) estimated that the recycling ratio for moisture from the Congo Basin at about 25%, while in both rainy seasons the southwestern Indian Ocean contributed about 21%. They claimed that the hydrology in areas with high recycling ratios are most sensitive to forest clearing because of the impact of changes in ET on precipitation.

The scale of change in forest conversion over a large region is a critical factor. Coe et al (2009) found that for the Amazon River “at the micro scale to meso scale, deforestation generally results in decreased ET and increased runoff, and discharge” and at the larger scale “atmospheric feedbacks may significantly reduce precipitation regionally and, if larger than the local ET changes, may decrease water yield, runoff and discharge.” Their simulations indicate that where deforestation has not yet exceeded 25% of the watershed area, any changes to discharge are probably too small to be detected (<10%). They also concluded that where it has exceeded this, the decrease in the net discharge indicated that the regional precipitation changes resulting from

the feedback with deforestation were larger than the local ET decreases and thus dominated the discharge response.

These studies corroborate Shukla et al (1990), who previously simulated Amazonian forest conversion and regional hydrology. In their model, the removal of Amazon forests and its replacement by a degraded pasture reduced annual precipitation by 642 mm y<sup>-1</sup>, or 26%, and reduced ET by 496 mm y<sup>-1</sup>, or 30%. The authors explained that because ET from the forest is one of the important sources of water vapor for precipitation in the Amazon, a reduction in ET should lead to a reduction in precipitation. Their value of modeled ET minus precipitation increased in the deforestation simulation and modeled runoff decreased as a result because the decrease in precipitation was more than the decrease in ET. Their results suggest that a complete and rapid conversion of Amazonian forest could have irreversible impacts on hydrology.

#### 4.1.4. Hydrological dynamics and land cover change

Understanding the hydrology of the Congo River requires a model-based approach given the paucity of gauge data. As described in the previous chapter, Munzimi et al (2019) developed, calibrated and validated a model of Congo River daily flow. The Geospatial Streamflow model (GeoSFM) has proven to be particularly suitable for characterizing flow in regions with limited *in-situ* monitoring such as the Congo Basin. The GeoSFM takes physical parameters, including soil characteristics associated with land-cover types, as inputs. For a given model parameter, the value assigned to sub-basins corresponds to the dominant land cover class, soil class and/or terrain represented in a sub-basin.

When studying hydrological responses to land cover and climate changes, Zhou et al (2014) suggested that water retention, i.e. water residence time in soil, and soil infiltration capacity are the most critical parameters, in combination with the ratio of precipitation to ET. The model sensitivity they reported corroborates the importance of the four most impactful GeoSFM parameters identified in Munzimi et al (2019) Congo Basin modeling: residence time for the interflow reservoir and for the base-flow reservoir, river-loss factor, river floodplain loss factor and kinematic wave celerity.

Munzimi et al (2019) adjusted these parameters in GeoSFM for the current LC distribution in the Congo Basin and produced an accurate simulation of flow timing and low-flow and peak-flow magnitudes over a 15-y period for the Congo River at the Kinshasa gauge site (Figure 4.1). Model results for average daily flows at this site are within 1% of the reference data from the gauge (Munzimi et al 2019). This gauge is the closest to the Inga site, situated 225 km downstream Kinshasa, and we expect model performance to be similar for the Congo River at Inga. The flow of the Congo River is strongly seasonal. Rainfall comes from both northern and southern hemispheres of the Basin, with alternate and asymmetrical dry and rainy seasons between both hemispheres (Munzimi et al, 2015). Southern-hemisphere rainfall peaks in October, providing the greatest contribution to the river's annual flow, while northern-hemisphere rainfall peaks in March. This results in a high-flow period for the Congo River in November-December, a lesser one in April, a minimum-flow period in May and an extended period of modest flow from May through September.

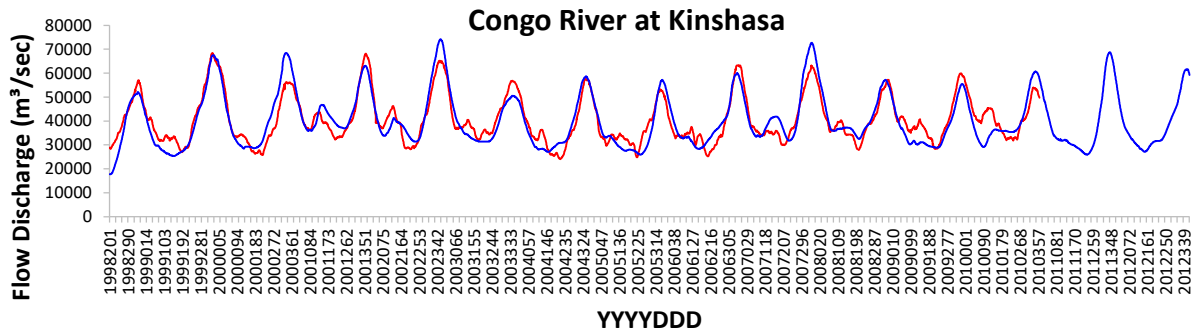


**Figure 4.1** Fifteen years of observed (red) and simulated (blue) daily flow discharge of Congo River at Kinshasa from Munzimi et al (2019). As shown for each year there are two peak flows and two low flows, which are also featured/found at Inga, denoting a bimodal flow regime. The bimodal flow exhibits a peak in December timeframe and a secondary peak in May that is approximately 50% of the December streamflow. The two low-flow periods occur in March and July (Munzimi et al, 2019).

Direct effects of LCLUC can be simulated by altering land cover, which alters the associated key parameters, for different LCLUC scenarios. Since users can adjust ET and precipitation values based on assumptions about changes associated with LCLUC, the GeoSFM model can also be used to assess indirect effects and combined effects by simulating climatic feedbacks of forest conversion. As an indication of precipitation change impact on discharge, Laraque, et al (2001) compared observed precipitation and discharge in the Congo Basin based on few gauges with long-term data from rain and river gauges. They compared decadal averages for the Ubangi and Sangha basins and the overall Congo Basin. Annual precipitation during the last dry period, 1971-1993, was on average less than the 1951-1993 by 4% for the Ubangi, by 6% for the Sangha and by 4% for the entire Congo Basin. The decreases in discharge during the same dry-period and for the same basins were much larger, 34%, 22% and 13%, respectively. By 2000 less than one percent of the forests in these basins had been cleared (Hansen et al, 2008). These differences suggest that LCLUC was unlikely the cause for the reductions in flow reported in the latter period, although it does not exclude the possibility larger areas of LCLUC could in the future. They also suggested

that very modest reductions in precipitation can cause large reductions in discharge in the Congo River and its major sub-basins.

The same conclusions have been drawn from two studies in large basins within the Amazon. In a study in the Xingu River in eastern Amazonia, Panday *et al.* (2015) reported that model simulations over the period from the 1970s to the 2000s suggest that climate variations alone accounted for a 14% decrease in annual discharge, due to a 2% decrease in precipitation and 3% increase in evapotranspiration. They also reported that deforestation alone caused a 6% increase in annual discharge, as a result of a 3% decrease in evapotranspiration. Mohor *et al.* (2015) also found that when changes in precipitation are small in the Amazon Basin, there is a greater influence of evaporation changes on the Amazon discharges, resulting in opposite sign between precipitation and discharge changes. They added that strong impacts on the dry-season discharges have also been verified in the observed discharges in the Amazon basin; they are related to the late demise of the dry season associated with the warming in the tropical North Atlantic. They concluded that on average, changes in the annual hydrological cycle indicate a longer duration of low discharges in most of the projected scenarios associated with precipitation decreases. Thus, according to them, Amazon hydrological regime is very sensitive to environmental changes and seasonal changes in precipitation, together with the limitation of the maximum installed capacity, explain the decreasing energy production, even when the annual average precipitation increases.

#### 4.1.5. Purpose

Motivated by the importance of the Congo Basin as a water resource for Africa and proposed expansions of hydropower, we sought to estimate the direct and indirect effects of expansion of the rural complex into forest on the river's hydrology and hydropower potential. Using the

GeoSFM calibrated by Munzimi et al. (2019), we modeled the impact of LCLUC on flow regimes by setting input parameters based on current LC and modifying them for a series of LCLUC scenarios. Hydropower potential was evaluated based on modeled total annual and seasonal flow.

## 4.2. Data and Methods

### 4.2.1. Data

Fifteen years of daily precipitation derived from the joint NASA/JAXA TRMM 3B42 product (Huffman *et al.* 2007) and daily ET from NOAA Global Daily Reference Evapotranspiration product (GDET; Senay *et al.* 2008) converted to potential evapotranspiration by GeoSFM provided the baseline for current climate. Precipitation was averaged over 15 years (1998-2012) per sub-basin unit (Figure 4.2). Current land conditions are from raster data on soil type and texture from the United Nations Food and Agriculture Organization (FAO) Digital Soil Map of the World (FAO 1995; 1971–1981), and topography is from NASA’s Shuttle RADAR Topography Mission (SRTM; Van Zyl 2001; Rodriguez *et al.* 2006), resampled from 90 m to 180 m to increase computational efficiency. Land cover for the basin is compiled from raster data on tree cover and vegetation type (Potapov *et al.* 2012), derived from Landsat and MODIS imagery, and wetlands extent, derived from Landsat, MODIS and MERIS (Bwangoy *et al.* 2010; Clevers *et al.* 2004). The land-cover map estimates that the basin is 59% forest and woodland, 11% wetland, 7% water bodies, and the remainder savannah and human settlements (Munzimi et al. 2019). This product was then used to assign majority land-cover classes to each sub-basin unit (Figure 4.3).

GeoSFM partitioned these data into 2,950 sub-basins, the modeling units, averaging 1501 km<sup>2</sup> each and covering the study area, the Congo Basin (Munzimi et al. 2019). We assigned averages for continuous variables and majorities for discrete variables to each sub-basin to

parameterize a baseline. We defined four scenarios of LCLUC, where 25%, 50%, 75% and 100% of forest in the basin was converted to rural complex. New areas of rural complex were distributed spatially by buffering around existing ones, based on Molinario et al. (2015). If this caused a change in the majority land cover from forest to rural complex in a sub-basin, then the new majority class was assigned (Figure 4.4). This requires a re-calculation of land-cover derived attributes, which are calculated in GeoSFM based on the combination of land cover, on which surface roughness depends, topography and soil type.

To account for indirect effects, precipitation and ET were adjusted per sub-basin depending on majority land cover. We used a recycling ratio for precipitation of 25%, from Dyer et al (2017), where forest is converted to rural complex.

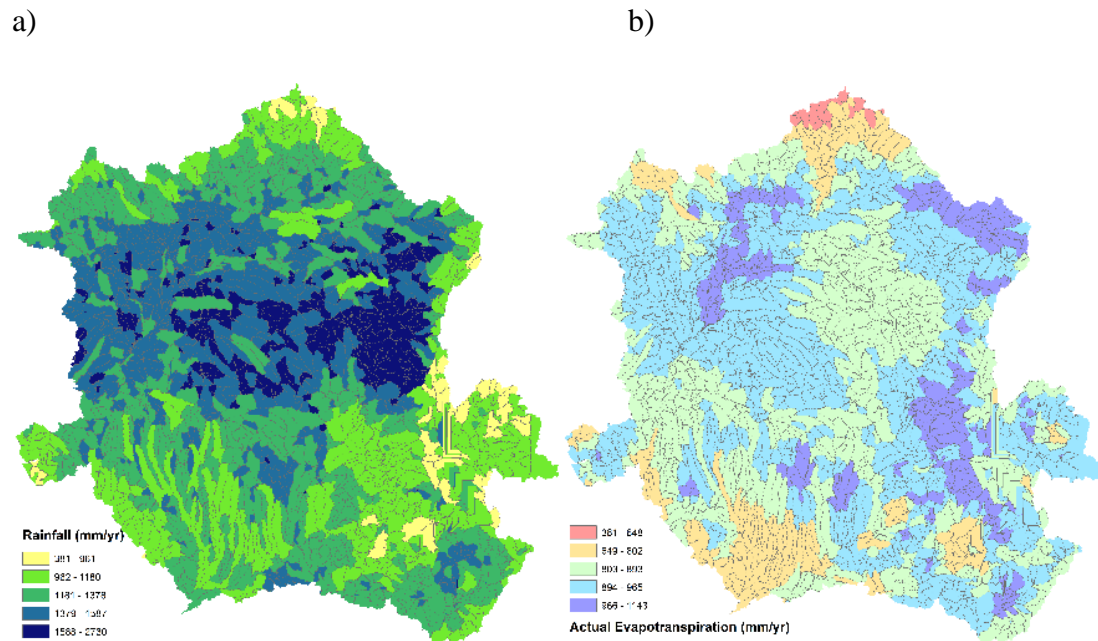


**Figure 4.2** Satellite-derived estimates of bioclimatic data inputs used in the GeoSFM model: a) current annual precipitation and b) evapotranspiration. See main text for data sources.

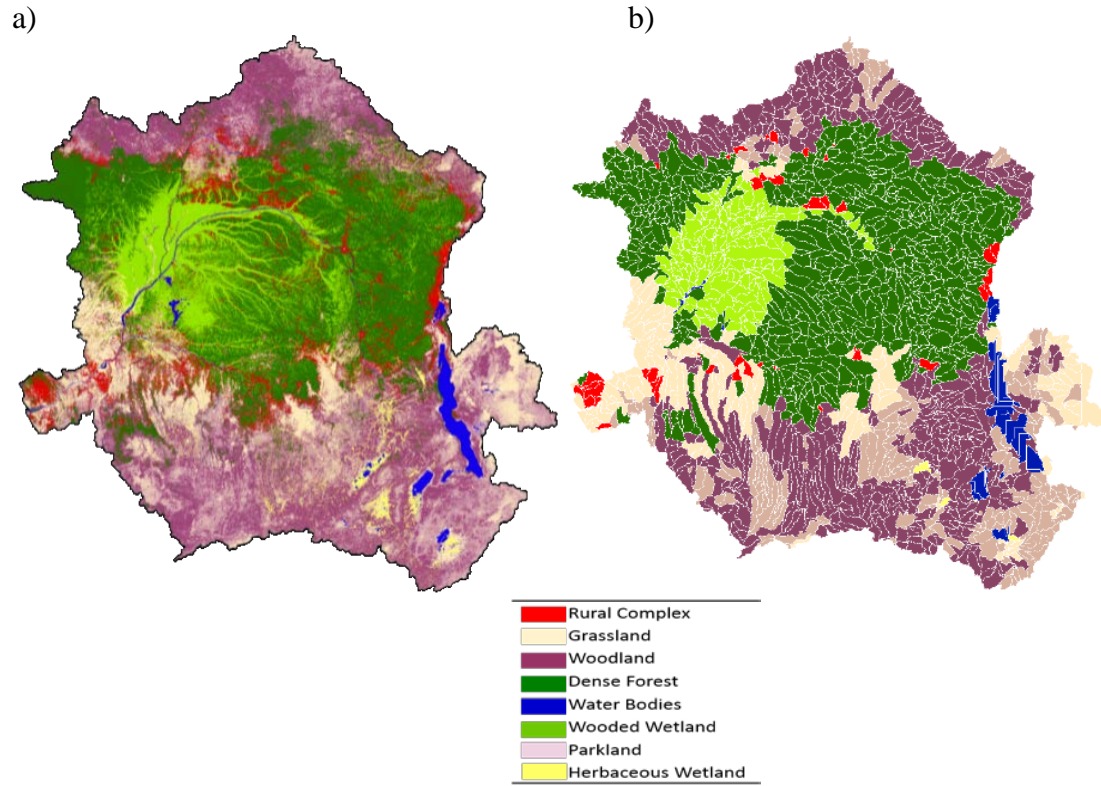


**Figure 4.3** Land cover classes used in the GeoSFM model: a) at full resolution compiled from a suite of existing, satellite-derived data products and b) majority values assigned to the 2,950 sub-basin units of the model. See main text for data sources.

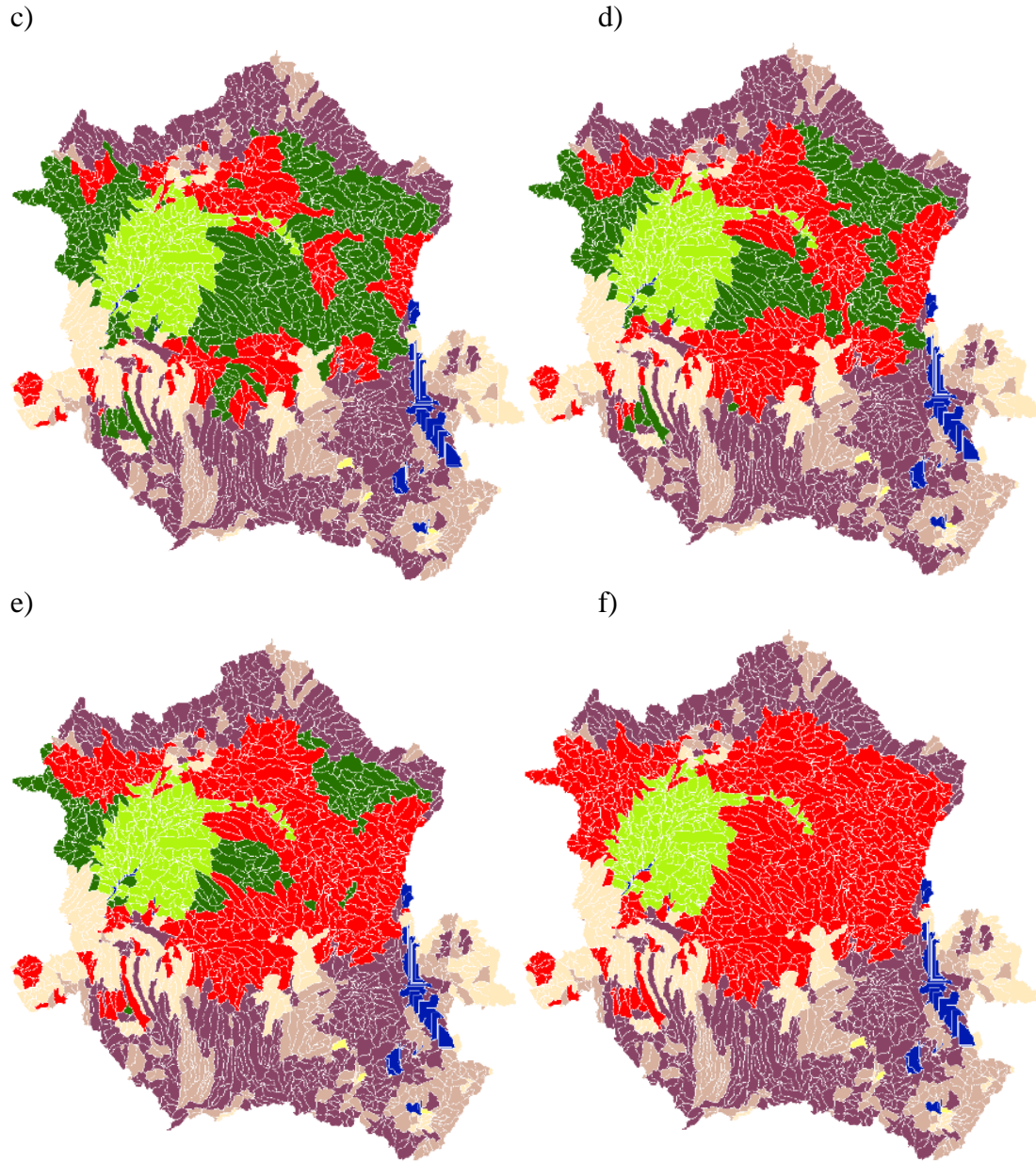


**Figure 4.4** Definition of four scenarios of land-cover change where a) 25%, b) 50%, c) 75% and d) 100% of forest is converted to rural complex and the resulting majority land-cover class is assigned to each sub-basin polygon. Legend is the same as in Figure 4.3.

#### 4.2.2. Direct effects

We prepared the input files, performed a soil-moisture accounting, and then routed the output through the river system. GeoSFM contains algorithms for estimating 30 flow-simulation parameters for each catchment and river reach, based on elevation, land cover and soil data. Land

cover influences both the rate of runoff generation and the rate of overland-flow transport. Its derived parameters are either from land cover alone or land cover combined with elevation and/or soil derivatives (Asante *et al.* 2008).

GeoSFM's hydrologic module then calculated water balance from time series-data of precipitation and ET and routes the balance through the river basin based on the above pre-processed data, estimating simulated soil moisture, runoff and transport. Accounting of soil moisture allowed us to estimate water directed to streamflow through the soil. We used a non-linear soil-moisture accounting routine, one of the two routines available in GeoSFM to perform the vertical separation of precipitation into atmospheric releases, surface runoff, and sub-surface flows. We then used a diffusion-analog routine, one of the three river-flow transport routines in the module, for simulating the horizontal movement of water through the river network.

We repeated this process for each scenario, with parameters values based on the distribution of LCLUC in each, including the four most impactful parameters related to surface roughness and soil infiltration. In GeoSFM, the residence time for the interflow reservoir and the residence time for the baseflow reservoir are required for soil moisture accounting, while river loss factor, river floodplain loss factor and kinematic wave celerity are required for river flow transport. In implementing the soil-moisture accounting and diffusion-analog routines, a series of algorithms relate these parameters to land-cover characteristics, as described in Asante et al (2008). The Non-linear Soil Moisture Accounting (NSMA) module represents sub-surface processes by creating separate soil layers within which interflow and baseflow occur. The runoff-curve number method from the Soil Conservation Service (SCS), which takes into account vegetation, soil type and antecedent moisture, is used to partition runoff into surface and interflow components. The Green and Ampt equation is used for extracting water from the interflow soil layer to feed the baseflow

soil layer. The curve number is used to generate excess precipitation when the daily precipitation is higher than 20% of the runoff:

$$\text{RUNOFF} = (\text{precipitation} - 0.2((1000/\text{CN}) - 10))^2 / (\text{precipitation} - 0.8((1000/\text{CN}) - 10)) \quad (1)$$

where RUNOFF is runoff from excess precipitation in mm, precipitation is in mm and CN is runoff-curve number (unitless). Water infiltrated in the soil is gradually released from the interflow and baseflow reservoirs for transfer to the nearest stream, downstream through the stream network and finally to a terminal point in an ocean or inland lake. The rate of release of water from each of these reservoirs is governed by a linear-response function with residence times obtained from the input river characteristics. The responses for the fast- and slow-interflow and baseflow reservoirs are:

$$\text{INTERFLOW}_{\text{fast}} = \text{INTERFLOWSTOR}_{\text{fast}} / \text{LAGIRF} \quad (2)$$

$$\text{INTERFLOW}_{\text{slow}} = \text{INTERFLOWSTOR}_{\text{slow}} / (0.5 / \text{LAGIRF}) \quad (3)$$

$$\text{BASEFLOW} = \text{GWSTOR} / \text{LAGGWT} \quad (4)$$

where INTERFLOW is the response for the fast or slow interflow (interflow residence time) in days, INTERFLOWSTOR is the reservoir for soil moisture storage (mm), LAGIRF is the linear reservoir routing constant for interflow runoff, BASEFLOW is the baseflow residence time in days, GWSTORE is the storage in the ground water reservoir (mm) and LAGGWT is the linear reservoir routing constant for groundwater runoff.

#### 4.2.3. Indirect effects

To model the additional effect of climatic feedback, the LCLUC in each scenario is used to adjust precipitation and ET and the resulting water-balance input to the model. For polygons that changed

from majority forest to majority rural complex, ET is reduced by 8% and precipitation by 2%. To obtain these values, we retrieved and compared ET from the two land cover classes, which differ per their tree density and canopy cover. In less dense class such as rural complex, ET is 8% less than in forested areas in the baseline data. Since we assume a recycling ratio of 25%, we adjusted precipitation proportionally, resulting in a precipitation reduction of 2%, where sub-basin polygons changed from majority forest to majority rural complex. This results in an adjustment factor of 0.92 for ET and 0.98 for precipitation in converted areas. The new values of water balance were used for a second series of scenarios that simulated the combined direct and indirect effects of forest conversion.

#### 4.2.4. Hydropower potential

The Inga site has a high-flow profile and low head, i.e. a small vertical distance between the highest and lowest water surface within a specified distance, the penstock length. The two key calculations to estimate the variation in the dam's hydropower potential are the flow discharge variation and the head at stream level. We simulated monthly means of potential from monthly means of flow discharge, with the head at stream level, calculated from NASA SRTM digital elevation model (DEM), held constant. The head grid was computed by:

$$\text{Head} = L \sin \theta \quad (5)$$

where L is penstock length, set at 100 meters and  $\theta$  is the slope generated from the elevation grid. We aggregated and averaged monthly-flow discharge from the daily flows estimated by Munzimi et al. (2019) for the baseline and then from the daily flows for the model results of each scenario. The variation of the gross hydropower potential was computed for a 100-m section of the Congo

River at Inga using the head at that location, extracted from the head grid computed from slope derived from the elevation grid (equation (5)). The variation of power available at Inga was calculated from the variation of flow discharge in each scenario:

$$\Delta\text{Power} = H \Delta Q \rho g * 0.001 \quad (6)$$

where  $\Delta\text{Power}$  is change in hydropower potential in Kilowatts (KW),  $H$  is head in m,  $\Delta Q$  is change in flow in  $\text{m}^3/\text{s}$ ,  $\rho$  is water density set at  $1000 \text{ kg m}^{-3}$ , and  $g$  is gravitational acceleration  $9.81 \text{ m s}^{-2}$  (adapted from Asante et al, 2007).

### **4.3. Results**

#### 4.3.1. Flow discharge

Routines for river-flow transport simulated the horizontal movement of water through the river network. As surface runoff is channelized, the timing and amount of runoff generation affects the routing of the water in the river channel. The timing and magnitudes of peak and low flows of the Congo River at Inga for all conversion scenarios are shown in Figure 4.5. Their magnitudes and trends of change differ across conversion scenarios and seasons. The basin has two dry seasons and two rainy seasons, which are of different lengths. These can be characterized as a minor dry season from January 1 to February 14 (Early dry season, ED), a minor rainy season from February 15 to May 14 (Early wet season, EW), a major dry season from May 15 to September 14 (Late dry season, LD) and a major rainy season from September 15 to December 31 (Late wet season, LW) (Figure 4.6).

Figure 4.5 illustrates significant changes from baseline peak flow after forest conversion for all scenarios. However, change of peak flows are not as significant as changes low flows across the

four conversion scenarios without and with climatic feedback. Additionally, as more forest is converted, the rise time and recession time of the hydrographs get faster. With more forest converted, there is more rainfall-runoff on the surface rising fast to the peak during the rainy season but there is less water available from soil during the dry season, explaining the faster recession.

Regarding the magnitude and trend of change of the secondary peak, from April to May (EW following the ED season), a delay can be observed in comparison to the baseline for all conversion scenarios. This might be caused by major decrease and slow-down of groundwater recharge during the ED that precedes EW as a result of forest conversion.

All LCLUC scenarios without climatic feedback produce higher peak hydrographs at the Congo River at Inga (Figure 4.5). They also produce minimums in the ED season that significantly decrease such that the annual minimum has shifted from the LD season to the ED season. Changes in lag time can be observed for each of those seasonal minimums. The low-peak flow and the low minimum are delayed by up to three and four weeks, respectively.

The trends in peak flow (LW) are similar to those found in previous studies although with different magnitudes. A subtle gradual trend in the increase in peak flow, from 6.9% to 7.9 % (~7% to 8%), is observed at the Congo River at Inga with increasing forest conversion (Table 4.1 and Figure 4.5). However, in the indirect-effects model, the hydrographs consistently decrease for all four scenarios.

#### 4.3.2. Surface runoff

Annual surface runoff volume has been derived from simulated daily flow discharge at the Congo River outlet. Model results of changes in annual surface runoff volume caused by LCLUC without and with climatic feedback are shown in Table 4.1 and Figure 4.7. Without climatic feedback,

annual surface volumes of runoff are greater than the baseline in all scenarios. However, the increase relative to the baseline is greatest, 4.7%, for the 25%-conversion scenario and progressively smaller for the subsequent three scenarios, down to 1.6%. When we include the climatic-feedback component of the model, i.e. ET and precipitation both decrease for sub-basins that have changed from majority forest to majority agricultural mosaic, annual surface runoff volumes are 7.5% smaller for the 25%-conversion scenario and decline to 9.1% smaller for the 100%-conversion scenario. Annual surface runoff volume is thus more sensitive to the cumulative effect of LCLUC when combined with the simulated decreases in ET and precipitation. Scenarios with indirect effects all produce rates of annual runoff lower than the baseline (Table 4.2).

#### 4.3.3. Hydropower potential

Following Congo Basin forest clearing and conversion to rural complex, hydropower potential is affected by both higher peak flows and lower peak and low flows. Estimates of changes in hydropower potential at Inga are proportional to those of the flow magnitudes. Under current conditions, estimated hydropower potential during peak flow is 44,293 MW, from an estimated peak flow of 56,439 m<sup>3</sup>/s and an average head of 80 meters. During the LD season in particular, the streamflow under current conditions reaches its lowest and is estimated at 30,502 m<sup>3</sup>/s, corresponding to a hydropower potential of 23,938 MW.

Peak flow following LCLUC simulations with no consideration to climatic feedback goes up to 65,199 m<sup>3</sup>/s. This corresponds to an increased hydropower potential of 51,168 MW, which could exceed plant capacity limitations. However, the substantial decreases of low flow are of particular concern for hydropower potential. It could possibly cause disruptions during these

periods. Indeed “low discharge variability has an important influence on the energy production of the run-of-river plants because the plants do not have reservoirs that allow for the storage of water during the wet season or regulation of discharges during the dry season” (Mohor *et al.* 2015). Under simulations that include indirect effects of LCLUC, increasing forest conversion causes decreases in low flow to 28,761 m<sup>3</sup>/s (25% forest conversion) to 23,115 m<sup>3</sup>/s (100% forest conversion). These correspond to estimated losses of hydropower potential from 1,366 MW to 5,797 MW for the LCLUC scenarios.

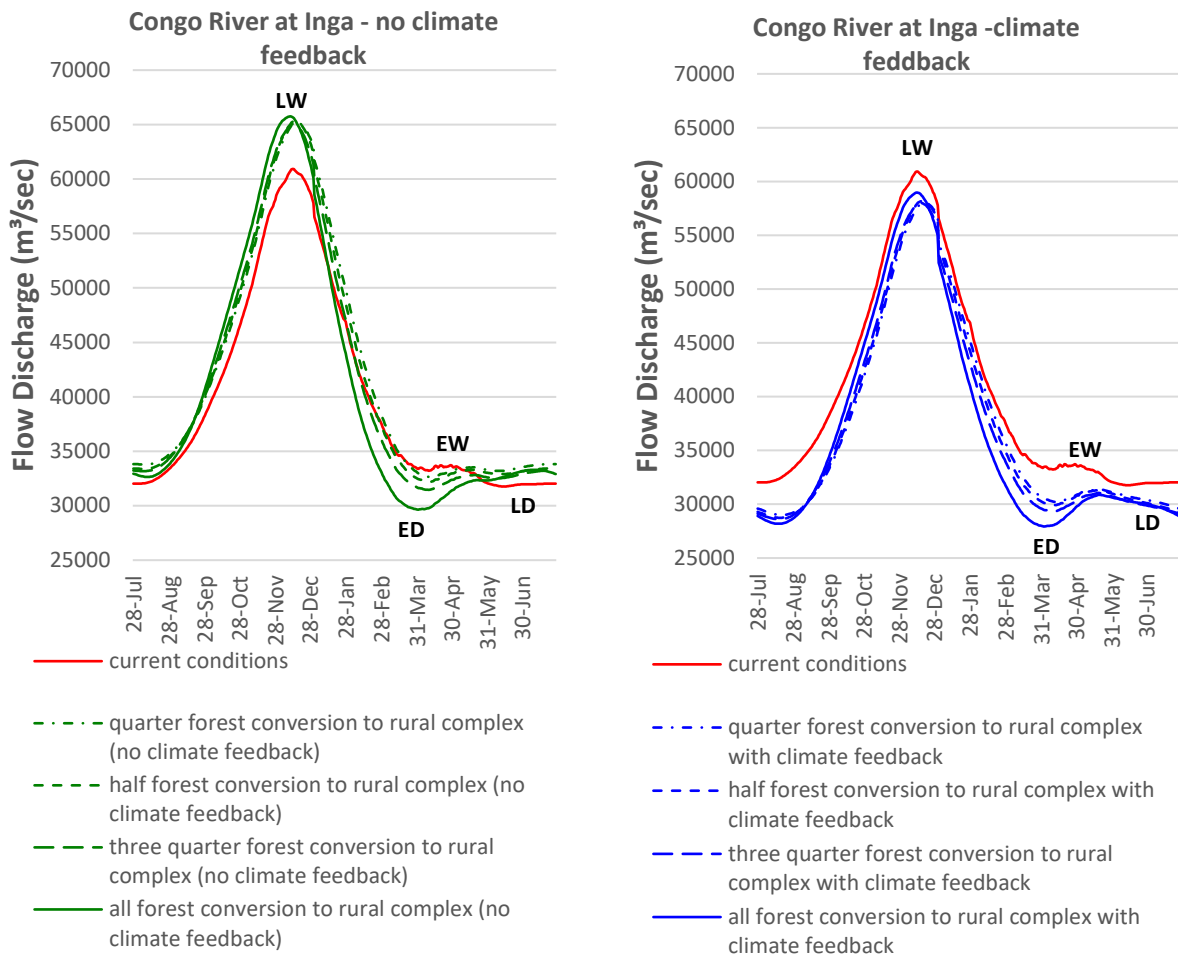


**Figure 4.5** Daily average hydrograph at the Congo River at Inga under four scenarios (25, 50, 75% and all forest conversion to rural complex) with and without consideration to climatic feedback. With forest conversion to rural complex, the rising limb get steeper, the rise time get slightly shorter and the peak discharge get slightly higher. In red, current daily average hydrograph. Increase of runoff contribute to a slightly higher peak flow. Yet, the increase of runoff occurs at the cost of groundwater recharge impacting low flow by a noticeable decrease.

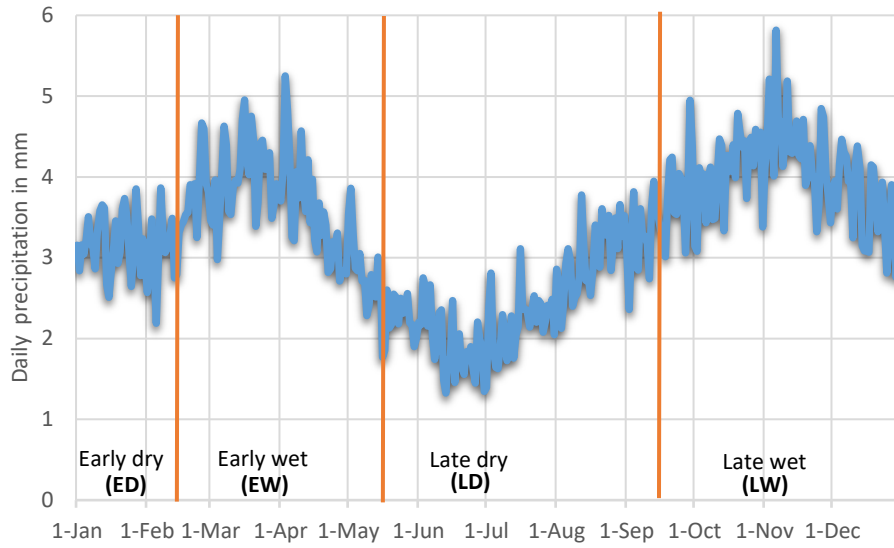


**Figure 4.6** Daily mean precipitation (1998-2012) in the overall Congo Basin

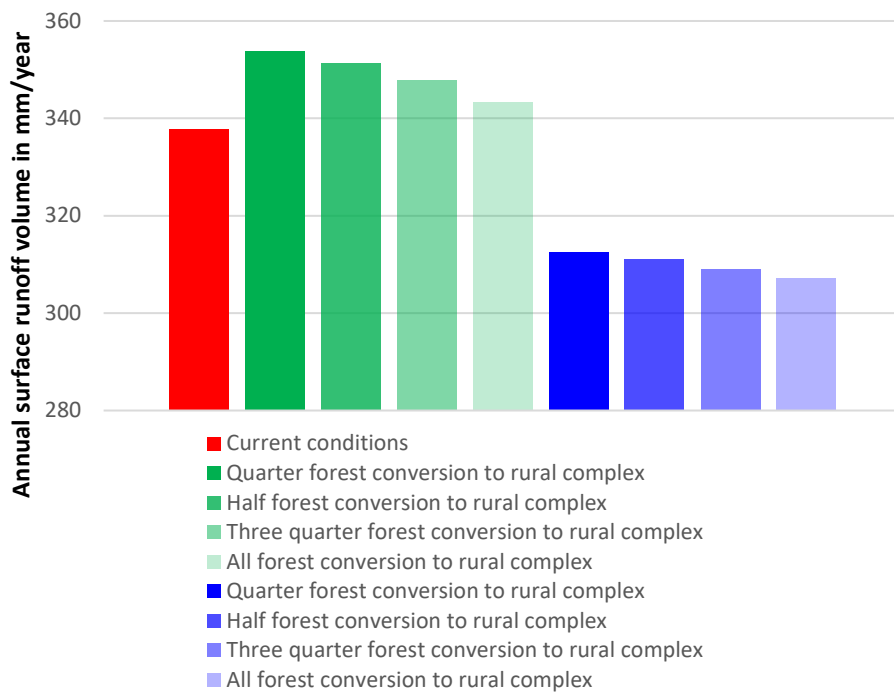


**Figure 4.7** Change in annual runoff volume/depth induced by LCLUC without and with climatic fee

**Table 4.1** Maximum (peak) and minimum (low) flow magnitude and percent of flow decrease/increase under the eight scenarios with no climatic feedback and with climatic feedback

	<i>Peak flow in m<sup>3</sup>/sec</i>	<i>Low flow in m<sup>3</sup>/sec</i>	<i>Percent increase/ decrease</i>	<i>Percent increase/ decrease</i>
<b>Current conditions</b>	60391	30956		
<b>No climatic feedback</b>				
<i>Quarter forest conversion to rural complex</i>	64596	31806	7	3
<i>Half forest conversion to rural complex</i>	64739	31384	7	1
<i>Three quarter forest conversion to rural complex</i>	64471	30663	7	-1
<i>All forest conversion to rural complex</i>	65199	28956	8	-6
<b>Climatic feedback</b>				
<i>Quarter forest conversion to rural complex</i>	56131	28485	-7	-8
<i>Half forest conversion to rural complex</i>	56293	28217	-7	-9
<i>Three quarter forest conversion to rural complex</i>	56136	28068	-7	-9
<i>All forest conversion to rural complex</i>	57087	27627	-5	-11

**Table 4.2:** Change in annual surface runoff volume/depth induced by LCLUC without and with climatic feedback

	<i>Average discharge at Inga</i>	<i>Runoff depth</i>	<i>Runoff increase</i>
	<i>m3/sec</i>	<i>mm/year</i>	<i>%</i>
<b><i>Current conditions</i></b>	39530.73607	337.88	
<b><i>No climatic feedback</i></b>			
<i>Quarter forest conversion to rural complex</i>	41386.89191	353.75	4.70
<i>Half forest conversion to rural complex</i>	41093.88387	351.25	3.95
<i>Three quarter forest conversion to rural complex</i>	40695.64631	347.84	2.95
<i>All forest conversion to rural complex</i>	40164.57754	343.30	1.60
<b><i>Climatic feedback</i></b>			
<i>Quarter forest conversion to rural complex</i>	36556.11379	312.46	-7.52
<i>Half forest conversion to rural complex</i>	36393.87054	311.07	-7.94
<i>Three quarter forest conversion to rural complex</i>	36156.23322	309.04	-8.54
<i>All forest conversion to rural complex</i>	35935.78314	307.16	-9.09

#### 4.4. Discussion

Our model simulation of the effects of LCLUC on Congo Basin's hydrology indicates the importance of considering both the direct effects, where LCLUC alters land-surface conditions, and the indirect effects, where LCLUC also alters local ET and precipitation. Accounting only for direct effects, the model shows increases in total annual flow relative to the baseline for all LCLUC scenarios, although these increases are progressively smaller as more forest is converted. Increases in annual flow with forest conversion is from large increases during the high-flow season that more than offset decreases in flow during the low-flow season (Figure 4.5, Table 4.1). This is likely a result of an increase in surface runoff following rains during the high-flow season, the surface runoff rapidly reaching the Congo River, compared to groundwater that can take as long as one year (Munzimi et al, 2019). Although, groundwater-surface water interactions are not completely captured by GeoSFM because of the model structure presenting certain limitations in characterizing groundwater storage, water balance is partitioned to surface runoff and to water infiltrated in the upper and lower soil layers by GeoSFM. It is thus possible to gain some useful insights into the plausible groundwater contribution to dry-season flows.

With no climatic feedback, Congo River maximum flow is fairly stable at 7% to 8% above the baseline with increasing forest conversion (Figure 4.5). In contrast, the minimum flows decrease progressively from 1% to 6% below the baseline with increasing forest conversion. The gradual decrease of dry-season flows with increasing forest conversion suggests an impact on groundwater. Forest conversion reduces

surface roughness and soil infiltration. Consequently, the ED season characterized by months of no rains leads to no groundwater recharge, particularly affecting the seasonal flow as relatively more water is extracted from than recharged to the ground. This appears to impact groundwater storage and thus decreases baseflow, the main source of water for the river during the dry season. “Streamflow is maintained by groundwater discharge known as baseflow, as long as the water table remains above the stream bottom (Delleur 1999). Yet, by taking long to reach the river, the water extracted from groundwater to feed surface water also affects the flow during the following wet season (EW). This might explain the prolonged low flow during the EW and the later resurgence of flow above baseline flow during the LD. Indeed, later in the LD season, flows under all four forest-conversion scenarios increase, surpassing the baseline levels. In summary, of these two indicators, surface runoff and groundwater recharges, the most sensitive, both in terms of change from baseline and trend among the four scenarios, is groundwater recharge. Since groundwater reaches the river much more slowly than does surface runoff, the groundwater recharge has a large effect and may be the main component driving the results of the flow timing seen in Figure 4.5.

In the combined-effects model, when we add indirect effects by including LCLUC effects on ET and precipitation, we find that a modest percent decrease in seasonal rainfall can contribute to larger changes in the Congo Basin’s hydrological regime. This agrees with the historical assessment by Laraque, et al (2001), whose comparisons of decadal averages show reductions in river discharge from 13% to 34% associated with reductions in precipitation of only 4% to 6%. The combined-effects model produces reductions in flow relative to the baseline levels across all seasons.

Peak flows no longer increase, rather they are all less than the baseline for all levels of forest conversion. It also produces progressively larger reductions with more forest conversion. Furthermore, the largest reductions now occur in the late-dry season, as opposed to the early-dry season when only direct effects are modeled.

There are large differences during the LD season between the results of the direct-only scenarios versus those of the combined-effects scenarios. These differences suggest that when precipitation is reduced the negative groundwater recharge and other losses that occur in the ED season extend into the LD. The reduction in precipitation is sufficient to alter the contribution of the northern rains in the LD season to the seasonal recovery of river flow. In the ED season, the reduction in flow estimated from combined effects are from 7% for the 25%-conversion scenario to 17% for the 100%-conversion scenario. In the LD season these reductions are 8% to 18%.

We know of no previously published simulations of LCLUC effects on the Congo Basin's hydrology and River's flow, although several exist for the Amazon Basin and its major sub-basins, which is of a similar geographic scale yet has much more data from rain and stream gauges as well as a research base. In their model simulations of river discharge under conversion to pasture and its subsequent climatic feedback, Coe et al (2009) found that in the absence of any significant atmospheric feedbacks to precipitation, deforestation of 7%, 25% and 40% caused increases in discharge at the mouth of the Amazon of 2%, 5% and 7%, respectively. When they included climatic feedback from deforestation, precipitation usually decreased, and flow discharge varied with not just the amount of decrease in precipitation but also with the location and the extent of the deforestation. For instance, in the case of the Rio

Negro 15% deforestation caused an 8% decrease in precipitation and a 10% decrease in discharge. In the Xingu, 26% deforestation caused a 15% decrease in precipitation and a 11% decrease in discharge. However, in the Tocantins and Araguaia Rivers of north-eastern Amazonia, 25% deforestation caused no significant change in precipitation and showed an increase discharge.

In another simulation of land use and hydrology the Xingu river, Stickler et al (2012) reported on the effects deforestation impacts on local ET within the watershed versus impacts on regional precipitation and the resulting impacts of both on river discharge and energy-generation potential for the Belo Monte energy complex on the Xingu River in the eastern Amazon. In these simulations, impacts on ET of deforestation levels of 20% and 40% increased discharge by 4% to 8% and 10% to 12%, respectively, with similar increases in energy generation. When the impacts on regional precipitation from these same deforestation rates were included in the simulations, reductions in precipitation offset the above increase and instead led to decreases in discharge of 6% to 36%. They found that under business-as-usual projections of 40% deforestation for 2050, simulated power generation declined to only 25% of maximum plant output and 60% of the industry's own projections. These studies corroborate the previously mentioned study of Panday, et al (2015), who found that when excluding the effects of deforestation on precipitation, deforestation caused increases in discharge, but including them more than offsets these increases, leading to net decreases in discharge. Mohor, et al (2015), in the simulations with a set of climate projections, also found large decreases in discharge, around 40% and 75%, under projected decreases in precipitation of 15% and 25%, respectively.

In summary, these studies of the Amazon Basin corroborate the major findings of this chapter of the Congo Basin. Forest conversion to non-forest land cover directly causes increases in annual discharge and higher peak flows. Conversion also decreases ET and thus decreases precipitation, decreasing the net water balance. The relatively small decreases in this balance consistently cause large decreases in the flow discharge of rivers in large basins. In almost all cases of simulations in the Amazon Basin, and in our study of the Congo Basin, these decreases more than offset the increases from the direct impacts, dominating the net result of decreasing river-flow discharge. The impacts in the Amazon Basin are in some cases similar in magnitude and in other cases larger. The larger impacts found for the Amazon Basin compared to our study might be due to forest conversion to pasture in the Amazon Basin versus to rural complex, a mosaic of agricultural fields and forest fallows.

Considering Congo Basin location astride the Equator, the alternate seasonal pattern of rainfall that feeds streams situated upstream Inga hydroelectric site will eventually be disrupted because of the climatic feedback. Indeed, following an eventual Congo Basin forest conversion to rural complex and its resulting climatic feedback, potential change of flow discharge could, depending on the land cover land use change magnitude, decrease hydropower generation at the Inga facility downstream Congo River. The modeled changes in hydropower potential particularly during dry season range from -1,366 MW to -5,797 MW, the latter corresponding to the hydropower potential of countries such as Zambia or Angola and of grand projects such as the Grand Ethiopian Renaissance Dam. These losses would necessitate management strategies

that might be different from the current ones, to compensate for flow modifications (Majone et al, 2016).

Greater than usual water balance has the potential to damage hydroelectric power plants structures. For example, the Guajataca Dam in Puerto Ricco was damaged when experiencing a structural failure on September 22, 2017, due to the hit from Hurricane Maria, requiring the evacuation of thousands of people downstream. The water balance increase was caused by days of heavy rain following Hurricane. The potential for rare but large storm events following LCLUC should be taken into consideration in planning for the Inga and other dams.

The most consistent results among all scenarios modeled is the reduction in flow in the dry season caused by forest conversion. The amount and duration of this reduction varies with the amount of forest conversion and whether or not indirect effects are included. Given the ample studies on deforestation impacts on ET and precipitation, and increasing demand for agricultural land in the Congo Basin, the 25%-conversion scenario with indirect impacts is a scenario of reasonable assumptions. In various regions including the Congo Basin, worsening droughts are already a threat to the ability of dams to meet their power production targets (Imhof et Lanza, 2010). The impacts of this scenario on flow throughout the entire early and late dry seasons are large, warrant further investigation, and warrant consideration in current planning of the Inga dam. All of these results could be either exacerbated or mediated by future global climate change. GCM results and regional climate change model results for precipitation in the Congo Basin disagree from a modest wetting to a modest drying (Sori et al 2017; Tshimanga et Hughes 2012; Mukheibir 2007; Paeth et Thamm 2007).

Thus far, GCMs do not indicate large enough changes that would change the general results and implications of this chapter.

#### **4.5. Conclusion**

This chapter hinted on the significance of the impact of forest loss on the hydrological system. The Congo Basin faces conflicting interests: the development of agriculture inducing the intrusion of the rural complex in the forest domain and the conservation of the Congo Basin water resources integrity by keeping the forest cover intact. This conversion will not only affect terrestrial characteristics of the watershed including soil infiltration and surface roughness but will also affect the water balance through a climatic feedback of the LCLUC depending on the change magnitude. Conversion of forest to rural complex has the potential to alter streamflow regime to the detriment of Congo Basin ecosystem services and even to the detriment of existing infrastructures such as the Inga hydropower facility downstream Congo River.

Our model simulations predict large impacts of LCLUC on river flows and hydropower potential. In the wet season, possible extreme flow events could stress power stations. In dry season, flows may not suffice to meet demands. If indirect effects are considered, major concerns in early through late dry seasons, comprising half of the calendar year. We find very different results when we do or do not include indirect effects in the model. This model also was by necessity parameterized, and calibrated, with very few available data. We recommend, given the ecological and economic importance of the Congo River, and given the potential range of impacts estimated in

this model, prioritizing further data collection required to enable further simulations. These data include: additional rain and stream gauges, field measurements of soil key parameters in forest and converted land. These would enable more robust models, model validation, sensitivity analyses and model inter-comparison.

## Chapter 5: Summary of findings, significance and future research directions

Quantitative and spatially explicit data on rainfall and streamflow discharge are necessary to advance research and to support informed decision-making on issues related to water sector. This dissertation investigates the development of hydrological modeling supported by remote sensing in an effort to quantify rainfall and streamflow data in the Congo Basin. The research provides key baseline information on current rainfall and streamflow regimes in the Congo Basin and assesses the hydrological response to potential LCLUC in the region.

### **5.1. Summary**

The contemporary rainfall regime is characterized by the statistical re-calibration of TRMM data, providing accurate rainfall data and proposing a new classification of the Congo Basin climate using our re-calibrated TRMM product (Chapter 2). A discussion on seasonal rainfall patterns across the Basin and its relationship with Congo River streamflow regime is also conducted. Our goal was to assess standard and regionally-calibrated TRMM products for future Basin-scale hydrological modeling of the Congo Basin that will employ the improved rainfall data in characterizing Basin streamflows. The resulting estimates of seasonal rainfall patterns and their relationship with Congo River streamflow regime guided the methodological development used for the modeling effort in chapter 3. The monthly

re-calibrated TRMM estimates are not used to drive our daily flow model in the following chapters. A re-calibration of daily rainfall was not possible since daily gauge data were not available at that time. We concluded that the importance of the daily time step of input rainfall is greater than the adjustment of the monthly data, and so we used an approach in the following chapters that takes the original TRMM daily data but conducts a calibration of the streamflow model based on the flow data from the *in-situ* gauges.

Chapter 3 describes the establishment of the baseline information on daily flows throughout the Congo Basin, which in turn provide a basis for assessing future hydrologic changes caused by changes in land cover and climate. The results of this chapter can be used to support operational short-term management and planning in the Congo Basin. In Chapter 4 we use the improved daily streamflow to study the hydrological responses to LCLUC across the Congo Basin. In doing this, the study explored four scenarios of potential forest conversion to the agriculture-dominated rural complex and quantified their impacts on flow and hydropower potential downstream Congo River at Inga.

## **5.2. Major findings and contributions**

This research indicates that TRMM 3B42 Version 6 data are appropriate for quantifying Congo Basin rainfall regimes and for deriving climate maps when calibrated by ground gauge data sets from within the region. TRMM data re-calibration with contemporary ground data from rain gauges from the core of our region of interest was validating by WORLCLIM data. Results illustrate the value of statistical

derivatives of the daily TRMM data in predicting monthly precipitation, although the generalized bagged regression tree model was very conservative in not predicting monthly rainfall greater than 300mm. This was due to the limited number of high monthly input observations coupled with a lack of separability of these months in the statistical feature space.

The model was differentially additive in augmenting monthly TRMM 3B42 data, particularly during dry season months characterized by light rain events, representative of stratiform rain in the Congo Basin. Convective storms, intense and of short duration, characteristic of the rainy season months in the Congo Basin were also subject to this model augmentation. The results indicate a lack of sensitivity of TRMM data to these two different types of rain. The chapter explained the two sources of rain event omission by TRMM sensors, omitting missing rainy-season convective and omitting dry-season stratiform rain events, explaining the overall underestimation of rainfall throughout the year in the Congo Basin.

The climate map based on the re-calibrated TRMM data has some strengths. First, the tropical rain forest and monsoon climates characteristic of the Congo Basin are more accurately depicted than in previous maps. Second, the hot semi-arid climate and the hot desert climate erroneously depicted in the map of Peel et al. (2007), the most-widely used climate map for the region to date, are not mis-characterized. Third, the highland climate, absent in Peel's map, is captured. The overall performance of the re-calibrated TRMM-derived climate classifier is promising, although its application in other regions would most likely require local TRMM re-calibration with appropriate ground data specific to the region of interest.

We examined seasonality of rainfall in the Congo Basin using the re-calibrated TRMM product of this study and were able to correlate it with the ITCZ in terms of rainfall timing (Waliser and Gauthier 1993) and in terms of rainfall amounts (Tsuneaki 2011). The ITCZ passes through the Southern hemisphere from October to April and the Northern hemisphere from April to October. Our results show April and October to be the peak rainfall months for both hemispheres, which is consistent with Waliser and Gauthier's model that places the ITCZ position near the equator during these two months. Tsuneaki (2011) explained the driving forces of the seasonal variation of the ITCZ, and found that the origin of the water vapor fluxes feeding the ITCZ varied by season. In April, the water vapor flux is mostly derived from the Indian Ocean via Tanzania. In October, the water vapor flux is supplied from within the Congo Basin. Varying sources of water vapor could explain the difference between the two peak rainfall months (April and October) observed across the Basin in this study. It receives more rain in the August to December time-frame than the mirrored period of year of February to June, confirming that the southward movement of the ITCZ is the dominant rain mechanism over the Basin.

The rainfall results of this study explain the two peak flows of the stream hydrograph at Kinshasa, the capital of the Democratic Republic of the Congo. The Kinshasa gauge station is situated along the lower reaches of the Congo River, roughly 400km from the ocean, close to the Basin outlet, providing an accurate representation of the Basinwide flow dynamic. There are two peaks of high streamflow, one in November with maximum annual flow and the other in April with 50% to 80% of that

of November. Testing against the stream gauge data of Kinshasa, including time lags, a high correlation of 0.81 between rainfall and streamflow was found for the re-calibrated TRMM model with a one month lag. The re-calibrated TRMM product of this chapter is consistent in the depiction of intra-annual rainfall variation and its influence captured in observed downstream Congo River hydrographs.

The third chapter describes the application of remotely-sensed data for hydrological modeling of the Congo Basin. Satellite-derived data, including TRMM precipitation, were used as inputs to drive the GeoSFM model to estimate daily river discharge records over the basin from 1998 to 2012. However, the daily temporal resolution of the climatological data, precipitation and evapotranspiration, required to drive the daily model prevented the use of the re-calibrated monthly TRMM data processed in our previous chapter. Temporal downscaling procedures would have required a much greater coverage of gauge data, as would any other option for re-calibrating daily data. This lack of daily-observed rainfall data prevented us from re-calibrating TRMM product on a daily scale in the previous chapter, explaining our focus on a monthly re-calibrated product in chapter 2.

A physically-based parameterization of the USGS hydrological model (Geospatial streamflow model, GeoSFM) is augmented with a spatially-distributed calibration that enables GeoSFM to simulate hydrologic processes. One major process is the slowing effect on downstream flow of the *Cuvette Centrale*, the bowl-shaped depression with wetlands, which lies in the center of the basin and extends in all directions along the arc of the Congo River. Wetlands such as the inland drainage of

the *Cuvette Centrale* have a substantial impact on river basin flow rates, as wetland water depths are shallow within a diffuse channel geometry (Betbeder *et al.* 2014, Alsdorf 2016). The model is able to account for the detention of water in the floodplain. Our overall approach consisted of an initial model parameterization for basin-wide daily flow, a basin-level calibration for the Congo River downstream the *Cuvette Centrale*, and a subbasin level calibration for Congo River's tributaries upstream the *Cuvette Centrale*.

The annual average flow from the model simulations of daily flow and the observed flow at the Kinshasa gauge were very similar, 40,631 m<sup>3</sup>/s and 40,638m<sup>3</sup>/s respectively, over the 7-year validation period average (2004 - 2010). The simulations show no significant bias and a Nash-Sutcliffe model efficiency coefficient of 0.70. Comparisons of modeled daily flows and aggregated monthly river outflows to historical averages for additional sites confirm the model's reliability in capturing flow timing and seasonality across the basin.

The results of this model can be useful in research and decision-making contexts and validate the application of satellite-based hydrologic models driven for large, data-scarce river systems such as the Congo Basin. Our results also corroborate findings from our previous chapter: the peak flows at Kinshasa in November-December and April-May are driven by the November and March rainfall peaks with about a month lag, and these rainfall timing were accurately estimated by the TRMM product. As the passage of ITCZ drives rainy and dry seasons in the Congo Basin, the seasonal progression of the ITCZ influences surface waters of the basin as well. The geographical distributions of the day of minimum and peak flow, shown in Figure 3.13,

illustrates day of minimum flow trends southward from the from early February to late October, with the exception of the northern-most part of the Basin where it occurs in April-May. The trend is reversed for day of peak flow that progresses northward from early February to late October. From July to August, peaks occur mostly in the northern-most part of the Basin. In addition, the equatorial belt is dominated by peak flows in November and December. These spatial patterns can be interpreted in the context of the migration of the ITCZ and the different origins of the water vapor fluxes feeding the ITCZ, which varies in different seasons. The month of maximum precipitation for re-calibrated TRMM data (Figure 2.8a ) and of the day of peak flow (Figure 3.13) show a strong agreement.

Corroborating previous studies, the streamflow model from the present study captured the difference between the equatorial rivers having in two peaks flows per year, whereas non-equatorial rivers basins have only one peak flow annually; as the varying sources of water vapor have explained the difference between the two peak rainfall days and months in April and October, which consequently drive the high streamflow of the Congo River in November and December, benefiting from the larger volume of water brought in by the ITCZ in October.

Despite some limitations in streamflow modeling, the basin-wide level and subbasin wide calibrations successfully accounted for the majority of the spatial and temporal hydrological patterns of the Congo Basin when evaluated over the entire validation period. More challenging was capturing temporal patterns (timing and shape of seasonal cycle) at the daily level, and here the range of  $r^2$  values from regressing modeled versus observed daily flows were encouraging. However, even though

temporal patterns (seasonality and timing) were successfully captured at all locations, discrepancies in magnitude of the seasonal cycle at some locations suggest that flow discharge may still be biased for some streams within the basin. Nonetheless, these limitations did not prevent us from assessing the hydrological response downstream Congo River of potential LCLUC in the Congo Basin in chapter 4.

In chapter 4, we present a model-based assessment of hydrological responses to land cover land use change (LCLUC) in the Congo Basin, with and without climatic feedbacks, and resulting impacts on the Congo River's hydropower potential. We simulate streamflow data using GeoSFM) under current land-cover conditions of the basin and under a series of LCLUC scenarios where forest is replaced with agricultural mosaic. Hydropower potential was estimated for the Inga hydroelectric site, currently the largest installation in the region and proposed for major expansion. Direct effects of LCLUC were via changes in key model parameters related to surface roughness and soil infiltration, with precipitation and ET held constant at recent fluxes. Indirect effects of LCLUC from climatic feedbacks were via changes in precipitation and ET over areas of simulated LCLUC, accounting for precipitation recycling in the Congo Basin where ET fluxes may contribute 25% of precipitation. Simulations of the direct effects of conversion of 25% to 100% of forest upstream from Inga result in decreases in low flows during the early-dry season of 1.5% to 10.3% and increases in peak flows in the late-wet season of 6.7% to 8.0%. When indirect effects were included, the largest decreases were in low flows during the late-dry season, from 7.9% to 10.7%, and peak flows in the late-wet season decrease by 5.5% to 7.1% rather than increase. This study indicates the significance of the impact of forest loss on the Congo Basin's hydrological

system. It shows how forest cover potential conversion to a rural complex contributed to large declines in flow in dry season and decline or augmentation of peak flow in wet season depending on the scenario i.e. without or with consideration of climatic feedback respectively. A combination of changes in flow magnitude and reductions in rise and decline times of the streamflow hydrograph is projected to significantly impact hydropower potential, with possible disruptions during periods of low flow and possible flooding during those of peak flow. The estimated yearly loss of hydropower potential reaches ~ 6,000 MW, equivalent to the hydropower potential of Zambia or Angola or that of grand projects such as the Grand Ethiopian Renaissance Dam.

### **5.3. Future research directions**

An expected finding of this research is the limitation posed by the shortage of timely contemporary ground-gauge data at fine temporal scales. While remote sensing based modeling provides significant insight of the mechanisms governing these processes, the added value of using data from very few gauge stations in the Congo Basin is demonstrated in this work. Whether for calibration or for evaluation of the statistical and hydrological models used in this study, the integration of gauge information allowed the generation of improved contemporary satellite-derived products useful for crucial decision-making and research in the water sector. More gauge data would certainly increase research efforts regarding the Congo Basin hydrology. As recommended by Nicholson et al (2019), station data availability should be added in at least few key areas and collaborative relationships with local meteorological services should be increased. The approaches used in this study could certainly be improved with the augmentation of rainfall gauge data, including more

high monthly rainfall months in particular. The limited number of high monthly input observations coupled with a lack of separability of these months in the statistical feature space appeared to be the cause of limited characterization of rainfall through the recalibration of TRMM products in the Congo Basin. Our results illustrated the value of statistical derivatives of the daily data in predicting monthly precipitation. However, for the regression tree model to better fit outlier rainfall and to be more sensitive to particularly high rainfall months, more rainfall gauges would be necessary.

More streamflow gauges data would allow a more efficient bias correction to adjust model overestimation at subbasins level. The simple bias correction handled was a recognition of the limitations of available gauge data in executing a more robust regional calibration. The simple bias correction with one factor applied to all subbasins did not consider the possible differences across subbasins. A regionally-distributed calibration could be performed on subbasins to improve validity of streamflow simulations in rivers segments throughout the basin. The regional calibration method would involve disaggregating streamflow to each subbasin and independently readjusting model parameters to ensure generate the target streamflow.

A better understanding of the specific mechanisms of the present streamflow modeling such as the river and floodplain losses is something we look forward to in the future. The river and floodplain losses reported in table 3.2 explained to some extent the difference between water balance and runoff. While the basinwide water runoff generated by our model was 424 mm/year (Table 3.2), the discharge at the basin outlet was estimated at 302 mm/year while in-stream losses including floodplains losses make up the balance of 122 mm/year (Table 3.2). More accurate estimation of the magnitude

of the losses would probably require a focused study, likely with a field campaign to accurately capture the extent, evaporation rates and other losses from the floodplains. This would also improve the allocation of these losses in the forest conversion scenarios analysis as suggested in the fourth chapter.

The streamflow model was by necessity parameterized, and calibrated, with very few available data. Given the ecological and economic importance of the Congo River, and given the potential range of impacts estimated in the scenarios analysis of forest conversion to agricultural mosaic, we encourage a prioritization of further data collection required to enable further simulations. The additional rain and stream gauges, as well as field measurements of soil key parameters in forest and converted land would enable more robust models, model validation, sensitivity analyses and model inter-comparison.

More precise knowledge of flow characteristics of the Congo River Basin as well as others in data-scarce river systems are also required for future studies, such as the estimation of which watersheds are most sensitive to temperature and which watersheds have a hydrology dominated by the amount and timing of precipitation. The present rainfall-based climate classification of the Congo Basin derived from TRMM, could serve as a stratifier for further data collection and it could serve as a basis for grouping rivers and streams within the basin by climate type to facilitate comparisons of runoff characteristics. Finally, the improved estimates of streamflow from this study could support other more reliable assessments of possible future scenarios, including those accounting for the effects of the El Niño Southern Oscillation (ENSO) and other climatic cycles, apart from the effects of land use change on the Congo Basin's

hydrology handled in this study. Studies of the hydrological responses to climate change and seasonal variability could benefit from improved daily streamflow models.

The importance of the LCLUC effect on hydrology demonstrates the need for coordination and support between hydropower proponents and efforts for both additional data collection, gauges and other *in-situ* studies, and model simulations.

## Bibliography

- Adeyewa, Z.D., and K. Nakamura, 2003: Validation of TRMM radar rainfall data over major climatic regions in Africa. *Journal of Applied Meteorology and Climatology*, 42, 331–347.
- Afouda, Abel, Alain Ibikunlé Ague, and Flavien Lanhoussi. "Etude Comparative D'un Modèle Conceptuel Global (Gr4j) Et D'un modèle Semi-Distribue (Geosfm) Sur Le Bassin Versant De L'Ouémé A Save (Benin, Afrique De L'ouest)." *Revue Ljee* 24&25 (2015).
- Agunbiade, O.A. and Jimoh, O.D., 2013. Flood Modelling Of Upper Gurara Watershed Using Remote Sensing Data And The Geospatial Streamflow Model. *WIT Transactions on Ecology and the Environment*, 172, 39-49.
- Ajami, N.K., Gupta, H., Wagener, T. and Sorooshian, S., 2004. Calibration of a semi-distributed hydrologic model for streamflow estimation along a river system. *Journal of Hydrology*, 298 (1), 112-135.
- Al-Abed, N.A. and Whiteley, H.R., 2002. Calibration of the Hydrological Simulation Program Fortran (HSPF) model using automatic calibration and geographical information systems. *Hydrological processes*, 16(16), pp.3169-3188.
- Aloysius, N. and Saiers, J., 2017. Simulated hydrologic response to projected changes in precipitation and temperature in the Congo River basin. *Hydrology and Earth System Sciences*, 21 (8), 4115-4130.
- Alsdorf, D., Beighley, E., Laraque, A., Lee, H., Tshimanga, R., O'Loughlin, F., Mahé, G., Dinga, B., Moukandi, G. and Spencer, R.G., 2016. Opportunities for hydrologic research in the Congo Basin. *Reviews of Geophysics*, 54(2), pp.378-409.
- Amarasekera, K.N., Lee, R.F., Williams, E.R. and Eltahir, E.A., 1997. ENSO and the natural variability in the flow of tropical rivers. *Journal of Hydrology*, 200 (1-4), 24-39.
- Artan G.A., Asante K.O., Smith J.L., Pervez S., Entenmann D., Verdin J.P. and Rowland J., 2007a. *Users manual for the geospatial stream flow model (GeoSFM)*. Open-File Report 2007-1440. Reston, VA: US Geological Survey, 194.
- Artan, G., Gadain, H., Smith, J.L., Asante, K., Bandaragoda, C.J. and Verdin, J.P., 2007b. Adequacy of satellite derived rainfall data for stream flow modeling. *Natural Hazards*, 43 (2), 167-185.

Artan, Guleid, et al. "Streamflow Simulation Using Remotely Sensed Rainfall Data: Brahmaputra River." *Mekong River Commission* (2009): 478.

Asante, K.O., Famiglietti, J.S. and Verdin, J.P. Current and future applications of remote sensing for routine monitoring of surface water. *In: Global priorities in Land and Remote Sensing Conference: PECORA 16, 23 – 27 October 2005* Sioux Falls, South Dakota. American Society for Photogrammetry and Remote Sensing, 2005

Asante K.O., Artan G.A., Pervez S., Bandaragoda C. and Verdin J.P., 2007a. *Technical manual for the geospatial streamflow model (GeoSFM)*. Open-File Report 2007-1441. Reston, VA: US Geological Survey, 99.

Asante, K.O., Macuacua, R.D., Artan, G.A., Lietzow, R.W. and Verdin, J.P., 2007b. Developing a flood monitoring system from remotely sensed data for the Limpopo basin. *IEEE Transactions on Geoscience and Remote Sensing*, 45 (6), 1709-1714.

Asante, K.O., Arlan, G.A., Pervez, S. and Rowland, J., 2008. A linear geospatial streamflow modeling system for data sparse environments. *International Journal of River Basin Management*, 6 (3), 233-241.

Beighley, R.E., Ray, R.L., He, Y., Lee, H., Schaller, L., Andreadis, K.M., Durand, M., Alsdorf, D.E. and Shum, C.K., 2011. Comparing satellite derived precipitation datasets using the Hillslope River Routing (HRR) model in the Congo River Basin. *Hydrological Processes*, 25 (20), 3216-3229.

Bell, F.C., 1968. Estimating design floods from extreme rainfall. *Hydrology papers (Colorado State University); no. 29*.

Beniston, Martin, and Markus Stoffel. "Assessing the impacts of climatic change on mountain water resources." *Science of the Total Environment* 493 (2014): 1129-1137.

Betbeder, J., Gond, V., Frappart, F., Baghdadi, N.N., Briant, G. and Bartholomé, E., 2014. Mapping of Central Africa forested wetlands using remote sensing. *IEEE Journal of Selected Topics in Applied Earth Observations and Remote Sensing*, 7 (2), 531-542.

Bitew, M. M., and M. Gebremichael, 2011: Are satellite-gauge rainfall products better than satellite-only products for Nile hydrology? *Nile River Basin*, A. M. Melesse, Ed., Springer-Verlag, 129–141

Blanc, E. and Strobl, E., 2013. The impact of climate change on cropland productivity: evidence from satellite based products at the river basin scale in Africa. *Climatic change*, 117 (4), 873-890.

Blanc, E., and E. Strobl. "Water availability and crop growth at the crop plot level in South Africa modelled from satellite imagery." *The Journal of Agricultural Science* 153.02 (2015): 306-321.

Bonan, Gordon B. "Forests and climate change: forcings, feedbacks, and the climate benefits of forests." *science* 320.5882 (2008): 1444-1449.

Boysen, L. R., et al. "Global and regional effects of land-use change on climate in 21st century simulations with interactive carbon cycle." *Earth System Dynamics* 5.2 (2014): 309.

Breiman, L., 1996: Bagging predictors. *Machine Learning*, 24, 123-140.

Breiman, L., Friedman, J.H., Olsen, R.A., and Stone, C.J. (1984). *Classification and Regression Trees*. Wadsworth, Belmont (CA).

Brown, M.E., Racoviteanu, A.E., Tarboton, D.G., Gupta, A.S., Nigro, J., Policelli, F., Habib, S., Tokay, M., Shrestha, M.S., Bajracharya, S. and Hummel, P., 2014. An integrated modeling system for estimating glacier and snow melt driven streamflow from remote sensing and earth system data products in the Himalayas. *Journal of Hydrology*, 519, 1859-1869.

Brummett, Randall, et al. "Water resources, forests and ecosystem goods and services." *The forests of the Congo Basin: State of the forest 2008* (2009): 1411-1457.

Bwangoy, J. R. B., Hansen, M. C., Potapov, P., Turubanova, S., & Lumbuenamo, R. S. (2013). Identifying nascent wetland forest conversion in the Democratic Republic of the Congo. *Wetlands ecology and management*, 21(1), 29-43.

Bwangoy, J.R.B., Hansen, M.C., Roy, D.P., De Grandi, G. and Justice, C.O., 2010. Wetland mapping in the Congo Basin using optical and radar remotely sensed data and derived topographical indices. *Remote Sensing of Environment*, 114 (1), 73-86.

Campbell D. 2005. The Congo River Basin. In: Fraser LH, Keddy PA, eds. *The World's Largest Wetlands: Ecology and Conservation*. Cambridge, United Kingdom: Cambridge University Press, 149-165.

Chishugi, J.B. and Alemaw, B.F., 2009. The hydrology of the Congo River Basin: A GIS-based hydrological water balance model. In *World Environmental and Water Resources Congress 2009: Great Rivers* (1-16).

Clevers, J.G.P.W., Bartholomeus, H., Mücher, C.A. and de Wit, A.J.W., 2005. Land cover classification with the medium resolution imaging spectrometer (MERIS). In *Proceedings 24th EARSeL Symposium "New Strategies for European Remote Sensing"*, Dubrovnik, Croatia, 25-27 May 2004 (687-694).

Coe, MT. and Olejniczak, N., 1999. Global River Discharge Database (SAGE). Available online at [<http://www.sage.wisc.edu/riverdata/>] from the Center for Sustainability and the Global Environment (SAGE), Gaylord Nelson Institute for Environmental Studies, University of Wisconsin-Madison, Madison, Wisconsin, USA

Coe, Michael T., Marcos H. Costa, and Britaldo S. Soares-Filho. "The influence of historical and potential future deforestation on the stream flow of the Amazon River—Land surface processes and atmospheric feedbacks." *Journal of Hydrology* 369.1 (2009): 165-174.

Cole, M.A., Elliott, R.J. and Strobl, E., 2014. Climate Change, Hydro-Dependency, and the African Dam Boom. *World Development*, 60, 84-98.

Crowley, J.W., Mitrovica, J.X., Bailey, R.C., Tamisiea, M.E. and Davis, J.L., 2006. Land water storage within the Congo Basin inferred from GRACE satellite gravity data. *Geophysical Research Letters*, 33 (19).

Defourny, P., Delhage, C. and Kibambe, J.P., 2011. Analyse quantitative des causes de la déforestation et de la dégradation des forêts en République Démocratique du Congo. *Rapport UCL/FAO/CN REDD. FAO, Kinshasa, République Démocratique du Congo.*

Delbourg, Esther, and Eric Strobl. "Water conflicts and cooperations up and down African rivers." (2014).

Delleur, J.W., 1999. The Handbook of Groundwater Engineering. FL, USA, CRC Press, Boca Raton. Eckhar

Democratic Republic of the Congo, "The Democratic Republic of the Congo fixes October 2015 as the date for the launch of the first phase of the largest hydroelectric plant in the world," Paris, p. 3, 18-May-2013

Dessu, S.B., Seid, A.H., Abiy, A.Z. and Melesse, A.M., 2016. Flood forecasting and stream flow simulation of the upper Awash River basin, Ethiopia using geospatial stream flow model (GeoSFM). In: Melesse A., Abtew W. (eds). *Landscape Dynamics, Soils and Hydrological Processes in Varied Climates*. Springer Geography. Springer, Cham, 367-384.

Dinku, T., P. Ceccato, E. Grover-Kopec, M. Lemma, S. J. Connor, and C. F. Ropelewski, 2007: Validation of satellite rainfall products over East Africa's complex topography. *International Journal of Remote Sensing*, 28 (7), 1503–1524.

Dinku, T., S. Chidzambwa, P. Ceccato, S.J. Connor, and C. F. Ropelewski, 2008: Validation of high-resolution satellite rainfall products over complex terrain. *International Journal of Remote Sensing*, 29, 4097–4110.

Dinku, T., S. J. Connor, and P. Ceccato, (2010). Comparison of CMORPH and TRMM-3B42 over mountainous regions of Africa and South America. *Satellite Rainfall Applications for Surface Hydrology*, M. Gebremichael and F. Hossain, Eds., Springer-Verlag, 193–204.

Dyer, E.L., Jones, D.B., Nusbaumer, J., Li, H., Collins, O., Vettoretti, G. and Noone, D., 2017. Congo Basin precipitation: Assessing seasonality, regional interactions, and sources of moisture. *Journal of Geophysical Research: Atmospheres*, 122(13), pp.6882-6898.

Ebert, E. E., J. E. Janowiak, and C. Kidd, (2007). Comparison of near-real-time precipitation estimates from satellite observations and numerical models. *Bulletin of the American Meteorological Society*, 88, 47–64.

Eltahir, Elfatih AB, and Rafael L. Bras. "Precipitation recycling." *Reviews of geophysics* 34.3 (1996): 367-378.

Eltahir, E.A., Loux, B., Yamana, T.K. and Bomblies, A., 2004. A see-saw oscillation between the Amazon and Congo basins. *Geophysical Research Letters*, 31(23).

Ernst, C., Mayaux, P., Verhegghen, A., Bodart, C., Christophe, M. and Defourny, P., 2013. National forest cover change in Congo Basin: deforestation, reforestation, degradation and regeneration for the years 1990, 2000 and 2005. *Global change biology*, 19 (4), 1173-1187.

Fernandez, N., Jaimes, W. and Altamiranda, E., 2010. Neuro-fuzzy modeling for level prediction for the navigation sector on the Magdalena River (Colombia). *Journal of Hydroinformatics*, 12(1), pp.36-50.

Food and Agriculture Organization of the United Nations (FAO), 1971–1981. *Soil Map of the World*. UNESCO, 1:5,000,000. Paris, vol. 1-10 (1:5M scale maps and accompanying texts).

Food and Agriculture Organization of the United Nations (FAO), 1995. *Digital Soil Map of the World (DSMW)*. [CD-ROM] V.3.5. FAO, Rome, Italy

Gabella M., S. Michaelides, P. Constantinides, and G. Perona, 2006: Climatological validation of TRMM precipitation radar monthly rain products over Cyprus during the first 5 years (December 1997 to November 2002). *Meteorologische Zeitschrift*, 15 (5), 559–564

Gabella M., S. Athanasatos, R. Notarpietro, S. Michaelides, 2008: Climatological validation of TRMM radar monthly rainfall amounts over Cyprus during the first 8 years (December 1997– November 2005). *5th European Conference on Radar in Meteorology and Hydrology*, 21–25 July 2008, Helsinki, Finland

Goudie, A.S., 2005. The drainage of Africa since the Cretaceous. *Geomorphology*, 67 (3-4), 437-456.

Green, Nathaniel, Benjamin K. Sovacool, and Kathleen Hancock. "Grand designs: assessing the African energy security implications of the grand inga dam." *African Studies Review* 58.01 (2015): 133-158.

Gupta, H.V., Sorooshian, S. and Yapo, P.O., 1999. Status of automatic calibration for hydrologic models: Comparison with multilevel expert calibration. *Journal of Hydrologic Engineering*, 4 (2), 135-143.

Hammons, Thomas J., Pathmanathan Naidoo, and Lawrence Musaba. "Run of river bulk hydroelectric generation from the Congo river without a conventional Dam." *Natural Resources* 2.01 (2011): 18.

Hansen, M., et al, 2008, A method for integrating MODIS and Landsat data for systematic monitoring of forest cover and change in the Congo, *Remote Sens. Environ.*, 112, 5: 2495-2513

Hansen, M.C., Roy, D.P., Lindquist, E., Adusei, B., Justice, C.O. and Altstatt, A., 2008. A method for integrating MODIS and Landsat data for systematic monitoring of forest cover and change in the Congo Basin. *Remote Sensing of Environment*, 112 (5), 2495-2513.

Herrmann, S., and K. A. Mohr, 2011: A Continental-Scale Classification of Rainfall Seasonality Regimes in Africa Based on Gridded Precipitation and Land Surface Temperature Products. *Journal of Applied Meteorology and Climatology*, 50 (12), 2504-2513.

Hijmans, R.J., S. E. Cameron, J. L. Parra, P. Jones and A. Jarvis, 2005: Very high resolution interpolated climate surfaces for global land areas. *International Journal of Climatology*, 25, 1965–1978.

Houze, R. A., Jr., 1997: Stratiform precipitation in regions of convection: A meteorological paradox?. *Bulletin of the American Meteorological Society*, 78, 2179–2196.

Huffman, G.J., 1997: Estimates of root-mean-square random error for finite samples of estimated precipitation. *Journal of Applied Meteorology and Climatology*, 36, 1191-1201.

Huffman, G.J., 2013: README for Accessing Experimental Real-Time TRMM Multi-Satellite Precipitation Analysis (TMPA-RT) Data Sets. Mesoscale Atmospheric Processes Laboratory, NASA Goddard Space Flight Center and Science Systems and Applications, Inc.

Huffman, G.J., R.F. Adler, P. Arkin, A. Chang, R. Ferraro, A. Gruber, J. Janowiak, A. McNab, B. Rudolph, and U. Schneider, 1997: The global precipitation climatology project (GPCP) combined precipitation dataset. *Bulletin of the American Meteorological Society*, 78, 5-20

Huffman, G.J., R. F. Adler, D. T. Bolvin, G. Gu, E. J. Nelkin, K. P. Bowman, E. F. Stocker, and D. B. Wolff, 2007: The TRMM Multisatellite Precipitation Analysis (TMPA): Quasi-Global, Multiyear, Combined-Sensor Precipitation Estimates at Fine Scales. *Journal of Hydrometeorology*, 8, 38- 55

Huffman, G.J., R. F. Adler, D. T. Bolvin, and E. J. Nelkin, 2010: The TRMM Multisatellite Precipitation Analysis (TMPA). Chapter 1 in *Satellite Rainfall Applications for Surface Hydrology*, F. Hossain and M. Gebremichael, Eds. Springer Verlag, ISBN: 978-90-481-2914-0, 3-22.

Huffman, G.J. and D. T. Bolvin, 2012: TRMM and Other Data Precipitation Data Set Documentation. Mesoscale Atmospheric Processes Laboratory, NASA Goddard Space Flight Center and Science Systems and Applications, Inc.

Huffman, G.J. and D. T. Bolvin, 2014: TRMM and Other Data Precipitation Data Set Documentation. "Recent" News. Mesoscale Atmospheric Processes Laboratory, NASA Goddard Space Flight Center and Science Systems and Applications, Inc.

Ickowitz, A., Slayback, D., Asanzi, P. and Nasi, R., 2015. *Agriculture and deforestation in the Democratic Republic of the Congo: A synthesis of the current state of knowledge* (Vol. 119). CIFOR Occasional Paper. Bogor, Indonesia: Center for International Forestry Research (CIFOR).

Imhof, Aviva, and Guy R. Lanza. "Big dams have a serious record of social and environmental destruction, and there are many alternatives. So why are they still being built?." *World Watch* 23 (2010): 8-14.

Islam, Z., 2011. Physically based hydrologic modeling.

Kadima E, Delvaux D, Sebagenzi N, Tack L, Kabeya SM (2011) Structure and geological history of the Congo Basin: an integrated interpretation of gravity, magnetic and reflection seismic data. *Basin Res* 23(5):499–527

Kalyanapu, A.J., Burian, S.J. and McPherson, T.N., 2010. Effect of land use-based surface roughness on hydrologic model output. *Journal of Spatial Hydrology*, 9(2).

Kar, S.O., 1967. *Hydrograph rise times* (Doctoral dissertation, Colorado State University, Fort Collins).

Karekezi, Stephen. "Poverty and energy in Africa—A brief review." *Energy Policy* 30.11 (2002): 915-919.

- Karekezi, Stephen, Waeni Kithyoma, and Energy Initiative. "Renewable energy development." *workshop on African Energy Experts on Operationalizing the NEPAD Energy Initiative, June*. 2003.
- Khakbaz, B., Imam, B., Hsu, K. and Sorooshian, S., 2012. From lumped to distributed via semi-distributed: Calibration strategies for semi-distributed hydrologic models. *Journal of Hydrology*, 418, 61-77
- Kiluva, V.M., Mutua, F., Makhanu, S.K. and Ong'or, B.T.I., 2011. Application of the geological streamflow and Muskingum Cunge models in the Yala River Basin, Kenya. *Journal of Agriculture, Science and Technology*, 13 (2).
- Köppen W., 2011: The thermal zones of the Earth according to the duration of hot, moderate and cold periods and to the impact of heat on the organic world. *Meteorologische Zeitschrift*, 20, 351–360.
- Köppen, W., 1918: Klassifikation der Klimate nach Temperatur, Niederschlag und Jahreslauf. *Petermanns Geogr. Mitt.*, 64, 193-203, 243-248. [(Classification of climates according to temperature, precipitation and seasonal cycle), *Petermanns Geogr. Mitt.*, 64, 193–203, 243–248]
- Kottek, M., J. Grieser, C. Beck, B. Rudolf, and F. Rubel, 2006: World map of the Köppen-Geiger climate classification updated. *Meteorologische Zeitschrift*, 15 (3), 259–263.
- Laraque, A., Mahé, G., Orange, D. and Marieu, B., 2001. Spatiotemporal variations in hydrological regimes within Central Africa during the XXth century. *Journal of hydrology*, 245(1-4), 104-117.
- Larentis, Dante G., et al. "Gis-based procedures for hydropower potential spotting." *Energy* 35.10 (2010): 4237-4243.
- Lee, H., Beighley, R.E., Alsdorf, D., Jung, H.C., Shum, C.K., Duan, J., Guo, J., Yamazaki, D. and Andreadis, K., 2011. Characterization of terrestrial water dynamics in the Congo Basin using GRACE and satellite radar altimetry. *Remote Sensing of Environment*, 115 (12), 3530-3538.
- Lukong, Terence Kibula, Michel Mbessa, and Thomas Tamo Tatietsé. "Predictive Model of Rainfall-Runoff: A Case Study of the Sanaga Basin at Bamendjin Watershed in Cameroon." *Energy and Environment Research* 1.1 (2011): p193.
- Majone, B., Villa, F., Deidda, R. and Bellin, A., 2016. Impact of climate change and water use policies on hydropower potential in the south-eastern Alpine region. *Science of the Total Environment*, 543, pp.965-980.

- Malhi, Y., Adu-Bredu, S., Asare, R.A., Lewis, S.L. and Mayaux, P., 2013. African rainforests: past, present and future. *Phil. Trans. R. Soc. B*, 368(1625), 20120312.
- Mandelli, S., Barbieri, J., Mattarolo, L. and Colombo, E., 2014. Sustainable energy in Africa: A comprehensive data and policies review. *Renewable and Sustainable Energy Reviews*, 37, 656-686.
- McGregor, G. R., and S. Nieuwolt, 1998: *Tropical climatology*, 2nd edn. Wiley, Chichester, 339 pp.
- Mohammed, Y. S., M. W. Mustafa, and N. Bashir. "Status of renewable energy consumption and developmental challenges in Sub-Sahara Africa." *Renewable and Sustainable Energy Reviews* 27 (2013): 453-463.
- Mohor, G.S., Rodriguez, D.A., Tomasella, J. and Júnior, J.L.S., 2015. Exploratory analyses for the assessment of climate change impacts on the energy production in an Amazon run-of-river hydropower plant. *Journal of Hydrology: Regional Studies*, 4, pp.41-59.
- Molinario, G., Hansen, M.C. and Potapov, P.V., 2015. Forest cover dynamics of shifting cultivation in the Democratic Republic of Congo: a remote sensing-based assessment for 2000–2010. *Environmental Research Letters*, 10 (9), 094009.
- Motovilov, Yuri G., et al. "Validation of a distributed hydrological model against spatial observations." *Agricultural and Forest Meteorology* 98 (1999): 257-277.
- Mukheibir, P. "Possible climate change impacts on large hydroelectricity schemes in Southern Africa." *Journal of Energy in Southern Africa* 18, no. 1 (2007): 4-9.
- Munzimi, Y., 2008. Satellite-derived rainfall estimates (TRMM products) used for hydrological predictions of the Congo River flow: overview and preliminary results. START report. *Agronomy Sciences Department*, 31.
- Munzimi, Y.A., Hansen, M.C., Adusei, B. and Senay, G.B., 2015. Characterizing congo basin rainfall and climate using tropical rainfall measuring mission (trmm) satellite data and limited rain gauge ground observations. *Journal of Applied Meteorology and Climatology*, 54 (3), 541-555.
- Munzimi, Y.A., Hansen, M.C., Asante, K.O., 2019. Estimating daily streamflow in the Congo Basin using satellite-derived data and a semi-distributed hydrologic model. *Journal of Hydrological Sciences. In press*
- Nackoney, J., Molinario, G., Potapov, P., Turubanova, S., Hansen, M. C., & Furuichi, T. Impacts of civil conflict on primary forest habitat in northern Democratic Republic of the Congo, 1990–2010. *Biological Conservation*, 170 (2014), 321-328.

Naidoo, P. "New strategies for harvesting large scale bulk energy from the Congo River without a conventional dam." *Power & Energy Society General Meeting, 2009. PES'09. IEEE. IEEE, 2009.*

Nicholson, S.E. 2000: The nature of rainfall variability over Africa on time scales of decades to millennia. *Global and Planetary Change, 26*, 137–158

Nicholson, S.E., Klotter, D., Zhou, L. and Hua, W., 2019. Validation of satellite precipitation estimates over the Congo Basin. *Journal of Hydrometeorology, 20*(4), pp.631-656.

Nicholson, S.E., B. Some, J. McCollum, E. Nelkin, D. Klotter, Y. Berte, B. M. Diallo, I. Gaye, G. Kpabeba, O. Ndiaye, J. N. Noukpozoukhou, M. M. Tanu, A. Thiam, A. A. Nikolaos, S., Kleomenis, K., Elias, D., Panagiotis, S., Panagiota, L., Vagelis, P. and Christos, C., 2019. A Robust Remote Sensing–Spatial Modeling–Remote Sensing (RMR) Approach for Flood Hazard Assessment. In *Spatial Modeling in GIS and R for Earth and Environmental Sciences* (pp. 391-410). Elsevier.

Osman, Aboubaker Ahmed. *Use of Space Technology and GIS in Seasonal Water Course System (Case of Gash River Basin)*. Diss. UOFK, 2015.

Paeth, Heiko, and Hans-Peter Thamm. "Regional modelling of future African climate north of 15 S including greenhouse warming and land degradation." *Climatic Change* 83, no. 3 (2007): 401-427.

Panday, P.K., Coe, M.T., Macedo, M.N., Lefebvre, P. and de Almeida Castanho, A.D., 2015. Deforestation offsets water balance changes due to climate variability in the Xingu River in eastern Amazonia. *Journal of Hydrology, 523*, pp.822-829.

Partow, H. (2011). Water issues in the Democratic Republic of the Congo. Challenges and opportunities. Technical report. United Nations Environment Programme (UNEP). Available from: [http://postconflict.unep.ch/publications/UNEP\\_DRC\\_water.pdf](http://postconflict.unep.ch/publications/UNEP_DRC_water.pdf) [Accessed 30 March 2017].

Peel, M.C., B. L. Finlayson, and T. A. McMahon, 2007: Updated world map of the Köppen-Geiger climate classification. *Hydrology and Earth System Sciences, 11*, 1633–1644.

Pokhrel, Yadu Nath, Taikan Oki, and Shinjiro Kanae. "A grid based assessment of global theoretical hydropower potential." *水工学論文集* 52 (2008): 7-12.

Potapov, P.V., Turubanova, S.A., Hansen, M.C., Adusei, B., Broich, M., Altstatt, A., Mane, L. and Justice, C.O., 2012. Quantifying forest cover loss in Democratic Republic of the Congo, 2000–2010, with Landsat ETM+ data. *Remote Sensing of Environment, 122*, 106-116.

- Reitsma, R.F., 1996. Structure and support of water-resources management and decision-making. *Journal of Hydrology*, 177 (3-4), 253-268.
- Roca, R., P. Chambon, I. Jobard, P. E. Kirstetter, M. Gosset, and J. C. Berges, 2010: Comparing satellite and surface rainfall products over West Africa at meteorologically relevant scales during the AMMA campaign using errors estimates. *Journal of Applied Meteorology and Climatology*, 49, 715–731.
- Rodriguez, E., Morris, C.S. and Belz, J.E., 2006. A global assessment of the SRTM performance. *Photogrammetric Engineering & Remote Sensing*, 72 (3), 249-260.
- Rudolf, B. 1993: Management and analysis of precipitation data on a routine basis. *Proc. Int. WMO/IAHS/ETH Symposium on Precipitation and Evaporation*, Bratislava, Slovakia, Slovak Hydrometeorology Institute, 69–76.
- Rudolf, B., H. Hauschild, W. Ruth, and U. Schneider, 1994: Terrestrial precipitation analysis: Operational method and required density of point measurements. *Global Precipitations and Climate Change*, M. Dubois and F. Desalmand, Eds., Springer Verlag, 173–186.
- Sahin, Vildan, and Michael J. Hall. "The effects of afforestation and deforestation on water yields." *Journal of hydrology* 178.1-4 (1996): 293-309.
- Sahoo, G.B., Ray, C. and De Carlo, E.H., 2006. Calibration and validation of a physically distributed hydrological model, MIKE SHE, to predict streamflow at high frequency in a flashy mountainous Hawaii stream. *Journal of Hydrology*, 327 (1-2), 94-109.
- Sambo, A. S. "Electricity demand from customers of INGA hydropower projects: The case of Nigeria." *WEC Workshop on Financing INGA Hydropower Projects*. 2008.
- Samuels, William B., Rakesh Bahadur, and Christopher Ziemniak. "Waterborne Transport Modeling of Radioactivity from the Fukushima Nuclear Power Plant Incident." *Securing Water and Wastewater Systems*. Springer International Publishing, 2014. 135-148.
- Samuels, William B., et al. "Development of a global oil spill modeling system." *Earth Science Research* 2.2 (2013): p52.
- Sangvaree, Wiroj and Yevjevich, Vujica. "Effects of forest and agricultural land use on flood unit hydrographs." *Hydrology papers (Colorado State University)*; no. 92. (1977).

Santhi, Chinnasamy, Narayanan Kannan, J. G. Arnold, and Mauro Di Luzio. "Spatial Calibration and Temporal Validation of Flow for Regional Scale Hydrologic Modeling1." (2008): 829-846.

Schumacher, C., and R. A. Jr. Houze, 2003: Stratiform rain in the tropics as seen by the TRMM Precipitation Radar, *Journal of Climate*, 16, 1739–1756.

Senay, G.B., Verdin, J.P., Lietzow, R. and Melesse, A.M., 2008. Global daily reference evapotranspiration modeling and evaluation. *JAWRA Journal of the American Water Resources Association*, 44 (4), 969-979.

Shiklomanov, I.A., 2009. River runoff to oceans and lakes. *In: Igor Alekseevich Shiklomanov, eds. Hydrological Cycle Volume II. UNESCO - Encyclopedia of Life Support Systems (EOLSS)*, 70-97

Showers, Kate B. "Beyond mega on a mega continent: Grand Inga on Central Africa's Congo River." *Engineering Earth*. Springer, Dordrecht, 2011. 1651-1679.

Shukla, Jagadish, Carlos Nobre, and Piers Sellers. "Amazon deforestation and climate change." *Science(Washington)* 247.4948 (1990): 1322-1325.

Smith, L.C., Turcotte, D.L. and Isacks, B.L., 1998. Stream flow characterization and feature detection using a discrete wavelet transform. *Hydrological processes*, 12 (2), 233-249.

Sofreco Led Consortium. *Study on Programme for Infrastructure Development in Africa (Pida). Africa Energy Sector Outlook – 2040*, 2011.

Sorí, Rogert, Raquel Nieto, Sergio M. Vicente-Serrano, Anita Drumond, and Luis Gimeno. "A Lagrangian perspective of the hydrological cycle in the Congo River basin." *Earth System Dynamics* 8, no. 3 (2017): 653-675.

Stickler, C.M., Coe, M.T., Costa, M.H., Nepstad, D.C., McGrath, D.G., Dias, L.C., Rodrigues, H.O. and Soares-Filho, B.S., 2013. Dependence of hydropower energy generation on forests in the Amazon Basin at local and regional scales. *Proceedings of the National Academy of Sciences*, 110(23), pp.9601-9606.

Strayer, David L., et al. "Effects of land cover on stream ecosystems: roles of empirical models and scaling issues." *Ecosystems* 6.5 (2003): 407-423.

Suberu, Mohammed Yekini, et al. "Power sector renewable energy integration for expanding access to electricity in sub-Saharan Africa." *Renewable and Sustainable Energy Reviews* 25 (2013): 630-642.

Summerfield, M. A., 1991. *Global geomorphology: An introduction to the study of landforms*. London: Longman Scientific and Technical, 537 p.

Suzuki, T., 2011. Seasonal variation of the ITCZ and its characteristics over Central Africa. *Theoretical and Applied Climatology*, 103 (1-2), 39-60.

Taliotis, Constantinos, et al. "Grand Inga to power Africa: Hydropower development scenarios to 2035." *Energy Strategy Reviews* 4 (2014): 1-10.

Tegegne, Yitagesu T., et al. "Evolution of drivers of deforestation and forest degradation in the Congo Basin forests: Exploring possible policy options to address forest loss." *Land Use Policy* 51 (2016): 312-324.

Thieme, M.L., Abell, R., Burgess, N., Lehner, B., Dinerstein, E. and Olson, D., 2005. *Freshwater ecoregions of Africa and Madagascar: a conservation assessment*. Island Press, Washington D.C., U.S.A.

Tierney, J. E., J. M. Russell, J. S. Sinninghe Damste', Y. Huang, and D. Verschuren, 2011: Late Quaternary behavior of the East African monsoon and the importance of the Congo Air Boundary. *Quaternary Science Reviews*, 30, 798–807.

Toure, A. K. Traore, 2003: Validation of TRMM and other rainfall estimates with a high-density gauge dataset for West Africa. Part II: validation of TRMM rainfall products. *Journal of Applied Meteorology and Climatology*, 42, 1355–1368

Tshimanga, R.M., Hughes, D.A. and Kapangaziwiri, E., 2011. Initial calibration of a semi-distributed rainfall runoff model for the Congo River basin. *Physics and Chemistry of the Earth, Parts A/B/C*, 36 (14-15), 761-774.

Tshimanga, R. M., and D. A. Hughes, 2012. Climate change and impacts on the hydrology of the Congo Basin: The case of the northern subbasins of the Oubangui and Sangha Rivers. *Physics and Chemistry of the Earth, Parts A/B/C*, 50, 72 –83.

Tshimanga, R. M., and D. A. Hughes, 2014. Basin-scale performance of a semi-distributed rainfall-runoff model for hydrological predictions and water resources assessment of large rivers: The Congo River. *Water Resources Research*, 50 (2), 1174–1188.

Tsuneaki, S., 2011: Seasonal variation of the ITCZ and its characteristics over central Africa. *Theoretical and Applied Climatology*, 103, 39–60

Turkson, John, and Norbert Wohlgenuth. "Power sector reform and distributed generation in sub-Saharan Africa." *Energy Policy* 29.2 (2001): 135-145.

Turubanova, S., Potapov, P.V., Tyukavina, A. and Hansen, M.C., 2018. Ongoing primary forest loss in Brazil, Democratic Republic of the Congo, and Indonesia. *Environmental Research Letters*, 13(7), p.074028.

United Nations, Department of Economic and Social Affairs, Population Division. World Population Prospects: The 2017 Revision, Key Findings and Advance Tables. Working Paper No. ESA/P/WP/248 (2017).

Van Zyl, J.J., 2001. The Shuttle Radar Topography Mission (SRTM): a breakthrough in remote sensing of topography. *Acta Astronautica*, 48(5-12), 559-565.

Verdin, J., Funk, C., Senay, G. and Choularton, R., 2005. Climate science and famine early warning. *Philosophical Transactions of the Royal Society B: Biological Sciences*, 360(1463), pp.2155-2168.

Waliser, D.E., and C. Gauthier, 1993: A Satellite-derived climatology of the ITCZ. *Journal of Climate*, 6, 2162-2174.

Washington, R., James, R., Pearce, H., Pokam, W.M. and Moufouma-Okia, W., 2013. Congo Basin rainfall climatology: can we believe the climate models? *Philosophical Transactions of the Royal Society B: Biological Sciences*, 368 (1625), 20120296.

Wijesundera, I., Halgamuge, M.N., Nirmalathas, T. and Nanayakkara, T., 2012, September. A computationally efficient framework for stochastic prediction of flood propagation. In *2012 IEEE 6th International Conference on Information and Automation for Sustainability* (pp. 25-28). IEEE.

Winsemius, H. C., et al. "On the calibration of hydrological models in ungauged basins: A framework for integrating hard and soft hydrological information." *Water Resources Research* 45.12 (2009).

Yimer, F., et al. "Effects of different land use types on infiltration capacity in a catchment in the highlands of Ethiopia." *Soil use and management* 24.4 (2008): 344-349.

Zhang, Q., Justice, C.O., Jiang, M., Brunner, J. and Wilkie, D.S., 2006. A GIS-based assessment on the vulnerability and future extent of the tropical forests of the Congo Basin. *Environmental Monitoring and Assessment*, 114 (1-3), 107-121

Zhou, L., Y. Tian, R. B. Myneni, P. Ciais, S. Saatchi, Y. Y. Liu, S. Piao, H. Chen, E. F. Vermote, C. Song, and T. Hwang, 2014: Widespread decline of Congo rainforest greenness in the past decade. *Nature*, 509, 86–90

Zhou, Guoyi, et al. "Global pattern for the effect of climate and land cover on water yield." *Nature communications* 6 (2015): 5918.